GENETIC ANALYSIS OF SUBCELLULAR BRANCHING IN *DROSOPHILA* TRACHEAL TERMINAL CELLS

by

Tiffani Alvey Jones

A dissertation submitted to the faculty of
The University of Utah
in partial fulfillment of the requirements for the degree of

Doctor of Philosophy

Department of Human Genetics

The University of Utah

December 2013

The University of Utah Graduate School

STATEMENT OF DISSERTATION APPROVAL

The dissertation of **Tiffani Alvey Jones**

has been approved by the following supervisory committee members:

Mark Metzstein	, Chair	**7/12/13** Date Approved
Carl Thummel	, Member	**7/12/13** Date Approved
Charles Murtaugh	, Member	**7/12/13** Date Approved
Gillian Stanfield	, Member	**7/12/13** Date Approved
Jody Rosenblatt	, Member	**7/12/13** Date Approved

and by **Lynn Jorde** , Chair/Dean of

the Department/College/School of **Human Genetics**

and by David B. Kieda, Dean of The Graduate School.

ABSTRACT

All cells have distinct cellular architectures that are critical for their function. A dramatic example of this relationship can be observed in cells that undergo subcellular branching. In this case, cells must first specify distinct branch sites and then outgrow cellular projections from those sites, resulting in a branched cellular morphology. Branching morphology is a common type of cell shape, examples of which include glial oligodendrocytes found in the human brain, dendritic cells of the mammalian immune system and by far the best studied example, neurons. Tubulogenesis or lumen morphology is another type of cell formation common throughout biology. Cellular tubes transport liquids and gases within animal tissues and are often found in elaborate organ systems that span the entire body including the human respiratory and circulatory systems. Despite the importance of these forms of cell architecture, little is known about the genes and molecular machinery that are required for developing branched tubular cells. *Drosophila* larval tracheal terminal cells are single, highly branched cells that have a subcellular lumen running through each branch. These cells are located at the ends of a network of interconnected tubes and are the final, and critical step in delivery of oxygen and other gases to animal tissues. Terminal cell development, which occurs primarily during larval stages, includes three distinct morphological processes: cell growth, subcellular branching and tubulogenesis. Cell outgrowth is a general process that is used by many other cell types to enable the overall growth. Subcellular branching is a

specialized process that includes sending cellular projections out from the plasma membrane towards other cellular targets. Lastly, tubulogenesis is the process of forming a space or lumen within a cell through which gas can flow.

Here, we use *Drosophila* larval terminal cells, a component of the respiratory system, to investigate the cellular mechanisms required for development of two distinct cellular morphologies, subcellular branching morphogenesis and subcellular lumen formation. Work described here focuses primarily on progress made in elucidating mechanisms of branch specification and branch outgrowth. We have found that the PAR-polarity protein complex is required for terminal cell branching and that through the Rho GTPase Cdc42, and other PAR proteins, the exocyst facilitates polarized membrane addition required for terminal cell branch outgrowth.

This thesis if dedicated to my husband, Josh.

TABLE OF CONTENTS

ABSTRACT……..…….iii

LIST OF FIGURES……...…viii

ACKNOWLEDGMENTS…….……x

Chapter

1. INTRODUCTION……..1

The *Drosophila* larval tracheal system……3
Tracheal system development……..4
Tracheal system lumen formation……6
Summary……..9
References……..……12

2. A NOVEL FUNCTION FOR THE PAR COMPLEX IN SUBCELLULAR MORPHOGENESIS OF TRACHEAL TERMINAL CELLS IN *DROSOPHILA MELANOGASTER*…….…....14

Abstract……..15
Introduction……15
Materials and methods……...16
Results……17
Discussion……..23
Acknowledgments……..25
Literature cited……..25
Supporting information……..27

3. EXOCYST-MEDIATED MEMBRANE TRAFFICKING IS REQUIRED FOR BRANCH OUTGROWTH IN *DROSOPHILA* TRACHEAL TERMINAL CELLS……...37

Abstract……..37
Introduction……38
Materials and methods……...41
Results……45

Discussion……..50
References……..69

4. MOLECULAR INTERACTIONS OF THE PAR COMPLEX AND THE ROLE OF THE PAR- AND EXOCYST COMPLEX IN SUBCELLULAR TUBE FORMATION……...75

Introduction……....75
Material and methods……79
Results……82
Discussion……..87
References……102

5. EXAMINATION OF *DROSOPHILA* LARVAL TRACHEAL TERMINAL CELLS BY LIGHT MICROSCOPY……...105

Abstract……....106
Video link……106
Introduction……..106
Protocol……107
Representative results……..108
Discussion……....110
Disclosures……...111
Acknowledgments……111
References……....111

6. SUMMARY……....112

References……....119

LIST OF FIGURES

Figure

1.1 *Drosophila* larval tracheal system morphology……10

2.1 *par-6* is required for subcellular branching and lumen formation…….18

2.2 Quantification of terminal cell defects……...18

2.3 The PAR complex is required for subcellular branching, but not all components are required for lumen formation……...19

2.4 Localization of PAR-complex proteins in wild-type and mutant terminal cells...20

2.5 A direct interaction between Par-6 and aPKC is required for subcellular branching, but not for lumen formation…….…..22

2.6 Analysis of $par\text{-}6^{15N}$……...23

2.7 Par-6 is required for FGF-induced cell branching, but not cell growth…….23

S2.1 Molecular analysis of new *par-6* alleles……30

S2.2 *par-6* rescue experiments……...31

S2.3 Terminal cell defects in *Cdc42* mutants…….…32

S2.4 Staining of mutant cells showing specificity of antibody staining……33

S2.5 Localization of Baz and aPKC in mutant backgrounds…….34

S2.6 Baz does not function to bridge interactions between Par-6 and $aPKC^{psu69}$……..35

3.1 The exocyst complex is required for terminal cell morphogenesis……...55

3.2 The exocyst is required for terminal cell branch outgrowth……..…57

3.3 The PAR complex is required for exocyst membrane concentration in terminal cells……..……..59

3.4 Terminal cells defective for the exocyst complex or Cdc42 accumulate cytoplasmic vesicles……...61

3.5 Rab GTPases Rab10 and Rab11 are required for terminal cell branch development……...63

3.6 Branching morphogenesis model……...65

S3.1 Terminal cells expressing RNAi directed against exocyst complex members show branching and outgrowth defects……...66

S3.2 The PAR-polarity complex is not required for terminal cell branch outgrowth……...……67

S3.3 The endocytic recycling pathway is required for terminal cell branch development……...68

4.1 *baz 15N* double mutants show severe terminal cell defects……...91

4.2 Activated aPKC causes branching defects in terminal cells……..93

4.3 PI3K is required for branching in tracheal terminal cells……..94

4.4 PAR-polarity mutant terminal cells show accumulation of the apical membrane marker, Pio……...…..96

4.5 Ultrastructure of *15N* mutant terminal cells…….…..97

4.6 Exocyst complex members are required for lumen formation in terminal cells……98

4.7 Exocyst complex members are required for lumen maturation in terminal cells……..100

5.1 Larvae preparation and identification of terminal cells……...…109

5.2 Representative images…….……110

ACKNOWLEDGMENTS

I would like to thank my advisor, Dr. Mark Metzstein. It has been a privilege to be trained by such a brilliant and caring mentor. On a professional level Mark is a constant teacher, taking every opportunity to instruct and inform his students. We have worked closely together in the preparation of three manuscripts and each time was more delightful than the last. Mark has been instrumental in my decision to pursue a career in research science and has instilled a newfound confidence in by abilities as a scientist. On a personal level, Mark has become a friend. My experience in the Metzstein lab has changed me and opened my eyes to new ways of thinking, interpreting and approaching life. Mark is a constant professional, he strives to instill values such as hard work, perseverance and scholastic professionalism and he does this first and foremost by his example. Mark has created a lab environment that is extremely supportive, friendly and fun, which makes the learning experience easy and fulfilling. I have benefited greatly form my time in the Metzstein lab and will never forget Mark and his undying devotion to science.

I would like to thank my committee, Carl Thummel, Gillian Stanfield, Charles Murtaugh, and Jody Rosenblatt. Their support and guidance has been instrumental in my success and training as a graduate student. Committee meetings were always helpful and a place where I felt support for my plans and ideas. This committee helped me focus my efforts on the important experiments that eventually resulted in publication. I have also

had continued support from committee members in the form of reference letters and editorial critiques, as I have begun writing fellowship applications for my postdoctoral research. In particular I would like to thank, Carl Thummel for his help in preparing my first research in progress talk as well as his continued acknowledgment and support of my success and progress. Finally, I would also like to especially thank Gillian Stanfield for her encouragement, editorial feedback on multiple projects and most importantly her strong leadership. Gillian is an amazing and careful scientist that I admire and I hope to follow her example and position as a strong, successful female researcher.

I would like to thank the Department of Human Genetics, students, faculty and staff. Receiving feedback from faculty members after journal club and research in progress talks has been instrumental in my ability to present and communicate science. I appreciate the administrative staff, especially, Natalie Johnson, for handling insurance, stipends and tuition benefits and generally making my life easier.

I would like to thank my friends, the members of the Metzstein lab. Kim Frizzell, Alex Chapin and Jon Nelson have become my closest and dearest friends. Together, we have created a friendly, competitive, and fun work environment that makes me happy to go to work everyday. We have enjoyed each other's successes and failures and together we have grown from each experience. I will never forget the wonderful friendships we have made and will always remember our time together fondly.

I would also like to especially thank my friend, Hannah Gordon. Hannah is an amazing women and scientist. Her passion and excitement for science coupled with her sweet giving nature make her a person to be respected and admired. I love her dearly and will be forever grateful that we became friends. Additionally, I would like to also thank

my dear friends, Kim and Jesse Frizzell. Kim has become one of my greatest friends; her witty humor coupled with her devotion to our friendship has been a refreshing and life changing experience. I have admired Kim's devotion to science and living and enjoying life and I will miss her dearly. Importantly, I want to thank Kim and Jesse for helping and supporting Josh and I. We will be forever grateful for your house, your help, and your friendship, thank you.

I would like to thank my wonderful family. Specifically my parents, Mark and Teresa, are a constant source of support. Making my parents proud has been exceedingly fulfilling and I have benefited greatly form their love and support over the years. My Dad is the reason I wanted to attend college, his admiration for academics and his desire to "work smarter not harder" gave me the confidence to pursue a career in academic science and I will be forever grateful for his support. My Mom is a wonderful example of perseverance and ambition, she has lead by example and taught me to constantly accept new challenges and always push myself further than I think possible. My sisters, Tanna and Melyn, and my brother, Tayler have been extremely helpful and supportive each in their own way. They have provided support, understanding and love that has encouraged and contributed to my success. Lastly, my nieces and nephews, who I love dearly, provide the mental and emotional relief that I desperately need from time to time.

Lastly, I would like to thank my dear husband, Josh. No words can truly explain the appreciation I have for him. Josh has sacrificed so much to make my dream possible and has given me nothing but love and support. I look forward to our new adventure together and hope the next twelve years will be as wonderful as the last.

CHAPTER 1

INTRODUCTION

Each cell within an organism has a distinct morphology that is necessary for its success and participation as a single cell or as part of a tissue. The shape of some cells, such as cuboidal cells found in an epithelium, are very simple. Others, such as the shape of human sperm, melanocytes or muscle cells, are much more complex. One of the most intricate cell shapes is branched morphology. Branched cells are common throughout biology and include cell types such as glial oligodendrocytes, megakaryocytes, and by far the best-known and well-studied examples, neurons. Branched cells or systems have unique functional features that distinguish them from cells and tissues of other morphologies. For instance, branching allows for increased surface area, as can be observed in the mammalian lung, where alveolar sacs at the tips of branched bronchioles, have a large surface area to facilitate the diffusion of gases (Cardoso and Lü, 2006). Additionally, a branched morphology allows a single cell to make contacts with many other cells simultaneously. In this case, the ability to contact many cells at the same time creates the opportunity for multiplicative signal propagation and integration. Conserved cellular processes likely provide general mechanisms to generate a branched morphology. For branching to occur, three basic cellular steps are

required: cell polarization (orientation), branch site specification, and branch outgrowth. Cell polarization is the process of establishing spatial differences within a cell that are required for structure, morphology, and function. Polarization is not unique to branched cells and occurs in most cell types. Branch site specification is the process of defining regions within a cell that are competent to promote branch growth. Branch outgrowth requires polarized membrane addition to specific sites, and this process occurs in cells that undergo branching, ciliogenesis and cell budding (Babbey et al., 2010; Das and Guo, 2011; Lalli, 2009; Murthy et al., 2003; Sans et al., 2003).

Another distinct type of morphology is that of cellular tubes, which are used commonly throughout biology to transport liquids and gases within an organism. One example is the vertebrate circulatory system, which is a system of cellular tubes that extend throughout the organism to shuttle blood containing vital nutrients and gases within the animal (Lizama and Zovein, 2013). Interestingly, there are many examples of entire organ systems composed of cellular tubes that also undergo branching, such as the previously described respiratory and circulatory systems (Ochoa-Espinosa and Affolter, 2012). In these and other tubular networks, large diameter tubes are made up of multiple cells with many cell-cell contacts. These tubes tend to bifurcate into smaller tubes with fewer cell-cell junctions. This process continues as fewer and fewer cells make up the tube until, finally, a single tubular cell contacts its target tissues, where gas and nutrient diffusion occurs.

Despite the important functions and elaborate and beautiful architecture, surprisingly little is known about the molecular mechanisms that are necessary for the development of a branched cell. To investigate the genes and molecular machinery

required for branching morphogenesis and tubulogenesis we use a component of the *Drosophila* larval tracheal system, terminal cells.

The *Drosophila* larval tracheal system

The *Drosophila* larval tracheal system contains ~10,000 interconnected tubes that function in gas transport. Air enters through openings in the insect cuticle called spiracles and passes through the tubes of the tracheal system until it reaches target tissues (Figure 1.1A and B). The larval tracheal system is composed of multiple tubes of distinct morphology. The dorsal trunks (DT) are two large multicellular tubes derived from primary tracheal branches that run parallel to the long axis of the animal (Figure 1.1A-C, see arrows). These function primarily to collect and transport large volumes of gas through the animal by their direct connection to the spiracular openings at the posterior and anterior ends of the animal. Secondary tracheal branches are unicellular tubes (Figure 1.1 insert from A and C) that function primarily to connect the dorsal trunk to the cells specialized for supplying gas directly to tissues, the terminal cells. However, some secondary tracheal branches have more specialized functions. For example, fusion cells which function in the interconnectivity of the tracheal system and connect the two dorsal terminal cells. Lastly, terminal cells are located at the ends of the tracheal system and consist of a network of subcellular tubes contained within an elaborately branched cytoplasm (Figure 1.1D and E). These cells send cellular projections out from their cell body to ramify with target tissues, where they facilitate gas exchange. Together primary, secondary and terminal cell branches make up the highly connected and branched tubular network required for transporting gases to internal tissues.

Tracheal system development

The tracheal system has repeating segmental and bilateral symmetry, which is established during embryogenesis (Figure 1.1F). During early embryonic development tracheal precursor cells, expressing the bHLH-PAS domain transcription factor Trachealess invaginate from the ectoderm to form 10 bilateral clusters (pits) of ~80 tracheal precursor cells within each body segment (Ghabrial et al., 2003; Llimargas, 1999). Expression of *trachealess* in tracheal precursors induces expression of the FGF receptor, encoded by *breathless,* just prior to sprouting from placodes and developing as tracheal pits. An FGF ligand, encoded by the *branchless* (*bnl*) gene, is expressed in a fixed pattern, which is governed by global patterning hierarchies in the embryo (Lee et al., 1996). Bnl is responsible for directing tracheal cell migration from placodes and controls the highly stereotyped morphology observed in primary and secondary tracheal branching patterns (Sutherland et al., 1996). In contrast, terminal cells, located at the terminal tips of the embryonic tracheal system, are specified by FGF-induced expression of the transcription factor, *blistered,* the *Drosophila* homolog of mammalian serum response factor (Gervais and Casanova, 2011; Guillemin et al., 1996). It has been proposed that, after specification, a secondary round of Bnl signaling could trigger the activation of Blistered, which would be sufficient to induce terminal branch growth through downstream regulation of cytoskeletal components such as actin and microtubules. Interestingly, the requirement for *blistered* can be bypassed by over-expression of *bnl* (Gervais and Casanova, 2011). Although this is sufficient to induce subcellular branching and lumen formation, the branches are not properly organized, which suggests that two pathways contribute to embryonic terminal cell development. One pathway

controls organization and outgrowth of branches and requires Blistered, whereas the other, Blistered-independent, pathway is sufficient for processes required to differentiate a terminal cell, but lacks the necessary organizational cues for proper development (Gervais and Casanova, 2011).

It will be important to determine the specific molecular machinery that is required for embryonic terminal cell development. However, the development of terminal cell structures during embryonic stages is minor in comparison to the dramatic morphological changes that occur during larval stages. Unlike other types of tracheal cells, terminal cell morphology is highly dependent upon oxygen requirement in target tissues. Just after hatching terminal cells are induced to branch and undergo outgrowth in response to the chemoattractive signal, Branchless, which is secreted by hypoxic tissue (Lee et al., 1996; Sutherland et al., 1996). This process continues throughout larval stages, with iterative rounds of specification and outgrowth until the oxygen demands of the tissue have been met. This process results in a dynamic and highly variable branching pattern between individual cells that is representative of the oxygen requirement of the target tissues (Ghabrial et al., 2003). Interestingly, the general shape of an individual terminal cell is conserved within repeating body segments and between animals, but differs only in the exact positioning of individual branches. A mature terminal cell will show an average of thirty-two subcellular branches per cell. These branches extend in different directions, never crossing over, away from the cell body and towards target tissues (Figure 1.1D). Terminal cells undergo the same three previously mentioned morphological processes that contribute to a branched morphology; cell growth, branch specification, and branch outgrowth. Cell growth is a general process required for making a cell larger in all

directions, which likely occurs in all cell types as a growth mechanism. Branch specification, however, is a much more specialized process that requires polarization and regionalization of a cell. Finally, branch outgrowth requires addition of membrane to a specific site on the plasma membrane. The general cell growth machinery could control this process, or specialized protein complexes that facilitate concentrated growth may be required. Together these three cellular processes result in a highly branched cellular morphology.

Using both forward and reverse genetic approaches, I have begun to elucidate some of the genetic and molecular components required for terminal cell branching morphology. Chapter 2 of this dissertation describes the identification and characterization of genes required for terminal cell branching morphogenesis. Chapter 3 focuses on the mechanisms of polarized membrane addition and vesicle trafficking events required for terminal cell branch outgrowth. Chapter 4 discusses the consequences of misregulating polarity proteins with respect to terminal cell branching morphology. This identification and characterization of the machinery required for the cellular processes, of branching and outgrowth has provided valuable information about terminal cell development and general mechanisms used to elaborate a branched cell.

Tracheal system lumen formation

In addition to establishing the highly branched network of interconnected cells, the tracheal system must also form cellular tubes through which gas will flow (Figure 1.1C). The dorsal trunks (DTs), are made up of a polarized epithelial sheet that appears to have folded upon itself until the edges met. This results in a multicellular tube with

many cell-cell junctions, an apical domain adjacent to the lumen, and a basal domain facing the inside of the animal (Samakovlis et al., 1996). Secondary branches also undergo tube formation, giving rise to unicellular tubes (Figure 1.1C), which occurs by a process termed budding. In this case, individual cells migrate out from a polarized epithelial sheet and elongate along their long axis, again with an apical domain adjacent to the lumen, and a basal domain facing the inside of the animal (Samakovlis et al., 1996). In contrast to multi- and unicellular tubes, which undergo lumen formation during embryogenesis, terminal cells generate a subcellular tube only after establishing the branched network of cellular projections during larval stages. Terminal cell lumens are characterized by the absence of cell-cell junctions and are thought to develop through a process called cell hollowing (Figure 1.1C). This process requires multiple steps, including cellular regionalization (polarization, defining the region for lumen assembly), membrane accumulation (organization, trafficking and assembly of membrane), and lumen clearing or maturation (Ghabrial and Krasnow, 2006; Jarecki et al., 1999).

In addition to the *de novo* generation of a subcellular lumen, tracheal tubes must also generate a protective cuticle that lines the lumen to prevent dehydration, infection, and provide mechanical support (Moussian, 2010; Payre, 2004). This protective cuticle is continuous with the entire tracheal system and the larval cuticle that covers the exterior of the animal. The cuticle is made up of three distinct layers; the envelope, the epicuticle and the procuticle (Figure 1.1C, see insert). The envelope is composed of proteins and lipids that provide a waterproof protective layer. The epicuticle, which is located directly under the envelope, is composed of cross-linked proteins, which confer stiffness and provide structure. Finally, the procuticle, which lies adjacent to the surface of the apical

membrane, consists of the polysaccharide chitin, and is responsible for the flexibility of the cuticle (Moussian, 2010). Together these three layers comprise a mature cuticle, which is critical for gas filling of the tracheal system.

Recently, genetic analysis has revealed several mechanisms involved in subcellular lumen formation. For example, a conserved protein, *Zinc finger protein 1 (Zpr1)* was shown to be required for subcellular lumen maturation (Ruiz et al., 2012). Terminal cells homozygous for *Zpr1* show no gas-filled lumens by brightfield microscopy, and ultrastructural analysis reveals the defects appear to be in the development or maturation of the cuticle lining the lumen. Zpr1 binds the cytoplasmic tail of inactivated EGF receptors and is thought to participate in mediating a short range EGF signal required for lumen formation in terminal cells (Ruiz et al., 2012). However, Zpr1 may also participate in cross talk with the FGF receptor, Breathless, which is also required for lumen formation. Additionally, Enabled, expressed downstream of Blistered, promotes asymmetric actin accumulation in terminal cells, which results in microtubule organization and establishment of apical/basal domains that eventually drive cell elongation and lumen formation (Gervais and Casanova, 2010). In support of this model, other groups have shown the dynein motor complex transports vesicles required for subcellular lumen formation towards the minus-end of acetylated microtubules, found near branch tips (Schottenfeld-Roames and Ghabrial, 2012). These vesicles presumably localize to branch tips by the action of a Rab GTP binding protein, Rab35 and its specific Rab-GAP, Whacked. Loss of either of these proteins results in aberrant lumen formation around the cell nucleus (Schottenfeld-Roames and Ghabrial, 2012), suggesting Rab35 and Wkd participate in a localization step, but not lumen formation *per se*.

Despite this growing body of knowledge, subcellular lumen formation remains poorly understood. Chapter 2 of this dissertation describes work investigating the role of common polarity proteins in the development of a subcellular lumen in terminal cells. Finally, Chapter 4 investigates the molecular machinery required for distinct phases of subcellular lumen formation, maturation, and gas filling.

Summary

Terminal cell development embodies a number of important biological questions. How are growth signals propagated resulting in distinct cellular architectures? How are branch sites specified? How does localized receptor activation result in branch specification and eventually outgrowth? Where is the membrane required for branch growth and lumen formation generated? How is the molecular machinery necessary for branch outgrowth properly positioned within cells? How does a cell coordinate branch development and lumen formation? Work presented in this dissertation addresses three main questions about terminal cell development. Chapter 2 describes my work identifying genes required for terminal cell polarization and branching. Chapter 3 describes my work defining the cellular trafficking events required for branch outgrowth. Finally, Chapter 2 and Chapter 4 investigate mechanisms of subcellular lumen formation in terminal cells.

Figure 1.1 *Drosophila* larval tracheal system morphology. (A and B) Dorsal view of L3 larva. Branches are visualized by expressing GFP using the *breathless* promoter (A) and the air-filled lumens are visualized with brightfield microscopy (B). Insert in A indicates the dorsal trunk (1^{o}) with an arrow and a unicellular branch (2^{o}) with an arrowhead. (C) Diagram of tracheal tube morphologies. Insert shows the structure of the cuticle. (D and E) Morphology of a terminal cell from a L3 wandering larva. The homozygous mutant cell is labeled with GFP (D) to visualize the branching pattern and brightfield microscopy (E) shows the air-filled lumen within each branch. (F) Diagram of two body segments in an L3 larva. The location of terminal cells is designate by the small circles. A single body segment is highlighted in grey to show the repetitive pattern of terminal cell locations. Dorsal trunk (DT), lateral group (LG) terminal cells, fat body (FB) terminal cells. Dashed white lines indicate the proximal end of the terminal cells and red arrowheads show the air-filled lumen in D and E.

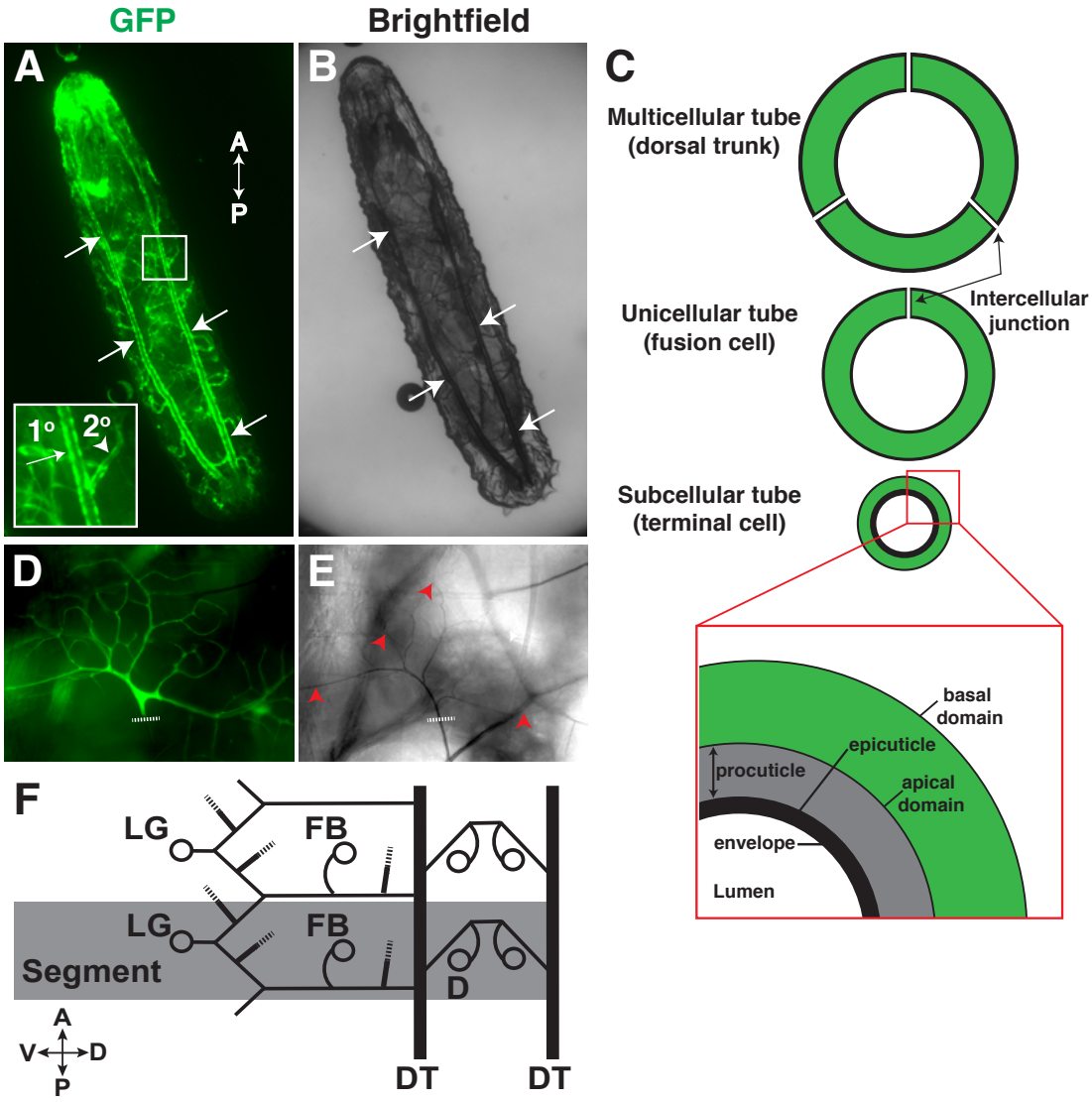
GFP
Brightfield
A
B
C
D
E
F
A
P
1°
2°
Multicellular tube
(dorsal trunk)
Unicellular tube
(fusion cell)
Intercellular
junction
Subcellular tube
(terminal cell)
basal
domain
epicuticle
procuticle
apical
domain
envelope
Lumen
LG
FB
LG
FB
Segment
D
A
V
D
P
DT
DT

References

Babbey, C.M., Bacallao, R.L., and Dunn, K.W. (2010). Rab10 associates with primary cilia and the exocyst complex in renal epithelial cells. Am. J. Physiol. Renal Physiol. *299*, F495–F506.

Cardoso, W.V., and Lü, J. (2006). Regulation of early lung morphogenesis: questions, facts and controversies. Development *133*, 1611–1624.

Das, A., and Guo, W. (2011). Rabs and the exocyst in ciliogenesis, tubulogenesis and beyond. Trends in Cell Biology *21*, 383–386.

Gervais, L., and Casanova, J. (2010). In vivo coupling of cell elongation and lumen formation in a single cell. Current Biology *20*, 359–366.

Gervais, L., and Casanova, J. (2011). The *Drosophila* homologue of SRF acts as a boosting mechanism to sustain FGF-induced terminal branching in the tracheal system. Development *138*, 1269–1274.

Ghabrial, A.S., and Krasnow, M.A. (2006). Social interactions among epithelial cells during tracheal branching morphogenesis. Nature *441*, 746–749.

Ghabrial, A.S., Luschnig, S., Metzstein, M.M., and Krasnow, M.A. (2003). Branching morphogenesis of the *Drosophila* tracheal system. Annu. Rev. Cell Dev. Biol. *19*, 623–647.

Guillemin, K., Groppe, J., Ducker, K., Treisman, R., Hafen, E., Affolter, M., and Krasnow, M.A. (1996). The pruned gene encodes the *Drosophila* serum response factor and regulates cytoplasmic outgrowth during terminal branching of the tracheal system. Development *122*, 1353–1362.

Jarecki, J., Johnson, E., and Krasnow, M.A. (1999). Oxygen regulation of airway branching in *Drosophila* is mediated by branchless FGF. Cell *99*, 211–220.

Lalli, G. (2009). RalA and the exocyst complex influence neuronal polarity through PAR-3 and aPKC. Journal of Cell Science *122*, 1499–1506.

Lee, T., Hacohen, N., Krasnow, M., and Montell, D.J. (1996). Regulated breathless receptor tyrosine kinase activity required to pattern cell migration and branching in the *Drosophila* tracheal system. Genes & Development *10*, 2912–2921.

Lizama, C.O., and Zovein, A.C. (2013). Polarizing pathways: balancing endothelial polarity, permeability, and lumen formation. Exp. Cell Res. *319*, 1247–1254.

Llimargas, M. (1999). The Notch pathway helps to pattern the tips of the *Drosophila* tracheal branches by selecting cell fates. Development *126*, 2355–2364.

Moussian, B. (2010). Recent advances in understanding mechanisms of insect cuticle differentiation. Insect Biochem. Mol. Biol. *40*, 363–375.

Murthy, M., Garza, D., Scheller, R.H., and Schwarz, T.L. (2003). Mutations in the exocyst component Sec5 disrupt neuronal membrane traffic, but neurotransmitter release persists. Neuron *37*, 433–447.

Ochoa-Espinosa, A., and Affolter, M. (2012). Branching morphogenesis: From cells to organs and back. (Cold Spring Harb Perspect Biol) *4*.

Payre, F. (2004). Genetic control of epidermis differentiation in *Drosophila*. Int. J. Dev. Biol. *48*, 207–215.

Ruiz, O.E., Nikolova, L.S., and Metzstein, M.M. (2012). *Drosophila* Zpr1 (Zinc Finger Protein 1) is required downstream of both EGFR and FGFR signaling in tracheal subcellular lumen formation. PLoS ONE *7*, e45649.

Samakovlis, C., Hacohen, N., and Manning, G. (1996). Development of the *Drosophila* tracheal system occurs by a series of morphologically distinct but genetically coupled branching events. Development *122*, 1395–1407.

Sans, N., Prybylowski, K., Petralia, R.S., Chang, K., Wang, Y.-X., Racca, C., Vicini, S., and Wenthold, R.J. (2003). NMDA receptor trafficking through an interaction between PDZ proteins and the exocyst complex. Nat Cell Biol *5*, 520–530.

Schottenfeld-Roames, J., and Ghabrial, A.S. (2012). Whacked and Rab35 polarize dynein-motor-complex-dependent seamless tube growth. Nature *14*, 386–393.

Sutherland, D., Samakovlis, C., and Krasnow, M.A. (1996). branchless encodes a *Drosophila* FGF homolog that controls tracheal cell migration and the pattern of branching. Cell *87*, 1091–1101.

CHAPTER 2

A NOVEL FUNCTION FOR THE PAR COMPLEX IN SUBCELLULAR MORPHOGENESIS OF TRACHEAL TERMINAL CELLS IN *DROSOPHILA MELANOGASTER*

Reprint of: Jones and Metzstein (2011) A Novel Function for the PAR Complex in Subcellular Morphogenesis of Tracheal Terminal Cells in *Drosophila Melanogaster*. *Genetics* 189, 1.

INVESTIGATION

A Novel Function for the PAR Complex in Subcellular Morphogenesis of Tracheal Terminal Cells in *Drosophila melanogaster*

Tiffani A. Jones and Mark M. Metzstein[1]
Department of Human Genetics, University of Utah, Salt Lake City, Utah 84112

ABSTRACT The processes that generate cellular morphology are not well understood. To investigate this problem, we use *Drosophila melanogaster* tracheal terminal cells, which undergo two distinct morphogenetic processes: subcellular branching morphogenesis and subcellular apical lumen formation. Here we show these processes are regulated by components of the PAR-polarity complex. This complex, composed of the proteins Par-6, Bazooka (Par-3), aPKC, and Cdc42, is best known for roles in asymmetric cell division and apical/basal polarity. We find Par-6, Bazooka, and aPKC, as well as known interactions between them, are required for subcellular branch initiation, but not for branch outgrowth. By analysis of single and double mutants, and isolation of two novel alleles of Par-6, one of which specifically truncates the Par-6 PDZ domain, we conclude that dynamic interactions between apical PAR-complex members control the branching pattern of terminal cells. These data suggest that canonical apical PAR-complex activity is required for subcellular branching morphogenesis. In addition, we find the PAR proteins are downstream of the FGF pathway that controls terminal cell branching. In contrast, we find that while Par-6 and aPKC are both required for subcellular lumen formation, neither Bazooka nor a direct interaction between Par-6 and aPKC is needed for this process. Thus a novel, noncanonical role for the polarity proteins Par-6 and aPKC is used in formation of this subcellular apical compartment. Our results demonstrate that proteins from the PAR complex can be deployed independently within a single cell to control two different morphogenetic processes.

FOR most cell types, morphology is key to cell function. A dramatic example of this association is seen in cells that undergo subcellular branching morphogenesis. In this process, cells send out extensions from their plasma membranes, which grow and undergo bifurcation events to form complex, branched networks. Examples of subcellular branching morphogenesis are seen in glial oligodendrocytes (Bauer *et al.* 2009) and in dendritic cells of the mammalian immune system (Makala and Nagasawa 2002), but by far the best studied examples of this process are in neurons (reviewed by Gibson and Ma 2011; Jan and Jan 2010). Indeed, neurons are frequently categorized entirely by differences in their branching morphologies (see Puelles 2009). However, despite the importance of subcellular branching morphogenesis, little is known about the molecular mechanisms that organize distinctive subcellular branching patterns.

We are studying the process of subcellular branching morphogenesis in *Drosophila* tracheal terminal cells, a component of the insect respiratory system. Terminal cells reside at the ends of a network of cellular tubes that functions in delivering air to internal tissues (Guillemin *et al.* 1996). The cells are specified during embryogenesis, primarily through a process of competitive FGF signaling and lateral inhibition among tracheal precursors (Llimargas 1999; Ghabrial and Krasnow 2006). At hatching, terminal cells occupy stereotypical positions within the larvae and have a simple morphology, typically consisting of a cell body, connected at its base to the rest of the tracheal system, with a single, subcellular cytoplasmic projection. During larval development, terminal cells undergo considerable growth and branching, such that in late larvae, the cells have an elaborate morphology composed of a branched network of cytoplasmic extensions (Figure 1A). Growth and branching are primarily under the control of the Branchless protein, an FGF growth factor, which is secreted by oxygen-starved target tissues

doi: 10.1534/genetics.111.130351
Manuscript received May 4, 2011; accepted for publication June 23, 2011
Supporting information is available online at http://www.genetics.org/cgi/content/full/genetics.111.130351/DC1.
[1]Corresponding author: Eccles Institute of Human Genetics, 15 N. 2030 E., Salt Lake City, UT 84112. E-mail: markm@genetics.utah.edu

(Jarecki *et al.* 1999). The mechanisms for outgrowth are not well understood, though likely involve cytoskeletal components, including actin (Levi *et al.* 2006; Gervais and Casanova 2010); how branch sites are selected is currently unknown.

In addition to the process of cytoplasmic extension and branching, each subcellular projection forms an internal membrane-lined tube. The mechanism for tube formation is not well understood, but may involve vesicle trafficking to the center of the cell followed by vesicle fusion (Jarecki *et al.* 1999). The mature terminal cell lumen is lined by an apical membrane, which is continuous with the apical domains of other tubes of the tracheal system, but is distinguished from these other apical domains in that it forms without cellular junctions (Noirot-Timothee and Noirot 1982), typically found in polarized epithelia (Plaza *et al.* 2010).

Terminal cell development epitomizes a number of important questions in cell biology. How does local receptor activation regulate directional cell growth and migration? How are subcellular domains specified and organized? How are branch points patterned and molecularly defined? A common player in the regulation of subcellular organization is the evolutionarily conserved PAR-polarity complex (referred to here as the PAR complex), consisting of the scaffolding proteins Par-6 and Bazooka (Baz, the *Drosophila* homolog of Par-3), atypical protein kinase C (aPKC), and the small GTP-binding protein Cdc42 (reviewed by Suzuki and Ohno 2006; Goldstein and Macara 2007). In many contexts, these proteins function together (Welchman *et al.* 2007) to effect biological roles such as asymmetric cell division (*e.g.*, Kemphues *et al.* 1988; Prehoda 2009) and establishment and maintenance of apical/basal polarity in epithelial cells (reviewed by Martin-Belmonte and Mostov 2008). However, a role for the PAR complex in subcellular branching morphogenesis or subcellular lumenogenesis has not been directly assayed.

Here, we show that PAR-complex proteins are required for both subcellular branching morphogenesis and subcellular lumen formation in tracheal terminal cells. We find that all members of the complex, as well as known physical interactions among them, are required for subcellular branching, indicating that canonical complex activity contributes to this process. The defects we observe in branching suggest that interactions between PAR-complex proteins may regulate an iterative process that generates branch patterns in terminal cells. Surprisingly, although the PAR complex is well known to be required for apical/basal polarity in other epithelial cell types, we find that only a subset of the complex members is needed for subcellular lumen formation in terminal cells. Furthermore, the proteins that are required may be acting independently in this process. Therefore, we have identified both a novel role for the PAR complex in the control of subcellular branching morphogenesis and a novel mechanisms by which PAR-complex proteins participate in forming an apical domain.

Materials and Methods

Fly stocks and genetics

Flies were reared on standard cornmeal/dextrose media and larvae to be scored were raised at 25°. The control chromosomes used in experiments were *y w FRT^{19A}* (Xu and Rubin 1993) or *FRT^{G13}* (Chou and Perrimon 1992), unless otherwise stated. Alleles analyzed were *baz^{EH171}* (Eberl and Hilliker 1988), *baz^{FA50}* [(Simoes *et al.* 2010) a gift from T. Schüpbach (Princeton University, Princeton, New Jersey) via J. Zallen (Sloan-Kettering Institute, New York, New York)], *par-6$^{\Delta 226}$* (Petronczki and Knoblich 2001), *par-6^{f05334}* (Bellen *et al.* 2004), *par-6^{29VV}* and *par-6^{15N}* (this work), *aPKC^{k06403}* (Wodarz *et al.* 2000), *aPKC^{psu69}* and *aPKC^{psu265}* (Kim *et al.* 2009), and *Cdc42^{4}* (Fehon *et al.* 1997). For construction of the *baz par-6* double-mutant chromosome, see Supporting Information, File S1. For mosaic analysis we used the tracheal specific *breathless* (*btl*) promoter (Shiga *et al.* 1996) in the stocks *y w P{w$^+$, btl-Gal80} FRT^{19A}, hsFLP^{122}*; *btl-Gal4 UAS-GFP* (M. M. Metzstein, unpublished data) and *y w hsFLP^{122}*; *FRT^{G13} P{w$^+$, tub-Gal80}*; *btl-Gal4 UAS-GFP* [gift from S. Luschnig (University of Zurich, Zurich, Switzerland)]. The *par-6* genomic rescue transgene has been described previously (Petronczki and Knoblich 2001). To perform mosaic analysis, *par-6$^{\Delta 226}$*, *baz^{EH171}*, and *Cdc42^{4}* were recombined onto *FRT^{19A}* and *aPKC^{k06403}* was recombined onto *FRT^{G13}* using standard methods. *UAS-baz* RNAi lines (5055R-1 and 5055R-2) were obtained from National Institute of Genetics Fly Stock Center, Japan (NIG-Fly) and *UAS-par-6* RNAi lines (108560 and 19730) were obtained from the Vienna *Drosophila* RNAi Center (Dietzl *et al.* 2007). Homozygous mutant cells were generated using the mosaic analysis with a repressible cell marker (MARCM) technique (Lee and Luo 1999). We also used this technique to express λBtl, using UAS-λBtl (Lee *et al.* 1996), in GFP-marked terminal cells that were simultaneously mutant or wild type for PAR-polarity genes. To generate the mosaics, 0- to 6-hr embryos were collected in fly food vials at 25° and treated to a 45-min heat shock at 38° in a circulating water bath before being returned to 25° for development. For light microscopy, tracheal terminal cells were scored at wandering third instar.

Tracheal terminal cell screen

par-6^{29VV} and *par-6^{15N}* were isolated in a mosaic screen for mutations affecting terminal cell development, the details of which are to be published elsewhere (M. M. Metzstein and M. A. Krasnow, unpublished results). Briefly, mutations were induced on a *y w FRT^{19A}* chromosome using 25 mM EMS (Lewis and Bacher 1968). We made MARCM mosaics in ~900 lines carrying X-linked lethal mutations and scored for defects in terminal cells, using GFP expression to assess branching and brightfield microscopy to assess lumen formation. The lethality associated with *par-6^{29VV}* was mapped with respect to visible X-linked markers using standard methods. For basic characterization of *par-6^{15N}* obtained from this screen see File S1 and Table S1.

Immunofluorescence analysis

Wandering third instar larvae were dissected in 1× PBS to make fillets exposing the tracheal system. Fillets were fixed for 30 min in 4% paraformaldehyde in 1× PBS, rinsed three times for 15 min in 1× PBST (1× PBS + 0.1% TX100), blocked for 30 min at room temperature in PBSTB (1× PBST + 0.02% BSA), and then incubated with primary antibody overnight at 4°. Fillets were then rinsed three times for 15 min in 1× PBSTB and incubated with secondary antibody for 2 hr at room temperature. Fillets were then rinsed and mounted on glass slides in ProLong Gold antifade reagent (Invitrogen, Carlsbad, CA). Antibodies were used in the following concentrations: guinea pig anti-Baz, 1:500 (Wodarz *et al.* 2000); rabbit anti-Par-6, 1:500 (Petronczki and Knoblich 2001); goat anti-aPKC, 1:200 (Santa Cruz Biotechnology; sc-15727); and mouse anti-GFP, 1:1000 (Clontech; 632375). Secondary antibodies, conjugated to Alexa-488 or Alexa-568 (Molecular Probes, Eugene, OR), were used at 1:1000. Images were taken on a Zeiss (Carl Zeiss, Thornwood, NY) AxioImager M1 equipped with an AxioCam MRm.

Terminal cell branching and lumen quantification

For determination of the number of terminal cell branches and lumens in homozygous wild-type and mutant terminal cells, we collected fluorescent and brightfield images of lateral group branches [LF, LG, and LH terminal cells (Ruhle 1932)] in mosaic animals. Terminal cell branches and lumens from these images were traced manually using NeuronJ (Meijering *et al.* 2004). Branch order was assigned on the basis of the following criteria: each tracheal terminal cell has a single central branch that contains the cell body, class I terminal branches arise directly from the central branch, and class II terminal branches arise directly from class I branches. We extended this scheme for further orders of branches, if present. Lumens were quantified as a ratio of total lumen length to total branch length, and different orders of lumens were not separated. For statistical comparisons we used the two-tailed Mann–Whitney *U*-test (http://elegans.swmed.edu/~leon/stats/utest.cgi).

Results

par-6 is required for branching and lumenogenesis in Drosophila tracheal terminal cells

In a genetic mosaic screen, we identified a lethal mutation, designated *29VV*, that showed distinct branching defects in *Drosophila* tracheal terminal cells. Wild-type cells possess a single central branch containing the cell nucleus and a set of side branches (class I branches) sprouting from the central branch (Figure 1A). In wild-type cells, class I branches bifurcate to produce class II, class III, and so forth, branches (Figure 1, A and A′′). Homozygous *29VV* cells have normal class I branching, but subsequent branching is much reduced, so that cells contain many fewer higher-order branches (Figure 1, B and B′′, quantitated in Figure 2A). In addition, wild-type cells contain a gas-filled lumen running through each branch (Figure 1A′), but *29VV* homozygous cells lack gas-filled lumens (Figure 1B′, quantitated in Figure 2B), apart from a region at the proximal end of the cell near the nucleus. At this level of analysis, we cannot distinguish whether mutant cells generate a lumen that does not subsequently gas fill or whether no lumen is generated at all. Finally, in contrast to wild-type cells where branches continually reduce in diameter, leading to smooth, tapered branch tips (Figure 1D), *29VV* terminal cell tips often appear bulbous (Figure 1E). The morphology of these abnormal tip structures is quite variable; some appear to contain internal membranous structures, while others appear to be simple accumulations of cytoplasm (Figure 1E).

We mapped the lethality associated with *29VV* to a region ~2 map units to the right of the gene *forked*. This region contained a candidate for causing the observed tracheal cell defects: the PAR-complex gene *par-6*. We sequenced the coding region for *par-6* in *29VV* and found a single, non-conservative change altering the initiation codon (ATG → ATA, Figure S1A), suggesting that *29VV* leads to a severe loss or complete absence of *par-6* function. Consistent with this, we found that *29VV* fails to complement the *par-6* alleles Δ*226* (Petronczki and Knoblich 2001) and *f05534* (Bellen *et al.* 2004) for lethality. Furthermore, a genomic construct containing wild-type *par-6* (Petronczki and Knoblich 2001) rescued the lethality associated with *29VV* (data not shown). Importantly, all observed defects (branching, lumen formation, and tip abnormalities) in *29VV* terminal cells were rescued by the *par-6*$^{+}$ genomic construct (Figure S2, A and B) or by trachea-specific expression of a *par-6* cDNA (Doerflinger *et al.* 2010) under the control of the GAL4/UAS system (data not shown).

To compare the *par-6*^{29VV} terminal cell phenotype to a known null allele of *par-6*, we generated *par-6*$^{\Delta 226}$ mosaics. Δ*226* is an N-terminal deletion of *par-6* that lacks detectable Par-6 protein expression (Petronczki and Knoblich 2001). We found *par-6*$^{\Delta 226}$ mutant terminal cells had defects similar to *par-6*^{29VV} in branching (Figure 1C), lumen formation (Figure 1C′), and branch tip morphology (Figure 1F). The extent of these defects was quantitatively similar between *29VV* and Δ*226* cells in branching (Figure 2A, $P > 0.7$) and lumen formation (Figure 2B, $P = 0.029$). *par-6* is known to be required for proper development of the embryonic cuticle (Petronczki and Knoblich 2001), and cuticular phenotypes of *par-6*$^{\Delta 226}$ and *par-6*^{29VV} were identical, either as zygotic mutants or in germline clones (data not shown). From these data, we conclude that *par-6*^{29VV} is a null allele and shows that Par-6 is required for diverse aspects of tracheal terminal cell morphology.

The canonical PAR complex is required for terminal cell branching but not all components are required for lumen formation

Our results with *par-6* mutants led us to test whether other PAR-complex members also function in tracheal terminal

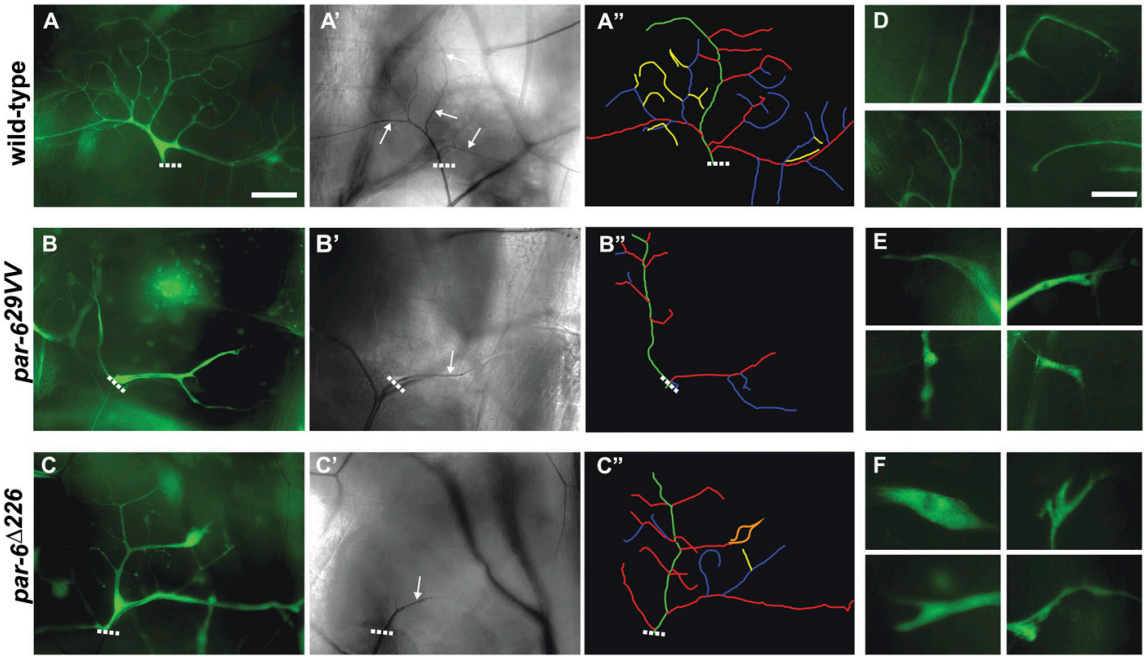

Figure 1 *par-6* is required for subcellular branching and lumen formation. Mosaic L3 larvae were generated using the MARCM system, such that only homozygous tracheal cells express GFP under the control of the tracheal-specific *breathless* promoter. Expression of GFP was used to identify homozygous cells and characterize the cellular branching pattern (A–C) and branch tips (D–F). The gas-filled intracellular lumen was examined using brightfield microscopy (A′–C′). Wild-type terminal cells have extensive outgrowth and subcellular branching (A), a single gas-filled lumen within each branch (A′), and normal tapered tip morphology (D). Terminal cells homozygous for *par-6*^{29VV} or *par-6*$^{\Delta 226}$ have branching defects (B and C), very little gas-filled lumen (B′ and C′), and abnormal tip morphology (E and F). Note that in B′ and C′ other non GFP-labeled (thus wild-type) terminal cells in the fields of view have normal, darkly contrasting, gas-filled lumens. (A′′–C′′) Tracing of the branching pattern observed in A–C. Branch hierarchy is indicated by color: green, central branch; red, class I terminal branches; blue, class II terminal branches; yellow, class III terminal branches; orange, tip abnormality. Dashed white lines demark the proximal end of GFP-labeled cells; arrows highlight gas-filled lumens. Bars: A–C, 75 μm; D–F, 25 μm.

cell development. First, we made mosaics of the *aPKC* null allele *k06403* (Wodarz *et al.* 2000; Rolls *et al.* 2003). We found that *aPKC*^{k06403} mutant terminal cells have branching (Figure 3A), lumenogenesis (Figure 3A′), and tip morphogenesis defects (Figure 3B) similar to *par-6* null alleles. Also, like *par-6*, loss of *aPKC* primarily affects class II and later-order branches (Figure 2A).

Mosaics of the null *baz* alleles *FA50* (Simoes *et al.* 2010) and *EH171* (Eberl and Hilliker 1988; Cox *et al.* 2001) display a similar branching defect to *par-6*, both qualitatively

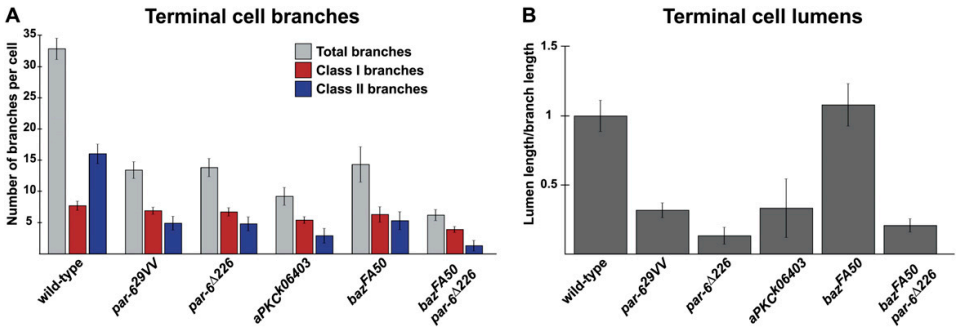

Figure 2 Quantification of terminal cell defects. (A) Quantification of mutant terminal cell branches, using tracings as shown in Figure 1. Gray bars, total number of branches per terminal cell; red bars, number of class I branches per cell; and blue bars, number of class II branches per cell. (B) Quantification of gas-filled lumens for terminal cells mutant for the indicated polarity gene calculated as a ratio of gas-filled lumen length to total branch length and normalized to wild-type cells. Error bars represent ±2 SEM (n = 10).

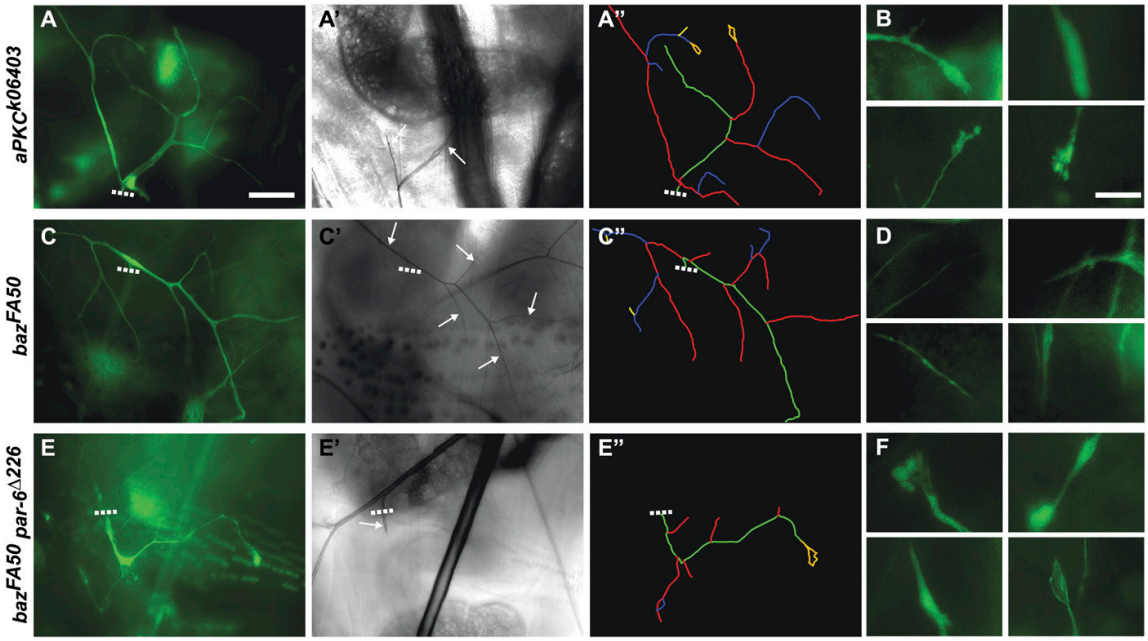

Figure 3 The PAR complex is required for subcellular branching, but not all components are required for lumen formation. As in Figure 1, homozygous terminal cell branches and tips were visualized by GFP expression in mosaic L3 larvae (A–F) and gas-filled lumens visualized by brightfield microscopy (A′, C′, and E′). Terminal cells homozygous for *aPKC*^{k06430} have branching defects (A), no gas-filled lumen (A′), and abnormal tip morphology (B). Terminal cells homozygous for *baz*^{FA50} have branching defects (C), but do contain gas-filled lumens (C′) and have normal tip morphologies (D). Terminal cells homozygous for *baz*^{FA50} *par-6*$^{\Delta 226}$ have branching defects (E), no gas-filled lumen (E′), and abnormal tip morphologies (F). (A′′, C′′, and E′′) Tracing of the branching pattern observed in A, C, and E. Branch hierarchy colors and other labels are as in Figure 1. Bars: A, C, and E, 75 μm; B, D, and F, 25 μm.

and quantitatively (Figures 3C and 2A and data not shown; $P > 0.6$ for total branches). Surprisingly, terminal cells mutant for either allele of *baz* appeared to have normal gas-filled lumens (Figures 3C′ and 2B and data not shown). In addition, tip morphology in *baz* mutant cells was similar to that of wild type, with a smooth tapered appearance (Figure 3D).

Mosaics of the *Cdc42* allele, *Cdc42*^{4} (Fehon *et al.* 1997) had very strong branching (Figure S3A) and lumen formation (Figure S3A′) defects. However, the cells also had a number of other morphological abnormalities (Figure S3A), confounding our analysis of tracheal defects. We have not characterized the role of *Cdc42* in tracheal terminal cells further.

In summary, we found that all components of the PAR complex are required for normal tracheal terminal cell branching and that the branching defect observed in each of the mutants consists primarily of a failure in higher-order bifurcation events. However, not all the components are required for subcellular lumen formation.

par-6 and baz are partially redundant for branching in tracheal terminal cells

When we compared terminal cells mutant for various members of the PAR complex, we noted a difference among them in the severity of branching defects. In particular, terminal cells mutant for the *aPKC* null allele had a significantly more severe branching defect than either *par-6* or *baz* null mutants (Figure 2A, $P < 0.01$). One interpretation of this result is that *baz* and *par-6* are partially redundant in regulating *aPKC*. To test this, we examined *baz par-6* double-mutant cells and found that they had severe branching defects (Figure 3E), quantitatively more similar to those observed in the *aPKC* null single mutant than in either *par-6* or *baz* single mutants (Figure 2A). These data are consistent with the idea that *par-6* and *baz* are partially redundant in terminal cell branching morphogenesis.

PAR-polarity proteins show distinct localization in tracheal terminal cells

We used immunocytochemistry to determine the localization of PAR-complex proteins within tracheal terminal cells in late L3 larvae (Figure 4). In all cases, no specific staining was observed in cells mutant for the corresponding gene, demonstrating the specificity of the antibodies used (Figure S4).

We found that in wild-type terminal cells, Par-6 protein is enriched adjacent to the intracellular lumen, with little staining observed in the rest of the cytoplasm (Figure 4A). The apical localization of Par-6 is lost in *baz* mutant cells, and instead staining is found throughout the cytoplasm (Figure

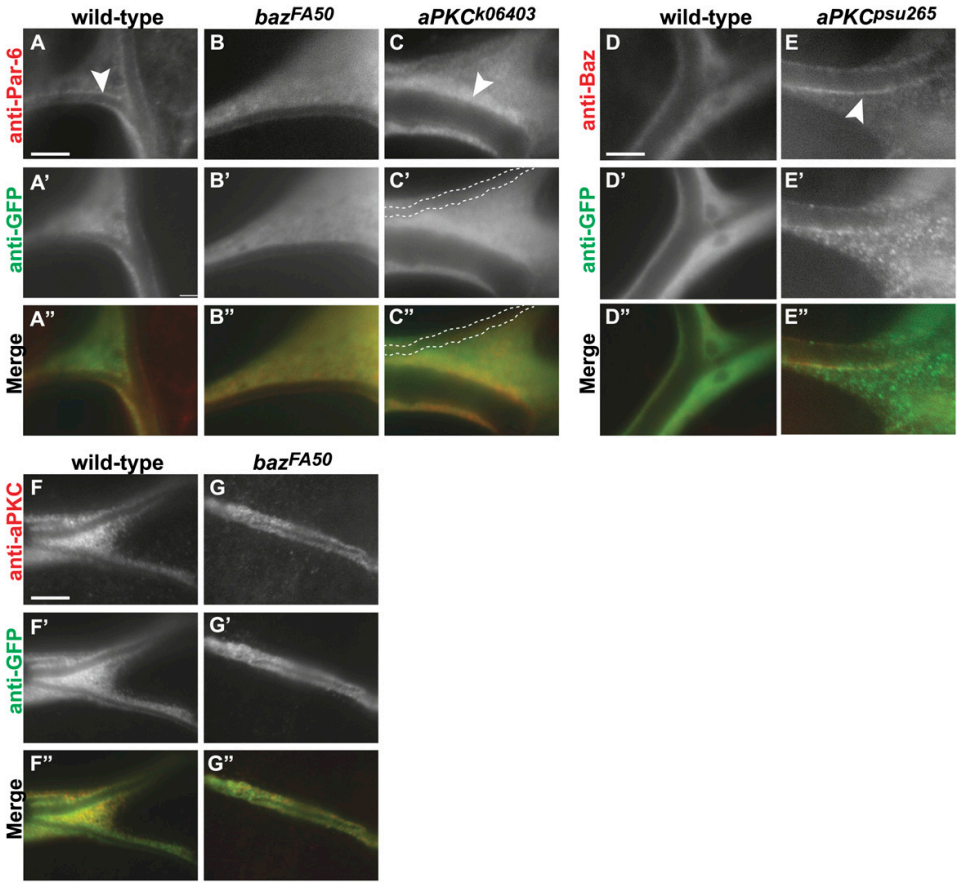

Figure 4 Localization of PAR-complex proteins in wild-type and mutant terminal cells. Individual homozygous terminal cells in L3 larvae were visualized with cytoplasmic GFP (A′–G′; green channel in A′′–G′′) and stained for the indicated protein (A–G; red channel in A′′–G′′). In wild-type cells, Par-6 is enriched at the lumen (A, arrowhead), distinct from the cytoplasmic GFP (A′′). In *baz*^{FA50} homozygous mutant cells, Par-6 loses luminal enrichment and is instead found throughout the cytoplasm (B), as seen by colocalization with GFP (B′′). *aPKC*^{k06430} homozygous mutant cells have patches of gas-filled lumen proximal to the cell body. In these regions, Par-6 is enriched around the lumen (C, arrowhead), but its domain is expanded compared to wild-type cells. Some regions in *aPKC*^{k06430} mutant cells contain reduced GFP expression, possibly indicative of a non-gas–filled lumen (outlined with dashed white lines in C′ and C′′). Par-6 is not enriched around such lumens. In wild-type cells, Baz is cytoplasmically localized (D) and overlaps with cytoplasmic GFP (D′′). In *aPKC*^{psu265} cells, which lack aPKC kinase activity, Baz is found enriched around the lumen (E, arrowhead). In wild-type cells, aPKC shows punctate cytoplasmic and luminal localization (F). This localization remains the same in *baz*^{FA50} mutant cells (G). Bars: 2 μm.

4B). This result is consistent with multiple reports showing that Baz is at the top of a PAR-complex localization hierarchy (reviewed in Harris and Peifer 2005). *aPKC* mutant cells mostly lack a gas-filled lumen, having this structure only in the proximal part of the cell. In these cells, Par-6 is found localized around this residual lumen, but in a broader domain than is found in wild-type cells (Figure 4C).

Baz shows no enrichment around the lumen in terminal cells that we examined, but is instead localized entirely in the cytoplasm (Figure 4D). This lack of luminal localization (and thus non-colocalization with Par-6) was surprising given our result that Par-6 accumulation at the lumen is dependent on Baz. However, this result is consistent with reports that Par-6 and Baz do not colocalize perfectly in other mature epithelia (Harris and Peifer 2005; Morais-de-Sa *et al.* 2010). The final localization of Baz is thought to occur by a two-step process: first, apically localized Baz recruits Par-6/aPKC; second, aPKC phosphorylates Baz, causing its relocalization to subapical junctions (Nagai-Tamai *et al.* 2002; Morais-de-Sa *et al.* 2010). We wanted to know whether such a mechanism might be displacing Baz from mature subcellular lumens, and since terminal cell branches lack cellular junctions, Baz relocalizes to the cytoplasm. To test this idea, we examined terminal cells mutant for the kinase-dead *aPKC* allele, *psu265* (Kim *et al.* 2009). We found that *aPKC*^{psu265} mutant cells have branching defects similar to aPKC null mutant cells, but contain gas-filled lumens (data not shown). In these cells, we found that Baz was

now localized to the lumen (Figure 4E), suggesting that aPKC-dependent phosphorylation indeed relocalizes Baz from the luminal membrane to the cytoplasm. Our results also indicate that kinase activity of aPKC is required for branching, but not for lumen formation. Finally, in *par-6* or *aPKC* null mutants, which lack lumens, Baz is found in the cytoplasm (Figure S5, A and B). Therefore, apical localization of Par-6 and Baz appears to occur by mechanisms similar to those occurring in other epithelia.

aPKC shows enrichment to the lumen, but rather than having a continuous domain of localization, is present in distinct puncta (Figure 4F). aPKC is also found in dispersed puncta within the cytoplasm. Unlike Par-6, aPKC luminal localization is unaffected by loss of *baz* (Figure 4G). In *par-6* mutant cells, aPKC shows punctate staining around the residual lumen, but expression levels appear to be reduced (Figure S5C). Thus, each of the three proteins examined showed distinct localization behavior within terminal cells.

Finally, we noted neither enrichment nor depletion of any PAR-complex protein around branch sites. Thus we conclude that it is the localized *activity* of the polarity complex, for instance by regulated interaction with downstream effectors, that mediates branching. Alternatively, the polarity complex may function within the whole cell to control branching, independent of specific sites.

par-6 and aPKC function independently in lumen formation

We have shown that Par-6 and aPKC are both required for branching and lumen formation in terminal cells. These proteins are known to have a direct interaction mediated through their respective PB1 domains (Lin *et al.* 2000; Hirano *et al.* 2005). To test whether this interaction is required for branching and/or lumen formation, we examined an allele of *aPKC*, *psu69*, that contains a single point mutation located just outside the PB1 domain. This mutation completely abolishes the interaction between aPKC and Par-6 (Kim *et al.* 2009). We found that tracheal terminal cells mutant for $aPKC^{psu69}$ have branching defects (Figure 5A) similar to those observed in *par-6* or *baz* null mutants and significantly less severe than those observed in the *aPKC* null (compare Figures 3A and 5A, quantitated in Figure 5D, $P < 0.01$). Interestingly, we observed that $aPKC^{psu69}$ mutant terminal cells have a normal gas-filled lumen running through each branch (Figure 5A′), suggesting that the physical interaction between aPKC and Par-6 is not required for normal lumen formation. $aPKC^{psu69}$ mutant terminal cells also differed from *aPKC* null cells in that they show normal branch tip morphology (data not shown). Finally, we found the defects observed in $aPKC^{psu69}$ mutant cells are independent of *baz* (Figure S6).

A further line of evidence suggesting *par-6* and *aPKC* function independently in lumen formation comes from experiments in which we used RNAi to reduce the activity of *par-6*. When expressed in the tracheal system, an RNAi transgene directed against *par-6* resulted in branching defects similar to those in *par-6*-null mutants (Figure 5B, quantitated in Figure 5D). However, we observed only weak defects in lumen formation (Figure 5B′, quantitated in Figure 5E), suggesting the knockdown is only partial. When we performed this *par-6* knockdown in an $aPKC^{psu69}$ mutant background, we found no difference in branching defects (Figure 5, C and D), but the lumen formation defects were partially ameliorated (Figure 5, C′ and E, $P < 0.05$). An explanation for this is that Par-6 functions in two pools, and disruption of binding to aPKC releases Par-6 into the lumen formation pool (Figure 5F).

The PDZ domain of Par-6 is required for branching and lumen formation

In our screen, we identified a second *par-6* allele, designated *15N* (see *Materials and Methods*). DNA sequence analysis revealed *15N* contains a 592-bp deletion in the *par-6* gene. This mutation is predicted to truncate the Par-6 protein within its single, C-terminally located PDZ domain (Figure S1, A and B). Similar to null mutations in *par-6*, terminal cells homozygous for $par\text{-}6^{15N}$ have defects in branching (Figure 6A), lumen formation (Figure 6A′), and tip morphology (Figure 6B). However, unlike null mutations, *15N* would not be expected to completely eliminate expression of Par-6 protein. In particular, while the deletion removes the C-terminal coding regions of *par-6*, the 3′-UTR is mostly left intact, missing only the first 97 (of 1677) bases. On the basis of this, we would predict that *15N* would not cause transcript instability, and while the PDZ domain is disrupted, the PB1 and semi-CRIB domains, which are required for interactions with aPKC and Cdc42, respectively (Lin *et al.* 2000; Yamanaka *et al.* 2001; Li *et al.* 2010) are left intact (Figure S1A).

To test residual activity in $par\text{-}6^{15N}$ we examined the cuticle phenotype of *par-6* zygotic mutants. Embryos hemizygous for null alleles of *par-6* are known to contain large cuticular holes, indicative of epithelial polarity defects (Petronczki and Knoblich 2001). We observed this defect in the *par-6* null allele *Δ226* (Figure 6D) and our new allele *29VV* (data not shown). However, we found that $par\text{-}6^{15N}$ mutants do not show large cuticular holes (Figure 6E). *Trans*-heterozygotes between *15N* and null alleles of *par-6* show occasional small holes (Figure 6F), suggesting that *15N* is hypomorphic for the regulation of embryonic epithelial polarity.

In contrast to this relatively mild embryonic cuticular defect, $par\text{-}6^{15N}$ homozygous terminal cells were quantitatively more severe than null alleles of *par-6* (Figure 6, G and H, $P < 0.001$) and quantitatively similar to *aPKC* null alleles. Furthermore, while $par\text{-}6^{29VV}$ homozygous cells contain a small portion of gas-filled lumen proximal in the cell, $par\text{-}6^{15N}$ cells have almost no observable gas-filled lumen (Figure 6A′). $par\text{-}6^{15N}$ homozygous terminal cell-tip abnormalities are extensive and include large varicosities and membrane-filled cytoplasmic swellings (Figure 6B). It is

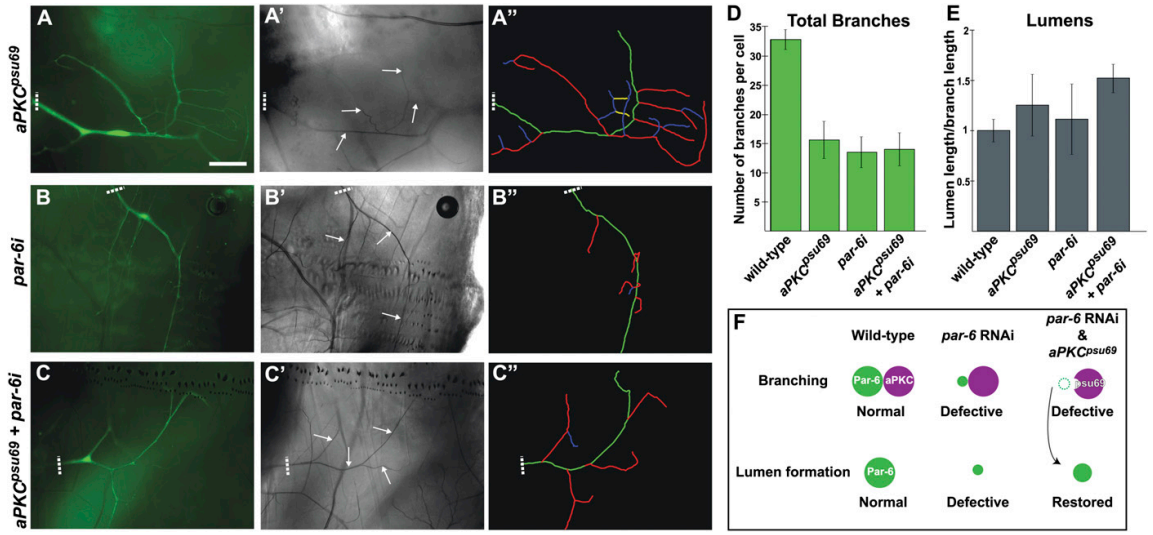

Figure 5 A direct interaction between Par-6 and aPKC is required for subcellular branching, but not for lumen formation. As in Figure 1, homozygous terminal cell branches were visualized by GFP expression in mosaic L3 larvae (A–C) and gas-filled lumens visualized by brightfield microscopy (A′–C′). Terminal cells homozygous for *aPKC^{psu69}* have branching defects similar to other polarity complex mutants (A), but have gas-filled lumens (A′). Expression of *UAS-par-6* RNAi leads to branching defects (B) similar to those seen in *par-6* null cells. These terminal cells also have lumen defects (B′), but these are not as severe as the defects observed in *par-6* null cells. Terminal cells homozygous for *aPKC^{psu69}* and also expressing the *par-6* RNAi show branching defects (C), but show more extensive gas-filled lumens than that seen in *aPKC^{+} par-6* RNAi cells (C′, compare to B′). (A′′–C′′) Tracing of the branching pattern observed in A–C. Quantitation of branching (D) and lumen formation (E) in cells was performed as in Figure 2. (F) Model for how *aPKC^{psu69}* ameliorates the lumen defects observed in *par-6* partial RNAi knockdown cells. In wild-type cells, Par-6 is present in two pools. One pool is complexed with aPKC and functions in branching, but not lumen formation. A second pool of Par-6 functions independently of aPKC and is required for lumen formation. In the *par-6* partial knockdown there are limited amounts of Par-6 available for both branching and lumen formation, and both processes are defective. In *aPKC^{psu69}* mutant cells, since aPKC and Par-6 can no longer interact, more of the limiting amount of Par-6 is now available for lumen formation, resulting in a weaker lumen formation defect. Bar: 75 μm. Branch hierarchy colors and other labels are as in Figure 1. Error bars represent ±2 SEM (n = 10 for *aPKC^{psu69}*; n = 5 for *par-6* RNAi and *aPKC^{psu69} par-6* RNAi).

important to note that *par-6$^{15N/+}$* heterozygotes have completely normal terminal cells, indicating *15N* is fully recessive (data not shown).

Thus, *15N* appears to have complex properties, showing weaker phenotypes in some contexts, but stronger phenotypes—even stronger than null alleles—in other contexts. Since the Par-6 PDZ domain is known to be required for its physical interaction with Baz (Lin *et al.* 2000), our data suggest that a direct protein–protein interaction between Par-6 and Baz is not required for embryonic epithelial polarity, but is required for branching morphogenesis and lumen formation in tracheal terminal cells.

PAR-polarity proteins function downstream of the FGF signaling pathway to regulate subcellular branching

Directional growth and branching in *Drosophila* tracheal terminal cells are known to be controlled by an FGF extracellular signal (Jarecki *et al.* 1999), potentiated by detection of intracellular oxygen tension (Centanin *et al.* 2008). Increase in FGF, either by reducing oxygen levels or by using a transgene to directly increase expression, results in increased growth and branching of terminal cells (Jarecki *et al.* 1999). We wanted to determine whether this increase in branching was dependent on PAR proteins. To test this, we made use of an activated form of the FGF Receptor, λBtl (Lee *et al.* 1996). We expressed λBtl in individual terminal cells and found that this leads to an increase in branch number, as well as cell growth, particularly obvious in the cell body (Figure 7A). While branch numbers were hard to determine precisely in this genetic background (due to the overall disorganized pattern and large number of overlapping branches), they were clearly significantly higher (>40) than those observed in wild-type cells (32 ± 2). However, when we expressed λBtl in cells that were also mutant for *par-6^{29VV}*, we found these cells did not show increased branching (Figure 7B). Indeed, the number of branches in these *par-6^{29VV}*; λBtl cells (10 ± 0.5) was very similar to that in *par-6^{29VV}* mutant cells not expressing λBtl (13 ± 2). In contrast, λBtl-stimulated cell growth, as determined by the increase in cell body size, was unaffected by *par-6^{29VV}* (Figure 7, A and B). We observed similar results for *baz*: *baz* mutant cells expressing λBtl show reduced branching compared to wild-type cells expressing λBtl (data not shown). From these data we conclude that Par-6 and Baz are downstream of FGF signaling for branching, but not for cell growth.

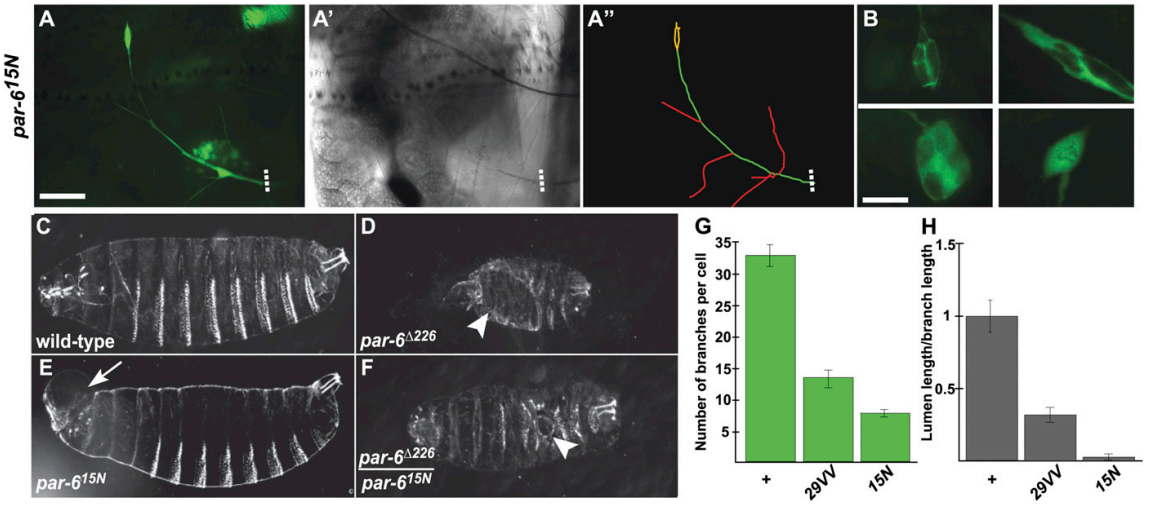

Figure 6 Analysis of *par-6*^{15N}. As in Figure 1, homozygous terminal cell branches and tips were visualized by GFP expression in mosaic L3 larvae (A and B) and gas-filled lumens visualized by brightfield microscopy (A′). Terminal cells homozygous for *par-6*^{15N} show severe branching defects (A), have no gas-filled lumen (A′), and have strong tip morphology defects (B). (A′′) Tracing of the branching pattern observed in A. (C–F) Darkfield image of embryonic cuticle preparations. (C) Wild-type embryo. (D) *par-6*$^{\Delta 226}$ hemizygote has a large cuticle hole (arrowhead), indicative of a polarity defect. (E) *par-6*^{15N} hemizygote has no cuticle hole. Arrow indicates a head involution defect in this genotype. (F) *par-6*$^{\Delta 226/15N}$ *trans*-heterozygote has a small cuticle hole (arrowhead). (G and H) Quantification of terminal cell branches (G) and lumen formation (H) in *par-6*^{15N} mutant cells. Wild-type and *par-6*^{29VV} data from Figure 2 are shown for comparison. Bars: A, 75 μm; B, 25 μm. Branch hierarchy colors and other labels are as in Figure 1. Error bars represent ±2 SEM (n = 10).

Discussion

The shape of branched networks is controlled by two parameters: the directional growth of extensions and the location of branching points. When combined in different patterns, these two processes can result in a great diversity of branched structures (Turcotte *et al.* 1998). Here, we have shown that mutations in PAR complex genes uncouple FGF-mediated growth from branching in tracheal terminal cells. We find that in PAR-complex mutants, terminal branches typically extend as far as they do in wild type and average branch length is not affected by mutations in any of the PAR-complex genes (data not shown), suggesting the PAR complex is not required for branch outgrowth, but is required for branch initiation. Furthermore, increase in branch numbers caused by overactivation of the FGF signaling pathway requires *par-6* and *baz*, while FGF-induced cell growth is independent of these genes. We propose that the FGF signal goes through two independent pathways; one controls growth and is independent of the PAR complex, while a second, PAR-complex–dependent mechanism, controls branching (Figure 7C).

Little is known about the cellular mechanisms that initiate subcellular branching, either for terminal cells or for other cells, such as neurons. There is considerable evidence that the PAR complex regulates different aspects of cytoskeletal organization (Nance and Zallen 2011) and it has been suggested that actin may play a role in outgrowth of at least the initial terminal cell branch (Gervais and Casanova 2010), although we find development of this branch

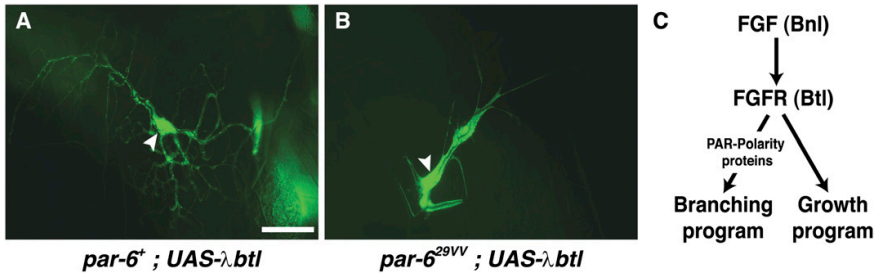

Figure 7 Par-6 is required for FGF-induced cell branching, but not cell growth. As in Figure 1, homozygous terminal cell branches were visualized by GFP expression in mosaic L3 larvae (A and B). *par-6*$^{+}$ terminal cells expressing activated FGF receptor (λBtl) show an increase in branch number (A) and cell growth, most obvious in the cell body (arrowhead). *par-6*^{29VV} terminal cells expressing λBtl do not show increased branch numbers (B), but still have increased cell growth (arrowhead). (C) Model for PAR complex in FGF-mediated branching in terminal cells. FGF stimulates outgrowth, independently of the PAR complex, and branching, dependent on the PAR complex. Bar: 75 μm.

is apparently not affected by PAR complex mutations. Since branch outgrowth occurs from the basal cell surface, one interesting possibility is that outgrowth is controlled by the counterpart to apical PAR proteins, basal polarity proteins that include Par-1 and Lethal (2) giant larvae (Lgl) (reviewed by Goldstein and Macara 2007). These apical and basal proteins are known to negatively regulate each other (Benton and St. Johnston 2003; Hao *et al.* 2006), and this cross-regulation is critical for establishing and maintaining stable apical/basal domains (reviewed by Prehoda 2009). One possibility is that basal proteins keep the basal surface in a nonbranching configuration until it is locally downregulated by the apical PAR complex, thus triggering branching events. Characterization of targets of both the apical and the basal PAR complexes should thus shed light on mechanisms of subcellular branching.

We have found that some, but not all, of the PAR-complex components are required for subcellular lumen formation. Specifically, both Par-6 and aPKC are required, while we cannot detect any role for Bazooka in this process. In other epithelia, it is well known that disruption of any of the four complex members generally leads to loss of epithelial integrity (Goldstein and Macara 2007). However, in these epithelia, the PAR complex is invariably associated with apical junctions that form between cells. Tracheal terminal branches do not possess such junctions, being seamless, intracellular tubes (Noirot-Timothee and Noirot 1982), so perhaps canonical complex function is required only for the formation and maintenance of junctions, rather than apical determination *per se*. Consistent with this, mutations in *crumbs*, a key apical junctional component that is generally required for stable epithelia, have no effect on terminal cell lumen formation (S. Luschnig, personal communication). Furthermore, we propose that Par-6 localization to the apical surface is a consequence of lumen formation, rather than a cause. One model suggests that the localization of PAR-complex proteins starts with a difference in lipid composition of the apical membrane. This composition allows binding by Baz (Gallardo *et al.* 2010; Krahn *et al.* 2010), which then functions to recruit Par-6/aPKC (Harris and Peifer 2005). We propose a similar mechanism for the terminal cell subcellular lumen: the lumen forms with a lipid composition similar to that of typical apical membranes, causing Baz localization, which in turn localizes Par-6.

We have multiple lines of evidence that Par-6 and aPKC may function independently of each other in the lumenogenic process. First, loss of interaction between Par-6 and aPKC, as in the $aPKC^{psu69}$ allele, has no effect on lumen formation, even in the absence of a potential bridging interaction through Baz. Second, the kinase activity of aPKC, which is regulated by Par-6, is not required for lumen formation. Finally, the localization of aPKC and Par-6 differs in terminal cells, with aPKC showing punctate, Baz-independent luminal localization, while Par-6 has a continuous, Baz-dependent luminal enrichment. These data suggest that Par-6 and aPKC may affect different steps in a lumen formation pathway. Other studies have identified Par-6- and aPKC-dependent, but Baz-independent cellular processes. Specifically, cell junction formation in imaginal epithelia is thought to be regulated by a Par-6- and aPKC-dependent endocytic pathway that regulates levels of E-Cadherin at cellular contacts (Georgiou *et al.* 2008; Leibfried *et al.* 2008). The phenotypes of *par-6* and *aPKC* mutant cells in these studies were similar, leading to the proposal that Par-6 and aPKC function together at a specific, but as yet unidentified, endocytic step. However, interfering with endocytosis even at biochemically distinct steps can lead to similar phenotypes (Babst *et al.* 2002). Hence, Par-6 and aPKC may function independently of each other in this cell junctional regulation, as we have proposed here for lumen formation.

The membranes that line intracellular lumens are thought to be generated by a process of vesicle biogenesis, trafficking of these vesicles to the center of the branch, and fusion (Jarecki *et al.* 1999; Ghabrial *et al.* 2003; but see Gervais and Casanova 2010, for an alternative model). One additional phenotype present in *par-6* and *aPKC* mutant terminal cells suggests a role in membrane trafficking. These terminal cells not only lack a subcellular lumen, but also have abnormal morphology at branch tips, showing swelling of their plasma membranes and sometimes the appearance of abnormal internal membranous structures. Both these defects are suggestive of ectopic membrane at branch tips. This defect is correlated with the lack of lumen formation. Mutants such as *baz* or $aPKC^{psu69}$ with abnormal branching, but no lumen defects, never show tip abnormalities. We propose that this ectopic membrane is material that normally contributes to the membrane surrounding the intracellular lumen. In this model, Par-6 and aPKC function to partition membranes between growing tips and intracellular lumens. In their absence, membrane intended for the lumen is trafficked to the tips and this excess membrane leads to the morphological defects observed.

Our genetic analysis of the PAR complex suggests that not all its components are required equally for branching. Specifically, aPKC mutant cells show a significantly more severe defect than either *par-6* or *baz* mutants. Also, we have found that *baz par-6* double mutants have a stronger defect than either of the single mutants. These data suggest the active form in branching is not the ternary Par-6/aPKC/Baz complex, since loss of any one of the components should give the same defect, and loss of any two should not give a stronger defect. Rather, we propose Par-6 and Baz act in parallel to regulate aPKC. Both the Par-6/aPKC and the Baz/aPKC complexes are required for branching, but either one has some activity on its own. Our multicomplex model may also explain why $par\text{-}6^{15N}$ leads to such strong branching defects, which are comparable to those of *aPKC* single mutants, but stronger than even null alleles of *par-6*. We propose that aPKC switching between the active Baz and Par-6 bound forms goes through a ternary complex, but this complex is not active for branching. Transition from this complex to one of the active binary complexes requires the

Par-6 PDZ domain, such that in *15N* mutants the components become locked into the inactive ternary complex and are thus unable to regulate branching. This model also explains why Par-6^{15N}, lacking the interaction between Par-6 and Baz, has defects in lumen formation, even though Baz itself is not required in this process: the locked ternary complex sequesters both Par-6 and aPKC from their function in lumen formation.

Finally, we suggest that the dynamic switching of partners within the PAR complex is not unique to subcellular branching. Rather, this may be a common phenomenon in cases in which the PAR complex must be remodeled during dynamic processes, such as asymmetric cell division, but it may be less critical for the complex to function in static systems, such as in apical/basal polarity. This is evident from the cuticles of *par-*6^{15N} zygotic mutant embryos that lack large holes, which are indicative of polarity defects. We further predict from this model that *par-*6^{15N} would lead to severe defects in other dynamic processes, such as asymmetric division of neuroblasts.

Acknowledgments

We are very grateful to Jürgen Knoblich, Jennifer Zallen, Natalie Denef, Trudi Schüpbach, Andreas Wodarz, Michael Krahn, Vincent Mirouse, Stefan Luschnig, and Christiane Nüsslein-Volhard for fly stocks and antibodies. We thank the Metzstein and Thummel laboratories, Michael Krahn, and Markus Babst for useful discussions; Stefan Luschnig for unpublished data; Joseph Smith and Charles Jones for preliminary *par-6* mapping experiments; Anthea Letsou for help with embryo cuticle preparations; and Gillian Stanfield, Carl Thummel, Stefan Luschnig, and members of the Metzstein laboratory for comments on the manuscript. Fly stocks were obtained from the Bloomington *Drosophila* Stock Center, the Vienna *Drosophila* RNAi Center, and the National Institute of Genetics Fly Stock Center, Japan.

Literature Cited

Babst, M., D. J. Katzmann, E. J. Estepa-Sabal, T. Meerloo, and S. D. Emr, 2002 Escrt-III: an endosome-associated heterooligomeric protein complex required for mvb sorting. Dev. Cell 3: 271–282.

Bauer, N. G., C. Richter-Landsberg, and C. Ffrench-Constant, 2009 Role of the oligodendroglial cytoskeleton in differentiation and myelination. Glia 57: 1691–1705.

Bellen, H. J., R. W. Levis, G. Liao, Y. He, J. W. Carlson *et al.*, 2004 The BDGP gene disruption project: single transposon insertions associated with 40% of *Drosophila* genes. Genetics 167: 761–781.

Benton, R., and D. St. Johnston, 2003 *Drosophila* PAR-1 and 14–3-3 inhibit Bazooka/PAR-3 to establish complementary cortical domains in polarized cells. Cell 115: 691–704.

Centanin, L., A. Dekanty, N. Romero, M. Irisarri, T. A. Gorr *et al.*, 2008 Cell autonomy of HIF effects in *Drosophila*: tracheal cells sense hypoxia and induce terminal branch sprouting. Dev. Cell 14: 547–558.

Chou, T. B., and N. Perrimon, 1992 Use of a yeast site-specific recombinase to produce female germline chimeras in *Drosophila*. Genetics 131: 643–653.

Cox, D. N., S. A. Seyfried, L. Y. Jan, and Y. N. Jan, 2001 Bazooka and atypical protein kinase C are required to regulate oocyte differentiation in the *Drosophila* ovary. Proc. Natl. Acad. Sci. USA 98: 14475–14480.

Dietzl, G., D. Chen, F. Schnorrer, K. C. Su, Y. Barinova *et al.*, 2007 A genome-wide transgenic RNAi library for conditional gene inactivation in *Drosophila*. Nature 448: 151–156.

Doerflinger, H., N. Vogt, I. L. Torres, V. Mirouse, I. Koch *et al.*, 2010 Bazooka is required for polarisation of the *Drosophila* anterior-posterior axis. Development 137: 1765–1773.

Eberl, D. F., and A. J. Hilliker, 1988 Characterization of X-linked recessive lethal mutations affecting embryonic morphogenesis in *Drosophila melanogaster*. Genetics 118: 109–120.

Fehon, R. G., T. Oren, D. R. LaJeunesse, T. E. Melby, and B. M. McCartney, 1997 Isolation of mutations in the *Drosophila* homologues of the human neurofibromatosis 2 and yeast CDC42 genes using a simple and efficient reverse-genetic method. Genetics 146: 245–252.

Gallardo, R., Y. Ivarsson, J. Schymkowitz, F. Rousseau, and P. Zimmermann, 2010 Structural diversity of PDZ-lipid interactions. ChemBioChem 11: 456–467.

Georgiou, M., E. Marinari, J. Burden, and B. Baum, 2008 Cdc42, Par6, and aPKC regulate Arp2/3-mediated endocytosis to control local adherens junction stability. Curr. Biol. 18: 1631–1638.

Gervais, L., and J. Casanova, 2010 In vivo coupling of cell elongation and lumen formation in a single cell. Curr. Biol. 20: 359–366.

Ghabrial, A., S. Luschnig, M. M. Metzstein, and M. A. Krasnow, 2003 Branching morphogenesis of the *Drosophila* tracheal system. Annu. Rev. Cell Dev. Biol. 19: 623–647.

Ghabrial, A. S., and M. A. Krasnow, 2006 Social interactions among epithelial cells during tracheal branching morphogenesis. Nature 441: 746–749.

Gibson, D. A., and L. Ma, 2011 Developmental regulation of axon branching in the vertebrate nervous system. Development 138: 183–195.

Goldstein, B., and I. G. Macara, 2007 The PAR proteins: fundamental players in animal cell polarization. Dev. Cell 13: 609–622.

Guillemin, K., J. Groppe, K. Ducker, R. Treisman, E. Hafen *et al.*, 1996 The *pruned* gene encodes the *Drosophila* serum response factor and regulates cytoplasmic outgrowth during terminal branching of the tracheal system. Development 122: 1353–1362.

Hao, Y., L. Boyd, and G. Seydoux, 2006 Stabilization of cell polarity by the *C. elegans* RING protein PAR-2. Dev. Cell 10: 199–208.

Harris, T. J., and M. Peifer, 2005 The positioning and segregation of apical cues during epithelial polarity establishment in *Drosophila*. J. Cell Biol. 170: 813–823.

Hirano, Y., S. Yoshinaga, R. Takeya, N. N. Suzuki, M. Horiuchi *et al.*, 2005 Structure of a cell polarity regulator, a complex between atypical PKC and Par6 PB1 domains. J. Biol. Chem. 280: 9653–9661.

Jan, Y. N., and L. Y. Jan, 2010 Branching out: mechanisms of dendritic arborization. Nat. Rev. Neurosci. 11: 316–328.

Jarecki, J., E. Johnson, and M. A. Krasnow, 1999 Oxygen regulation of airway branching in *Drosophila* is mediated by branchless FGF. Cell 99: 211–220.

Kemphues, K. J., J. R. Priess, D. G. Morton, and N. S. Cheng, 1988 Identification of genes required for cytoplasmic localization in early *C. elegans* embryos. Cell 52: 311–320.

Kim, S., I. Gailite, B. Moussian, S. Luschnig, M. Goette *et al.*, 2009 Kinase-activity-independent functions of atypical protein kinase C in *Drosophila*. J. Cell Sci. 122 (Pt 20): 3759–3771.

Krahn, M. P., D. R. Klopfenstein, N. Fischer, and A. Wodarz, 2010 Membrane targeting of Bazooka/PAR-3 is mediated by direct binding to phosphoinositide lipids. Curr. Biol. 20: 636–642.

Lee, T., and L. Luo, 1999 Mosaic analysis with a repressible cell marker for studies of gene function in neuronal morphogenesis. Neuron 22: 451–461.

Lee, T., N. Hacohen, M. Krasnow, and D. J. Montell, 1996 Regulated Breathless receptor tyrosine kinase activity required to pattern cell migration and branching in the *Drosophila* tracheal system. Genes Dev. 10: 2912–2921.

Leibfried, A., R. Fricke, M. J. Morgan, S. Bogdan, and Y. Bellaiche, 2008 *Drosophila* Cip4 and WASp define a branch of the Cdc42-Par6-aPKC pathway regulating E-cadherin endocytosis. Curr. Biol. 18: 1639–1648.

Levi, B. P., A. S. Ghabrial, and M. A. Krasnow, 2006 *Drosophila* talin and integrin genes are required for maintenance of tracheal terminal branches and luminal organization. Development 133: 2383–2393.

Lewis, E. B., and F. Bacher, 1968 Methods of feeding ethyl methane sulfonate (EMS) to *Drosophila* males. Dros. Inf. Serv. 43: 193.

Li, J., H. Kim, D. G. Aceto, J. Hung, S. Aono *et al.*, 2010 Binding to PKC-3, but not to PAR-3 or to a conventional PDZ domain ligand, is required for PAR-6 function in *C. elegans*. Dev. Biol. 340: 88–98.

Lin, D., A. S. Edwards, J. P. Fawcett, G. Mbamalu, J. D. Scott *et al.*, 2000 A mammalian PAR-3-PAR-6 complex implicated in Cdc42/Rac1 and aPKC signalling and cell polarity. Nat. Cell Biol. 2: 540–547.

Llimargas, M., 1999 The Notch pathway helps to pattern the tips of the *Drosophila* tracheal branches by selecting cell fates. Development 126: 2355–2364.

Makala, L. H., and H. Nagasawa, 2002 Dendritic cells: a specialized complex system of antigen presenting cells. J. Vet. Med. Sci. 64: 181–193.

Martin-Belmonte, F., and K. Mostov, 2008 Regulation of cell polarity during epithelial morphogenesis. Curr. Opin. Cell Biol. 20: 227–234.

Meijering, E., M. Jacob, J. C. Sarria, P. Steiner, H. Hirling *et al.*, 2004 Design and validation of a tool for neurite tracing and analysis in fluorescence microscopy images. Cytometry A 58: 167–176.

Morais-de-Sa, E., V. Mirouse, and D. St. Johnston, 2010 aPKC phosphorylation of Bazooka defines the apical/lateral border in *Drosophila* epithelial cells. Cell 141: 509–523.

Nagai-Tamai, Y., K. Mizuno, T. Hirose, A. Suzuki, and S. Ohno, 2002 Regulated protein-protein interaction between aPKC and PAR-3 plays an essential role in the polarization of epithelial cells. Genes Cells 7: 1161–1171.

Nance, J., and J. A. Zallen, 2011 Elaborating polarity: PAR proteins and the cytoskeleton. Development 138: 799–809.

Noirot-Timothee, C., and C. Noirot, 1982 The structure and development of the tracheal system, pp. 351–381 in *Insect Ultrastructure*, edited by R. C. King, and H. Akai. Plenum Press, New York.

Petronczki, M., and J. A. Knoblich, 2001 DmPAR-6 directs epithelial polarity and asymmetric cell division of neuroblasts in *Drosophila*. Nat. Cell Biol. 3: 43–49.

Plaza, S., H. Chanut-Delalande, I. Fernandes, P. M. Wassarman, and F. Payre, 2010 From A to Z: apical structures and zona pellucida-domain proteins. Trends Cell Biol. 20: 524–532.

Prehoda, K. E., 2009 Polarization of *Drosophila* neuroblasts during asymmetric division. Cold Spring Harbor Perspect. Biol. 1: a001388.

Puelles, L., 2009 Contributions to Neuroembryology of Santiago Ramon y Cajal (1852–1934) and Jorge F. Tello (1880–1958). Int. J. Dev. Biol. 53: 1145–1160.

Rolls, M. M., R. Albertson, H. P. Shih, C. Y. Lee, and C. Q. Doe, 2003 *Drosophila* aPKC regulates cell polarity and cell proliferation in neuroblasts and epithelia. J. Cell Biol. 163: 1089–1098.

Ruhle, H., 1932 Das larvale Tracheensystem von *Drosophila melanogaster* (Meigen) und seine Variabilitat. Z. Wiss. Zool. 141: 159–245.

Shiga, Y., M. Tanaka-Matakatsu, and S. Hayashi, 1996 A nuclear GFP/β-galactosidase fusion protein as a marker for morphogenesis in living *Drosophila*. Dev. Growth Differ. 38: 99–106.

Simoes, S. M., J. T. Blankenship, O. Weitz, D. L. Farrell, M. Tamada *et al.*, 2010 Rho-kinase directs Bazooka/Par-3 planar polarity during *Drosophila* axis elongation. Dev. Cell 19: 377–388.

Suzuki, A., and S. Ohno, 2006 The PAR-aPKC system: lessons in polarity. J. Cell Sci. 119: 979–987.

Turcotte, D. L., J. D. Pelletier, and W. I. Newman, 1998 Networks with side branching in biology. J. Theor. Biol. 193: 577–592.

Welchman, D. P., L. D. Mathies, and J. Ahringer, 2007 Similar requirements for CDC-42 and the PAR-3/PAR-6/PKC-3 complex in diverse cell types. Dev. Biol. 305: 347–357.

Wodarz, A., A. Ramrath, A. Grimm, and E. Knust, 2000 *Drosophila* atypical protein kinase C associates with Bazooka and controls polarity of epithelia and neuroblasts. J. Cell Biol. 150: 1361–1374.

Xu, T., and G. M. Rubin, 1993 Analysis of genetic mosaics in developing and adult *Drosophila* tissues. Development 117: 1223–1237.

Yamanaka, T., Y. Horikoshi, A. Suzuki, Y. Sugiyama, K. Kitamura *et al.*, 2001 PAR-6 regulates aPKC activity in a novel way and mediates cell-cell contact-induced formation of the epithelial junctional complex. Genes Cells 6: 721–731.

Communicating editor: T. Schupbach

GENETICS

Supporting Information
http://www.genetics.org/cgi/content/full/genetics.111.130351/DC1

A Novel Function for the PAR Complex in Subcellular Morphogenesis of Tracheal Terminal Cells in *Drosophila melanogaster*

Tiffani A. Jones and Mark M. Metzstein

DOI: 10.1534/genetics.111.130351

File S1

Supporting Material

Construction of *baz par-6* double mutant

Because *baz* and *par-6* are located close to each other on the *Drosophila* X chromosome (*baz* is ~1.3 m.u. to the left of *par-6*), we used a two step recombination process to construct the *baz par-6* double mutant. First, we recombined the visible marker, *scalloped* (*sd^1*), located about 7 m.u. to the left of *par-6* (thus ~5.7 m.u. from *baz*) onto *$par\text{-}6^{\Delta 226}$*. *$par\text{-}6^{\Delta 226}$ FRT^{19A}/FM7c* females were crossed to *sd^1/Y* males, non-balancer female progeny were collected and crossed to *Dp(1;Y)W73, y B f^+* bearing males. *Dp(1;Y)W73* is a Y-linked duplication that covers *par-6*, *baz*, but not *sd*. The progeny from this cross were selected for G418 resistance (neo^R) encoded by the *FRT^{19A}* transgene, and individual *sd* males were used to establish lines balanced with *FM7c*. Lethal lines, presumably carrying *$par\text{-}6^{\Delta 226}$*, were chosen and complementation tests, using two independent alleles of *par-6*, were performed to confirm the presence of *par-6*. Terminal cell defects were also evaluated in mosaic animals and found to be identical to those observed in the *par-6* null, also confirming the presence of *FRT^{19A}*. These *sd^1 $par\text{-}6^{\Delta 226}$ FRT^{19A}/FM7c* females were then crossed to *baz^{FA50} FRT^{19A}/Dp(1;Y)W73, y B f^+* males, non-balancer female offspring were collected and crossed to *Dp(1;Y)W73, y B f^+* bearing males. Single *sd^+* males were selected, and were crossed to *baz* and *par-6* carrying females. Animals that failed to complement both *par-6* and *baz* were used to establish lines.

Characterization of *$par\text{-}6^{15N}$*

When first isolated, we found that lethality associated with *15N* mapped ~2 m.u. to the right of the visible marker *forked* (*f*), located at ~57 m.u. on the X chromosome and our most rightward visible marker. We then mapped *15N* with respect to *FRT^{19A}*, using G418 resistance as a marker. We found 0 recombinants among ~10,000 flies scored. The inferred map distance was inconsistent with the previous mapped lethal location near *f*, since *FRT^{19A}* is at ~64 m.u., thus ~8 m.u. from *f*, and suggested the existence of an additional lethal very closely linked to *FRT^{19A}*. We have named these two putative lethals *let1* (~2 m.u. from *f*) and *let2* (close to *FRT^{19A}*).

To determine which, if either, of these two lethals corresponded to the *15N* tracheal cell defect, we performed experiments to separate and test the terminal cell phenotype of the two lethals independently of each other. Since *let2* maps very close to *FRT^{19A}*, we predicted that *Df(1)mal3*, an X terminal deficiency that removes chromosome segments 19A2--h26 (SCHALET and LEFEVRE 1973) would fail to complement *let2*, but would complement *let1*. We generated females of genotype *f^+ let1 let2 FRT^{19A}/f $let1^+$ $let2^+$ FRT^{19A}* and crossed them to males of genotype *f^1 Df(1)mal3/Dp(1;Y)y^+mal^{106}*, and collected *f^+* female progeny of putative genotypes *f^+ let1 $let2^+$ FRT^{19A}/f^1 $let1^+$ Df(1)mal3* or, less frequently, *f^+ $let1^+$ $let2^+$ FRT^{19A}/f^1 $let1^+$ Df(1)mal3*, which result from recombination between *let1* and *let2* (~6 m.u.) or recombination between *let1* and *f* (~2 m.u.), respectively. We then isolated and balanced the recombinant chromosome, confirmed lethality (thus is *f^+ let1 $let2^+$ FRT^{19A}*) and tested the chromosome in tracheal terminal cell mosaics. This chromosome showed identical terminal cell defects as did the original *15N* mutant isolate. Subsequent mapping experiments showed a single lethal locus,

mapping ~6 m.u. from *FRT*^{19A} consistent with the map distance from *f*. All subsequent analysis of *15N* was carried out using this recombinant chromosome.

To confirm the second putative lethal locus (*let2*), which is close to *FRT*^{19A}, did not contribute to the terminal cell phenotype, we generated females of genotype *f*$^{+}$ *let1 let2 FRT*^{19A}*/f let1*$^{+}$ *let2*$^{+}$ and crossed them to *FM0, f/Y* males. A number of resulting *f neo*^{R} progeny were selected (putative genotypes *f let1*$^{+}$ *let2 FRT*^{19A}*/FM0, f* or *f let1 let2 FRT*^{19A}*/FM0, f*) and tested for terminal cell defects. One line that was tested was found to be lethal, but terminal cells appeared completely wild-type in mosaic animals. This line thus contains the recombinant chromosome *f let1*$^{+}$ *let2 FRT*^{19A} and *let2* does not contribute to a terminal cell defect. We have not characterized *let2* any further.

The following data showed that *15N* is an allele of *par-6*. First, we found the lethality associated with *15N* (after removal of the irrelevant lethal mutation) mapped to a very small (59 kb) interval that contains *par-6*. Second, *15N* failed to complement known alleles of *par-6* for lethality (data not shown). Finally, *15N* lethality (data not shown) and terminal cell defects (Figures S2C and S2D) were rescued by the *par-6*$^{+}$ containing genomic transgene (PETRONCZKI and KNOBLICH 2001).

SNP mapping

To map the *15N* mutation, we used meiotic recombination with visible and single nucleotide polymorphism markers (SNPs). The mutations were induced on a *y w FRT*^{19A} chromosome. To map with respect with visible markers, we used the mapping chromosome *sc cv ct v g f*. We found that this chromosome is also highly polymorphic on the sequence level with the *y w FRT*^{19A} chromosome (M.M.M. and M.A.Krasnow, unpublished data), with a SNP variant approximately every 250 bp. To isolate recombination events, we took females of genotype *f*$^{+}$ *15N FRT*^{19A}*/f 15N*$^{+}$ (Since we found *15N* was to the right of *f*, this is the only visible marker relevant for recombination analysis) and crossed them to *FM7c/Y* males. To isolate recombination events to the left of *15N*, we selected for viable (i.e. *15N*$^{+}$) male offspring that were also *f*$^{+}$, thus had a recombination event between *f* and *15N*. To isolate recombination events to the right of *15N*, we selected for viable (i.e. *15N*$^{+}$) G418 resistant males. Individual males were then typed for SNPs in the *f-FRT*^{19A} interval. SNPs were typed by performing PCR to amplify a 500-1000 bp fragment around the SNP site followed by a diagnostic restriction enzyme digest or direct sequencing of the PCR product. Location of the SNPs and their relative position to *15N* are described in supplemental table 1. The smallest interval we determined to contain *15N* was ~59 kb (XE10-XE01).

PETRONCZKI, M., and J. A. KNOBLICH, 2001 DmPAR-6 directs epithelial polarity and asymmetric cell division of neuroblasts in *Drosophila*. Nat Cell Biol 3: 43-49.

SCHALET, A., and G. LEFEVRE, JR., 1973 The localization of "ordinary" sex-linked genes in section 20 of the polytene X chromosome of *Drosophila melanogaster*. Chromosoma 44: 183-202.

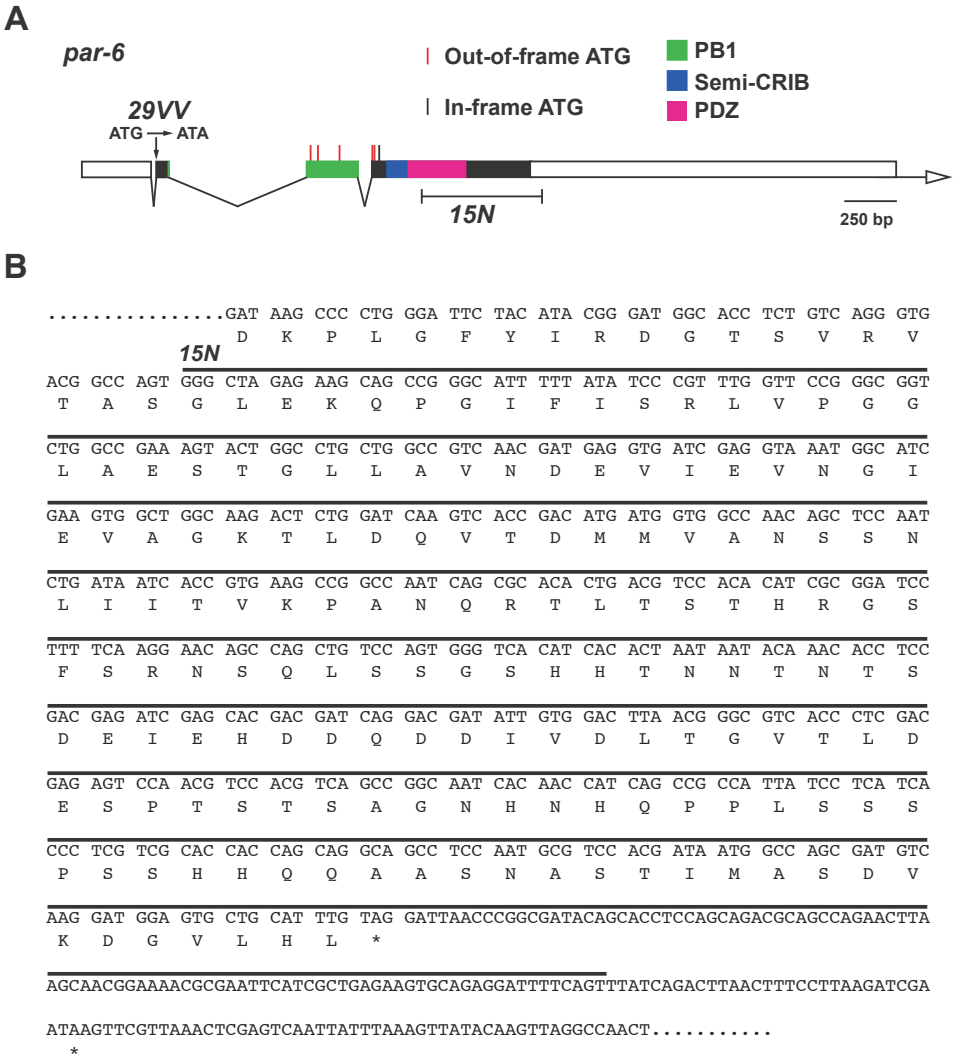

Figure S1 Molecular analysis of new *par-6* alleles. (A) Genomic structure of *par-6* showing location of the *29VV* mutation and the extent of the *15N* deletion. Filled boxes represent coding sequence, open boxes represent 5' and 3' UTRs, the open arrow indicates the direction of transcription. Colors represent different domains of Par-6: PB1 (green); semi-CRIB (blue); PDZ (magenta). Ticks above sequence show out-of-frame (red) and first in-frame (black) start codons after the usual start. The extent of the 15N deletion is bracketed under the structure. (B) Partial sequence of the final exon of *par-6*. The dark line represents the sequence deleted in *15N*. The first asterisk represents the normal par-6 stop codon and the second asterisk represents the inferred *15N* stop codon. *15N* is predicted to remove 64 amino acids of Par-6 and add 10 amino acids that are not normally coding before translation termination.

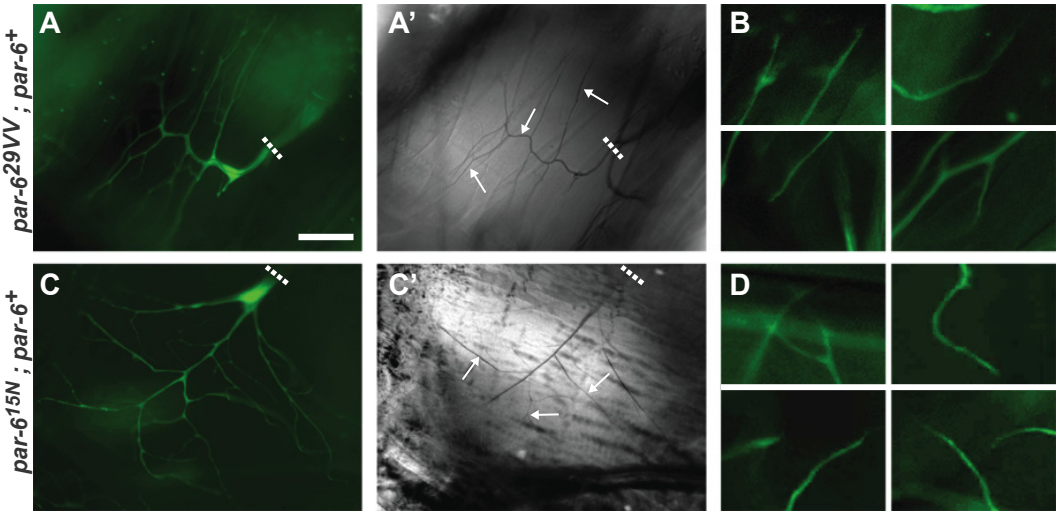

Figure S2 *par-6* rescue experiments. Homozygous terminal cell branches and tips were visualized by GFP expression in mosaic L3 larvae (A-D) and gas-filled lumens visualized by bright-field microscopy (A' and C'). Terminal cells homozygous for *par-6*^{29VV} (A, B) or *par-6*^{15N} (C, D) carrying one copy of a genomic *par-6*$^{+}$ containing transgene have normal branching (A, C), a complete gas-filled lumen (A', C') and normal tapered tip morphology (B, D). Dashed white lines demarks the proximal end of the cell; arrows point to gas-filled lumens. Scale bar; 75µm.

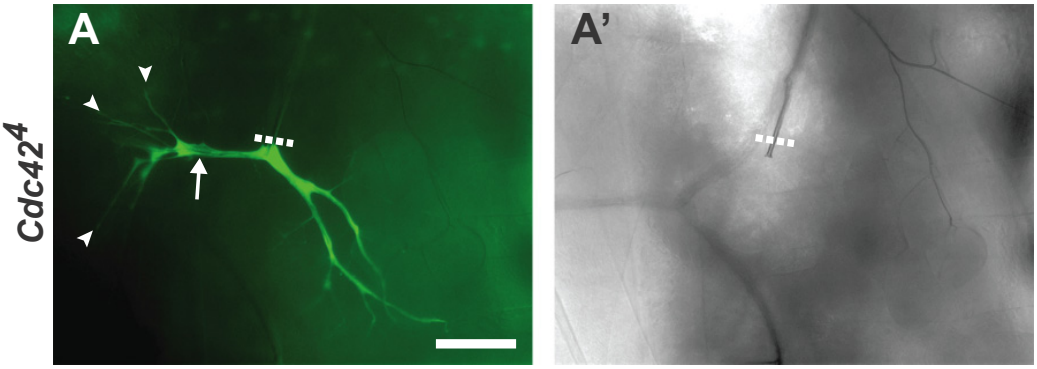

Figure S3 Terminal cell defects in *Cdc42* mutants. Tracheal terminal cells homozygous for *Cdc42*^{4} have branching defects (A) and no gas-filled lumen (A'). Dashed white lines demark where the homozygous GFP-labeled cell starts relative to other (wild-type) tracheal cells. Additional defects are observed in *Cdc42* mutants, including fine filopodial-like extensions (arrowheads) and regions of branches in which the cell membranes appear to spread out on the substrate, leading to a wider and thinner appearance (arrow). Scale bar; 75µm.

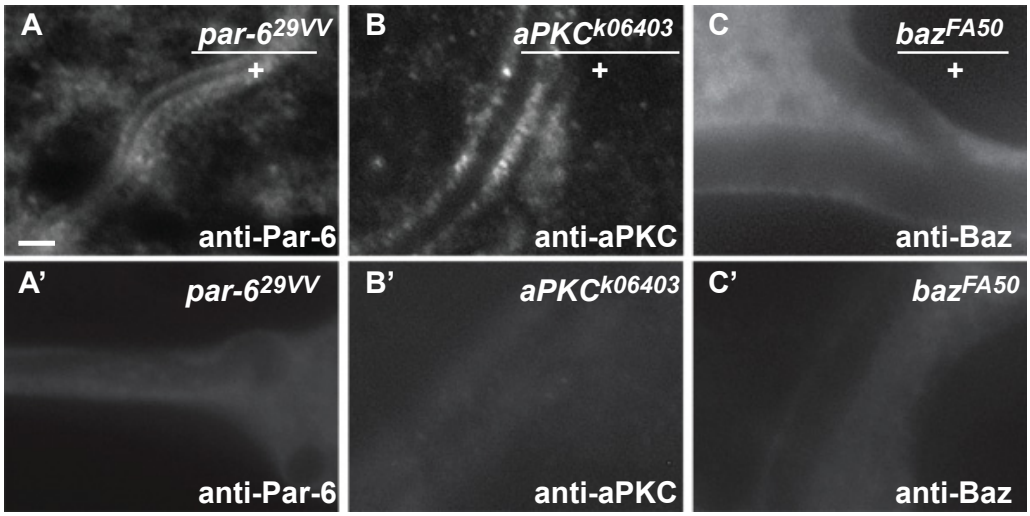

Figure S4 Staining of mutant cells showing specificity of antibody staining. Individual terminal cells in L3 larvae stained for the indicated protein (A-C). Par-6 is localized to the lumen in *par-6*^{29VV} heterozygous cells (A), but completely absent in terminal cells homozygous for *par-6*^{29VV} (A'). aPKC is detected in terminal cells heterozygous for *aPKC*^{k06403} (B), but absent in *aPKC*^{k06403} homozygous terminal cells (B'). Baz is cytoplasmically localized in terminal cells heterozygous for *baz*^{FA50} (C), but absent in *baz*^{FA50} homozygous terminal cells (C'). Heterozygous and homozygous mutant cells were scored within the same mosaic animals in each case. Scale bar; 2μm.

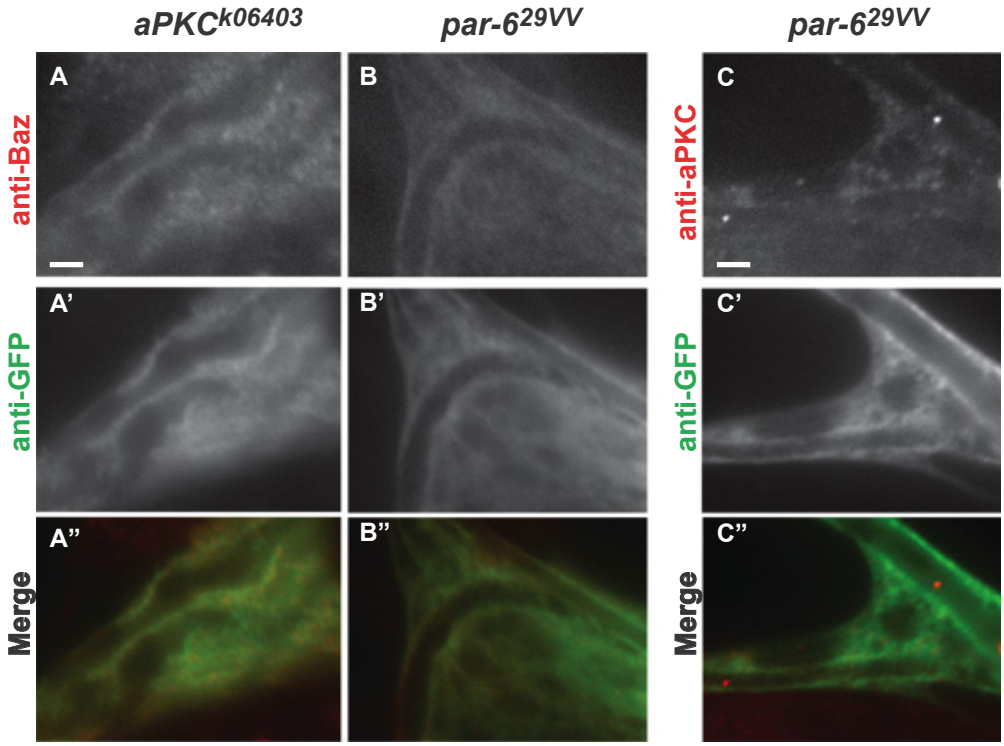

Figure S5 Localization of Baz and aPKC in mutant backgrounds. Individual homozygous terminal cells in L3 larvae visualized with cytoplasmic GFP (A'-C'; green channel in A''-C'') and stained for the indicated protein (A-C; red channel in A''-C''). Baz is cytoplasmically localized and overlaps with cytoplasmic GFP in *aPKC*^{k06403} (A-A"), and *par-6*^{29VV} (B-B") terminal cells. In *par-6*^{29VV} mutant cells, aPKC shows punctate cytoplasmic and luminal localization (C-C''), similar to that seen in wild-type cells. Scale bar; 2µm.

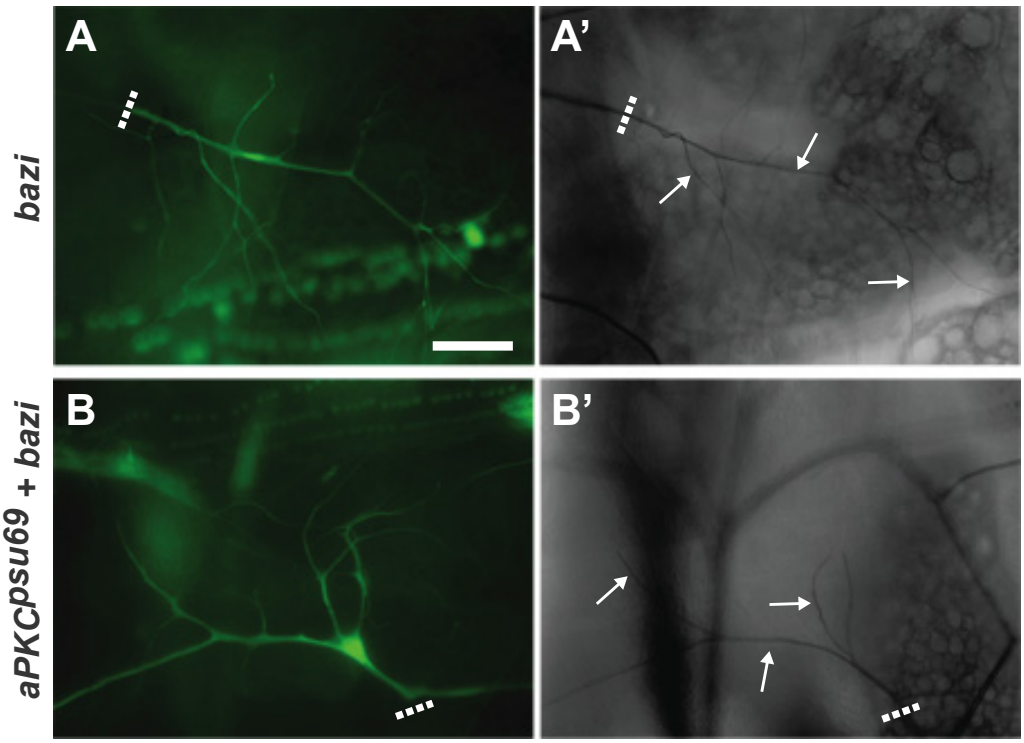

Figure S6 Baz does not function to bridge interactions between Par-6 and aPKC^{psu69} in lumen formation. Baz has protein-protein interactions with both aPKC and Par-6, and one possibility we considered is that Baz may act to bridge the interaction between aPKC and Par-6, missing in *psu69*, to allow lumen formation to occur. One prediction of this model is that baz, while not normally required for lumen formation, would be required in *psu69* mutant terminal cells. To test this, we made mosaics of *aPKCpsu69* in animals also expressing an RNAi transgene directed against *baz*. We first confirmed that terminal cells expressing the *baz* RNAi transgene, under the control of the tracheal-specific *breathless* promoter, show branching defects (A), but no lumen defects (A'), akin to *baz* mutant terminal cells. Next, we examined terminal cells mutant for *aPKC*^{psu69} that also expressed the *baz* RNAi transgene. We found that these cells still had a gas-filled lumen running through each branch (B'). These results indicate that the *aPKC*^{psu69} mutant terminal cells generate lumens independent of Baz, and therefore Baz does not bridge the interaction between aPKC and Par-6 in *psu69* mutant cells. Dashed white lines demarks the proximal end of the cell; arrows point to gas-filled lumens. Scale bar; 75µm.

TABLE S1 ***15N*** **SNP mapping data**

SNP ID	SNP position[1]	SNP sequence[2]	Detection method[3]	Position relative to *15N*
XA70	17405759	C -> G	*Scr*FI polymorphism	Left
XB78	17503989	A -> T	Sequencing	Left
XE07	17515033	T -> C	*Hae*III polymorphism	Left
XE10	17546733	A -> G	Sequencing	Left
XE01	17605985	G -> T	*Msl*I polymorphism	Right
XB92	17707066	15 bp insertion	Sequencing	Right
XB93	17766184	C -> T	*Aci*I polymorphism	Right

Notes:
1. Based on *D. melanogaster* genome release 5.30 (www.flybase.org). The XB92 insertion is after the base listed.
2. Difference between the *y w* FRT^{19A} (listed first) and *sc cv ct v g f* (listed second) chromosomes. For XB92, the insertion is present on *sc cv ct v g f*.
3. SNP changes a restriction enzyme recognition site or is scored by direct sequencing of PCR products.

CHAPTER 3

EXOCYST-MEDIATED MEMBRANE TRAFFICKING IS REQUIRED FOR BRANCH OUTGROWTH IN *DROSOPHILA* TRACHEAL TERMINAL CELLS

Abstract

Branching morphogenesis, the process by which cells or tissues generate tree-like networks that function to increases surface area or in contacting multiple targets, is a common developmental motif in multicellular organisms. We use *Drosophila* tracheal terminal cells, a component of the insect respiratory system, to investigate branching morphogenesis that occurs on the single cell level. Here, we show that the exocyst, a conserved protein complex that facilitates docking and tethering of vesicles at the plasma membrane, is required for terminal cell branch outgrowth. We find that exocyst-deficient terminal cells have highly truncated branches and show an accumulation of vesicles within their cytoplasm. We also show that vesicle trafficking pathways mediated by the Rab GTPases Rab10 and Rab11 are redundantly required for branch outgrowth. In terminal cells, the PAR-polarity complex is required for branching, and we find the PAR complex is required for proper membrane localization of the exocyst, thus identifying a molecular link between the branching and outgrowth programs. Together, our results

suggest a model where exocyst mediated vesicle trafficking facilitates branch outgrowth, while *de novo* branching requires cooperation between the PAR and exocyst complexes.

Introduction

Branching architecture is found in many biological contexts and facilitates numerous biological functions at both the multiple- and single-cell level. For instance, multicellular branching events in the vertebrate lung increase surface area available for gas diffusion (Gehr et al., 1981; Warburton et al., 2010), while branching in neurons allows individual cells to make numerous contacts with targets, which promotes multiplicative signal propagation and processing (Bilimoria and Bonni, 2013; Vetter et al., 2001). There has been significant progress in elucidating the mechanisms of multicellular branching (Carmeliet and Jain, 2011; Conway et al., 2001; Warburton et al., 2005; 2000), but much less is known about the mechanisms underlying subcellular branching. During subcellular branching, membrane bound cytoplasmic extensions emerge from a cell, these extension undergo further bifurcation events to make a network of membrane bound cellular branches. Such subcellular branching presumably depends on membrane addition to specific sites on the plasma membrane. Iterative rounds of such site specification and outgrowth produce a branched cellular morphology. However, the molecular machinery that regulates site specification and membrane addition required for subcellular branching, remains poorly understood.

We use terminal cells, a component of the *Drosophila* tracheal system, to investigate the molecular machinery required for the development of a branched cellular morphology. Terminal cells are located at the ends of a network of cellular tubes used

for insect respiration, where they elaborate processes onto target tissues to supply oxygen and other gases (Ghabrial et al., 2003; Locke, 1957; Samakovlis et al., 1996). Terminal cells are born during embryogenesis and maintain a simple unbranched morphology until hatching (Guillemin et al., 1996). Throughout larval stages, terminal cells grow and branch extensively in response to the fibroblast growth factor (FGF) Branchless (Bnl), which is secreted by hypoxic target tissues (Jarecki et al., 1999). Bnl activates the FGF receptor Breathless (Btl), expressed in terminal cells, to stimulate both outgrowth and branching (Gervais and Casanova, 2011; Jarecki et al., 1999; Lee et al., 1996; Sutherland et al., 1996). Concurrent with branching, terminal cells also form a subcellular lumen through which oxygen is supplied to hypoxic tissue (Gervais and Casanova, 2010; Jarecki et al., 1999; Ruiz et al., 2012; Schottenfeld-Roames and Ghabrial, 2012).

Genetic screens have identified a number of genes required for terminal cell branching morphogenesis (Baer et al., 2007; Ghabrial et al., 2011; Jones and Metzstein, 2011; B. Levi and Ghabrial, 2006). One mechanism identified in these screens involves the activity of the PAR-polarity complex (Par-6, Baz, aPKC, and Cdc42). In terminal cells the PAR complex is required for terminal cell branching but not outgrowth, demonstrating that these two processes can be decoupled (Jones and Metzstein, 2011). Here, we focus on the molecular machinery required for branch outgrowth in terminal cells and identify a role for the exocyst complex in subcellular branch outgrowth.

The exocyst is an octomeric protein complex consisting of the proteins Sec3, Sec5, Sec6, Sec8, Sec10, Sec15, Exo70, and Exo84, and was originally identified for its role in polarized membrane addition that precedes bud outgrowth and secretion in *S. cerevisiae* (TerBush et al., 1996). The exocyst complex also functions in other cellular contexts. For

instance, the complex has been shown to participate in neurite outgrowth and synapse formation in *Drosophila* (Mehta et al., 2005; Murthy et al., 2003), cilia formation in mammalian cells (Rogers et al., 2004; Zuo et al., 2009), and axon outgrowth and receptor positioning in mammalian neurons (Hazuka et al., 1999; Vega and Hsu, 2001), amongst many other processes. On a molecular level, the exocyst functions by facilitating tethering, docking, and fusion at the plasma membrane (Heider and Munson, 2012; Whyte and Munro, 2002) of vesicles derived from diverse cellular origins, including the Golgi and recycling endosome (He and Guo, 2009; Ponnambalam and Baldwin, 2003). Localization of the exocyst to the plasma membrane is dependent on Rho-family small GTPases (Estravís et al., 2011; Kanzaki and Pessin, 2003; Kawase et al., 2006; Ory and Gasman, 2011; X. Zhang, 2001), while trafficking of exocytic vesicles is controlled by Rab-family GTPases (Das and Guo, 2011; Novick et al., 2006; Pfeffer, 2012). In particular, Rab8, Rab10, and Rab11 have been shown to function with the exocyst in delivery of vesicles to the plasma membrane (Babbey et al., 2010; Chen et al., 1998; Feng et al., 2012; Satoh et al., 2005; Takahashi et al., 2012). Rab10 and Rab11 have also been shown to physically interact with the exocyst through directly binding Sec15 (S. Wu et al., 2005; X.-M. Zhang et al., 2004).

Here, we show the exocyst complex is required for branching and branch outgrowth in terminal cells. We provide evidence that the PAR complex controls terminal cell branching by regulating exocyst localization at the plasma membrane in developing terminal cells. Ultrastructural analysis reveals exocyst deficient terminal cells have defects in vesicle trafficking, implicating polarized membrane addition as a mechanism of branch outgrowth. Finally, we show that redundant vesicle trafficking

pathways converge on the exocyst to contribute to the outgrowth of terminal cell branches. These finding demonstrate how the interplay of several molecular mechanisms contribute to subcellular branching morphogenesis.

Materials and methods

Fly stocks and genetics

Flies were reared on standard cornmeal/dextrose food and larvae were raised at 25°C. The control chromosomes used were: *y w FRT^{19A}, FRT^{82B}* (Xu and Rubin, 1993) and *FRT^{G13}* (Chou, 1996), unless otherwise stated. Alleles analyzed were *sec5^{E10}* (Murthy et al., 2003), *sec6^{KG08199}* (Zhou et al., 2007), *sec10^{f03085}* (Bloomington *Drosophila* Stock Center), *sec15^{1}* (Mehta et al., 2005), *par-6^{29VV}* (Jones and Metzstein, 2011), *aPKC^{k06403}* (Wodarz et al., 2000), *baz^{FA50}* (Wodarz et al., 2000), *shi^{ts1}* (Masur et al., 1990), *Rab5^{k08232}* (Wucherpfennig et al., 2003). For mosaic analysis, we used the stocks: *y w P{w^{+},btl-Gal80} FRT^{19A}, hsFLP^{122}; btl-Gal4 UAS-GFP* (Jones and Metzstein, 2011), *y w hsFLP^{122}; FRT^{G13} P{w^{+}, tub-Gal80} ; btl-Gal4 UAS-GFP* (gift from S. Luschnig), and *y w hsFLP^{122}; btl-Gal4 UAS-GFP ; FRT^{82B} P{w+ tub-Gal80}/TM6B* (gift from A. Ghabrial). To perform mosaic analysis, *shi^{ts}*, *sec6*, and *sec10* were recombined onto *FRT^{19A}*, *FRT^{G13}* and *FRT^{82B}*, respectively, using standard methods. *UAS-Sec5* RNAi (27526), *UAS-Sec6* RNAi (27314), *UAS-Sec10* RNAi (27483), *UAS-Sec15* RNAi (27499), *UAS-Chc* RNAi (27530), *UAS-Rab11* RNAi (27730), *UAS-YFP-Rab11* DN (23261), *UAS-YFP-Rab10* DN (9786), and *UAS-Cdc42*^{N17} (6288) were obtained from the Bloomington *Drosophila* Stock Center (stock numbers shown in parentheses). *Rab5* (stock number 111-239) was obtained from the *Drosophila* Genetic Resource Center.

Homozygous mutant cells were generated using the mosaic analysis with a repressible cell marker (MARCM) technique (Lee and Luo, 1999). To generate mosaics, 0-6 hr embryos were collected in fly food vials at 25° C and treated to a 45 minute heat shock at 38° C in a circulating water bath, then reared at 25° C until the L3 stage (Jones and Metzstein, 2013). Temperature sensitive *shi* alleles were heat shocked and maintained at room temperature overnight then reared at the restrictive temperature of 29º C until they reached L3.

Light microscopy of terminal cells

Wandering third instar larvae were collected and heat-fixed according to a standard protocol developed in our lab (Jones and Metzstein, 2013). Images were taken on Zeiss AxioImager M1 equipped with an AxioCam MRm.

Immunofluorescence

Wandering third instar larvae were dissected in 1X PBS to make fillets exposing the tracheal system. Fillets were fixed for 30 minutes in 4% PFA in 1X PBS, rinsed 3 times for 15 minutes in 1X PBST (1X PBS + 0.1% TX100), blocked for 30 minutes at room temperature in PBSTB (1X PBST + 0.02% BSA), then incubated with primary antibody overnight at 4°C. Fillets were then rinsed 3 times for 15 minutes in 1X PBSTB and incubated with secondary antibody for 2 hr at room temperature. Fillets were then rinsed and mounted on glass slides in ProLong® Gold antifade reagent (Invitrogen). Antibodies were used in the following concentrations: goat anti-sec8 (Beronja et al., 2005), at 1:250 and mouse anti-GFP, at 1:1000 (Clontech, #632375). Secondary

antibodies, conjugated to Alexa-488 or Alexa-568 (Molecular Probes), were used at 1:1000. Imaging was performed using a Leica TCS SP2 confocal microscope. A Z-stack of 10-25 slices was imaged for each setting sequentially. An average intensity projection was generated in Image-J.

Terminal cell branching and outgrowth quantification

Terminal cell branch number and outgrowth were determined using methods described previously (Jones and Metzstein, 2011). Outgrowth was quantified as the ratio of the length of class I branches to the number of class I branches. For statistical comparisons we used the two-tailed Mann-Whitney U test.

Transmission electron microscopy

High pressure freezing

We fixed samples for TEM analysis using a protocol developed in our lab, the details of which will be published later. Briefly, larvae were picked at late L1 or early L2 and kept for a short time in a drop of 1X PBS prior to freezing. Larvae were loaded into Type A specimen carriers (Technotrade, cat. # 24150) and carriers were filled with *E. coli* as a cryoprotectant. Loaded Type A carriers were closed with the flat side of a Type B specimen carrier (Technotrade, cat. # 24250). Carriers were immediately subjected to high pressure-freezing using a BAL-TEC HPM 010 freezer (BAL-TEC, Inc., Carlsbad, CA). Carriers containing frozen larvae were quickly transferred to cryovials that contained a precooled (-90°C) mix of 2% osmium tetroxide (OsO_4) and 0.1% Uranyl Acetate in 97% acetone (McDonald and Müller-Reichert, 2002) in a Leica EM AFS

(Leica Microsystems, Vienna, Austria). To enhance membrane contrast 3% water was added to the fixative (Walther and Ziegler, 2002). Specimens underwent freeze substitution for 72 hrs at -90°C, were gradually warmed at the rate of 5°C/hrs to -20°C, and were kept at this temperature for 8-16 hrs. The temperature was slowly raised to 20°C at the rate of 10°C/hr, and samples then were removed from the AFS unit to room temperature and rinsed immediately with pure acetone 5 times as follows: 2x15 min, 1x30min, and 2x1 hr, before infiltration and embedding.

Resin infiltration and embedding

Infiltration was performed by incubating the specimens in a gradually increasing concentrations of Durcupan Fluka epoxy resin (Fluka Analytical cat. # 44610) at room temperature as follows: 30% epoxy resin in acetone for 5 hrs; 70% resin in acetone overnight; and 90% resin in acetone for 8 hrs-overnight. Specimens were transferred to 100% resin for 24 hrs with 2 changes, then transferred to fresh 100% resin with 2 changes over a 3 hr period, after which polymerization was performed at 60°C for 48 hrs.

Sectioning and imaging

Ultrathin (50-60nm) sections were obtained using a diamond knife (Diatome) and Reichert Ultracut E microtome. Sections were collected on coated copper grids and post-stained with 2.5% uranyl acetate for 10 minutes. Sections were imaged at 120 kV using a FEI Tecnai 12 transmission electron microscope.

Vesicle quantification

Vesicle accumulation was quantified by determining the average number of cytoplasmic vesicles per section, in ultrathin sections. From each genotype, a total of at least 8 sections were evaluated (2-6 sections from 3-4 cells each). Vesicles were defined as roughly circular membrane bound structures of 50 nm or greater in diameter lacking electron dense material in their lumens.

Results

The exocyst complex is required for terminal cell branch outgrowth

To test if the exocyst complex is required for terminal cell branching or outgrowth, we used the MARCM system (Lee and Luo, 1999) to generate mosaic animals with terminal cells mutant for exocyst components. The use of mosaics allowed us to investigate the cell autonomous role of the exocyst in terminal cells, as well as to bypass any other requirement for organismal development. We found that terminal cells homozygous for null alleles of *sec5, sec6, sec10,* and *sec15* showed similar defects, including fewer branches and shorter branch lengths (Figure 3.1A-E; quantitated in 3.1G and 3.1H). We used RNAi-mediated gene knockdown to test a role for other members of the exocyst complex for which null alleles were not available. We found RNAi-mediated knockdown of exocyst complex members *exo70* and *exo84* resulted in terminal cell defects qualitatively similar to those of other exocyst deficient cells (Figure S3.1). By contrast, as previously reported (Jones and Metzstein, 2011), PAR-polarity proteins such as Par-6 are required for terminal cell branching, but not outgrowth: terminal cells deficient for *par-6* and other PAR polarity genes have defects in the total number of

branches, but branches that are present extend as far as wild-type branches (Figure 3.1F-H and S3.2).

Our data suggests the exocyst complex is required for both branch specification and outgrowth. However, it is possible that the exocyst is primarily required for outgrowth but is less important in branch specification, but this cannot be observed since outgrowth is required to observe specified branches. To test this possibility, we used RNAi to partially inactivate exocyst complex members in terminal cells. We found RNAi-mediated knockdown of *sec5, sec6, sec10,* or *sec15,* resulted in similar branching defects to those observed in null alleles, but relatively mild outgrowth defects, suggesting the knockdown was indeed incomplete (Figure 3.2A-E; quantitated in Figure 3.2P). Interestingly, close examination of branches in these RNAi knockdown cells revealed small membrane protrusions along their lengths (Figure 3.2G-J). This morphology differed from that of wild-type (Figure 3.2F) or exocyst-complex null cells, in which branches nearly always have a smooth, tapered appearance. We interpret these protrusions to be primitive branch sites that have undergone specification, but fail to extend when exocyst function is reduced. These results suggest that the primary role of the exocyst complex is in branch outgrowth. We also note that these nascent branches are more numerous than established branches, suggesting a mechanism of lateral branch inhibition may help pattern terminal cells.

We next asked whether the PAR complex and the exocyst complex had independent roles in terminal cell branching, or whether they were participating together to facilitate this process. To do this we tested for exacerbation of branching defects in terminal cells that were mutant for a *par-6* null allele and simultaneously expressing

RNAi directed against exocyst complex members. We found branching defects observed upon RNAi of *sec5*, *sec6*, *sec10,* and *sec15* were not exacerbated by loss of Par-6 (Figure 3.2K-O); the double mutant branching defects are quantitatively similar to defects observed by RNAi expression alone (Figure 3.2P). This result suggests the exocyst complex and the PAR complex likely participate in a common process required for terminal cell branching.

The PAR-polarity complex is required for proper exocyst localization in terminal cells

The Rho GTPase Cdc42 has been shown to directly interact with exocyst-complex members Sec3 (X. Zhang, 2001) and Exo70 (H. Wu et al., 2010). Cdc42 is a component of the PAR-polarity complex, which is required for terminal cell branching morphogenesis (Jones and Metzstein, 2011). Thus, Cdc42 is a candidate to link polarized membrane addition by the exocyst with branch specification by the PAR complex. To investigate this, we determined if the PAR complex was required for localization of the exocyst in terminal cells. We used immunofluorescence to visualize localization of the exocyst-complex member Sec8 in wild-type and *Cdc42* mutant terminal cells (Figure 3.3A-F), since localization of Sec8 is representative of the localization of the assembled exocyst complex at the cell membrane (Rivera-Molina and Toomre, 2013). We found that in wild-type terminal cells, Sec8 protein is spread diffusely throughout the plasma membrane and also concentrated in distinct membrane-localized puncta (Figure 3.3B, B' and C). However, in the absence of Cdc42, the punctate membrane localization is completely lost (Figure 3.3E, E' and F), leaving only the diffuse membrane staining. We

obtained similar results when we examined a mutant of another PAR-complex member, *aPKC* (Figure 3.3G-I). Together, these results suggest the PAR-polarity complex is required for localized concentration of the exocyst on the terminal cell plasma membrane. Since the PAR complex is specifically required for terminal cell branching, these results imply the exocyst puncta are related to processes involved in new branch formation.

Vesicle trafficking is abnormal in exocyst and Cdc42 mutant terminal cells

Given the role of the exocyst complex in vesicle trafficking and fusion at the plasma membrane, one prediction is that loss of exocyst function would result in an accumulation of cytoplasmic vesicles in mutant terminal cells. Such a phenotype has been observed in exocyst defective yeast and mammalian cells (Guo et al., 1999; TerBush et al., 1996). We tested if this is the case in exocyst defective terminal cells using transmission electron microscopy (TEM). We found that in wild-type terminal cells, intracellular vesicles are rarely observed in the cytoplasm (0.13±0.35, vesicle per section; Figure 3.4A). However, when RNAi is used to reduce expression of either *sec5* (Figure 3.4B) or *sec15* (Figure 3.4C), we found the terminal branch cytoplasm contained many large intracellular vesicles, with *sec5*-deficient and *sec15*-deficient terminal cells containing an average of 4.7±1.5 and 1.9±1.0 vesicles per section, respectively. Since each section represents only a small fraction of the cell, these data indicate that exocyst-mutant terminal cells accumulate a large number of vesicles in their cytoplasm.

Since Cdc42 is required for localization of the exocyst to the plasma membrane, we predicted we would observe a vesicle accumulation phenotype similar to exocyst complex mutants in terminal cells defective for *Cdc42*. When we examined the

ultrastructure of terminal cells expressing dominant-negative Cdc42, we observed an accumulation of intracellular vesicles similar to that observed in *sec5* and *sec15* deficient cells. The defects observed in *Cdc42* defective cells are even more severe than those observed in exocyst-mutant terminal cells (8.1±2.5 vesicles per section). Our results suggest that vesicle trafficking in terminal cells is abnormal in the absence of the exocyst or Cdc42.

Multiple trafficking pathways contribute to branch outgrowth

Rab GTPases have been shown to work in concert with the exocyst complex to mediate trafficking of vesicles to the plasma membrane (Das and Guo, 2011). Rab10 is involved in trafficking of vesicles derived from the Golgi (Lerner et al., 2013; Sano et al., 2007; Wang et al., 2011), and Rab11 is primarily involved in trafficking of vesicles from recycling endosomes (Chen et al., 1998; Satoh et al., 2005; Takahashi et al., 2012). To determine the role of these Rab proteins in terminal cell development, and to identify the source of vesicles that contribute to branch outgrowth, we expressed dominant-negative forms of Rab10 or Rab11 (J. Zhang et al., 2007) in terminal cells. We found expression of either *rab10-DN* (Figure 3.5A) or *rab11-DN* (Figure 3.5B) resulted in strong defects in total branch number, but only mild outgrowth defects (quantified in Figure 3.5F and G). Interestingly, we found terminal cells coexpressing *rab10-DN* and *rab11-DN* (Figure 3.5C) show outgrowth defects that are much more severe than either of the single mutants and are comparable to those of an exocyst null mutant (Figure 3.5F and G). At the ultrastructural level, Rab10 and Rab11 defective terminal cells show cytoplasmic vesicle accumulation similar to that observed in exocyst complex and Cdc42 defective cells

(Figure 3.5D and E). These findings imply that redundant vesicle trafficking pathways contribute to terminal branch outgrowth and these pathways are likely to converge on the exocyst to facilitate this process.

Endocytosis is required for terminal cell branching

As Rab11 is primarily involved in trafficking from the recycling endosome to the plasma membrane, we predicted endocytosis might also be important for terminal cell development. To test this, we examined critical components of the clathrin-mediated endocytosis machinery: clathrin heavy chain, a major component of clathrin-coated pits (Conibear, 2010; Swan, 2013) and dynamin, a GTPase known to facilitate scission of endocytic vesicles from the plasma membrane (Ramachandran, 2011). We found terminal cells expressing RNAi directed against *Chc* (clathrin heavy-chain) or mutant for *shibire* (*shi*, the *Drosophila* homolog of dynamin) have severe defects in total branch number, but only mild defects in branch outgrowth (Figure S3.3). Additionally, terminal cells mutant for *Rab5*, a key regulator of early endosome formation (Pfeffer, 2001), show defects similar to *shi* or *Chc* mutant cells in branching and outgrowth (Figure S3.3). These defects are very similar to those caused by inhibiting Rab11, suggesting a trafficking pathway of endocytosis to recycling endosomes is required for terminal cell branching.

Discussion

Drosophila tracheal terminal cells have proven to be a powerful model for investigating molecular mechanisms controlling the formation of a branched cell. In

particular, much has been learned about the signaling pathways required for terminal cell specification and initial development (Gervais and Casanova, 2011; Ghabrial et al., 2003; Guillemin et al., 1996). However, much less is known about the mechanisms of terminal cell branching and branch outgrowth. Previously, we showed the PAR-polarity complex is necessary for branching and functions downstream of the FGF signaling pathway that regulates growth of terminal cells towards hypoxic tissue (Jarecki et al., 1999; Jones and Metzstein, 2011). However, the PAR-polarity complex is not in itself required for branch outgrowth. Here, we characterize a role for exocyst-mediated vesicle trafficking in terminal cell branch outgrowth. We find disruption of all tested exocyst-complex components results in severe branch extension defects in terminal cells. Branch outgrowth requires membrane addition at specific sites and the exocyst is known to facilitate docking and fusion of vesicles at target membranes (He and Guo, 2009; Lipschutz and Mostov, 2002). Our ultrastructural analysis of terminal cells defective for exocyst-complex components reveals an accumulation of vesicles within the cytoplasm. These vesicles are likely those that would deliver membrane required for branch extension, but in exocyst defective cells are unable to fuse with their target membranes and remain trapped in the cytoplasm. Thus, we propose that exocyst-mediated vesicle fusion is a key mechanism of branch outgrowth in terminal cells.

In various cellular contexts, the exocyst facilitates membrane addition required for both general and polarized cell growth (Cole and Fowler, 2006; Heider and Munson, 2012). General cell growth is a process of membrane addition that occurs throughout the entire plasma membrane and leads to an overall increase in cell size and length. Conversely, polarized outgrowth occurs at specific sites and results in extension of small

regions of the cell membrane. Terminal cells presumably employ both types of cellular growth: general growth, as established branches get longer and wider during larval development, and polarized outgrowth, required for new branch formation. We find that in terminal cells, the exocyst is localized diffusely throughout the cell membrane, as well as in greater concentrations at specific sites on the membrane. We find that these sites of membrane concentration are dependent upon the PAR complex, as the punctate localization is lost and we only observed diffuse membrane staining in PAR-complex mutant terminal cells. PAR complex mutants do not show defects in branch outgrowth, indicating that the diffusely localized pool of exocyst is sufficient for growth of the cell and for the extension of established branches. Thus, it appears that PAR complex-dependent membrane concentration of the exocyst is required only for *de novo* branching. We propose a model that *de novo* branch outgrowth is driven by a transient increase in exocyst complex concentration at branch sites (Figure 3.6). As a potential mechanism for such an increase, we propose that local FGF receptor activation at the plasma membrane promotes a transient increase in exocyst concentration, leading to exocyst-mediated membrane addition at these sites, resulting in new branch formation. This process continues through iterative rounds of specification and outgrowth to generate a branched cellular morphology. A potential molecular link between FGF receptor activation and exocyst localization, is the PAR complex component Cdc42. It is known that receptor tyrosine kinase activation can lead to the recruitment of PI3K (Funamoto et al., 2002) and thus to a local increase in phosphatidylinositol (3,4,5)-triphosphate (PIP_3) concentration. PIP_3 in turn can recruit GEFs that activate Cdc42 (Yang et al., 2012), and Cdc42 is known to stimulate assembly of the exocyst complex (Estravís et al., 2011; Kawase et al.,

2006; H. Wu et al., 2010). One part of this model is that the PAR complex is not specifically localized to branch sites, but instead is locally activated to promote branching. This is consistent with our previous observation that the PAR complex, despite being required for branching, is not specifically localized to branch sites in terminal cells. In this way the PAR complex facilitates branching but is not instructive for this process. Finally, it is important to note that concentrated exocyst localization is found throughout the membrane and not only at branch sites. Since branches in terminal cells are typically spaced apart it is likely that a mechanism of lateral inhibition occurs upon branch specification and outgrowth, as may be observed in our partial exocyst knockdown experiments. Testing whether these mechanism function in terminal cells will likely require the development of techniques that will allow live cell imaging and biochemical approaches to detect changes in local concentrations of the key components (Schottenfeld-Roames and Ghabrial, 2012).

The process of *de novo* branch formation requires addition of membrane to a specific site on the cell surface. Vesicles that deliver membrane to the plasma membrane are primarily derived from two intracellular compartments: the Golgi and the recycling endosome (Bryant et al., 2010; Pfeffer, 2012; Ponnambalam and Baldwin, 2003; Prigent et al., 2003; Whyte and Munro, 2002). To investigate which of these compartments is the likely source of membrane used for branch outgrowth, we examined terminal cells where we had inactivated pathway-specific vesicle-trafficking genes. We found that disruption of either Golgi to plasma membrane trafficking, through knockdown of *Rab10*, or disruption of recycling endosome to plasma membrane trafficking, through knockdown of *Rab11*, leads to only mild branch outgrowth defects. However, the simultaneous

inactivation of *Rab10* and *Rab11* leads to very strong outgrowth defects, comparable to loss of the exocyst. These results suggest that the vesicles required for branch outgrowth can be derived either from the Golgi or from the recycling endosome. Such a mechanism of terminal branch outgrowth contrasts with axonal growth, in which membrane is thought to be derived primarily from the Golgi (Tekirian, 2002), but may have parallels with dendritic morphogenesis, in which membranes can come from multiple sources (Sann et al., 2009). We do not yet know if the vesicles derived from these two sources have different functional properties, for instance in the delivery of proteins or other macromolecules required for later steps in terminal cell branch function, such as guidance (Englund et al., 2002; Steneberg and Samakovlis, 2001) or adhesion to underlying substrates (B. P. Levi et al., 2006).

Mechanisms of terminal cell branching morphogenesis encompass a number of important cell biological processes including, a unique combination of cellular organization and polarity, as well as trafficking processes. Here, we have shown exocyst-mediated vesicle trafficking is critical for terminal cell branch outgrowth and propose a model where localized PAR complex activity regulates localization of the exocyst. Continued genetic analysis of mutants obtained from this pliable genetic system should reveal more about the general processes necessary for subcellular morphogenesis, which are common to branched cells such as neurons, oligodendrocytes, and megakaryocytes.

Figure 3.1. The exocyst complex is required for terminal cell morphogenesis. (A-F) Terminal cells in MARCM mosaic L3 larvae, with homozygous cells labeled with GFP. (A) Wild-type terminal cells show extensive outgrowth and subcellular branching. (B-E) Terminal cells homozygous for exocyst complex members *sec5*, *sec6*, *sec10*, or *sec15* show a reduction in branching and branch outgrowth, showing only a few branches that are much shorter than those observed in wild-type. (F) Cells mutant for *par-6* have fewer branches than wild-type cells, but normal outgrowth. (G) Quantification of terminal cell branch number, measured by counting the total number of branches per cell. (H) Quantification of terminal cell outgrowth, measured as the average length of class I branches (the first side branches to emerge from a terminal cell). *Significant difference from *par-6* ($p<0.01$); n.s., not significant ($p>0.05$). Dashed white lines indicate the proximal ends of the GFP-labeled cell. Scale bar, 75 μm. Error bars represent ±2 SEM.

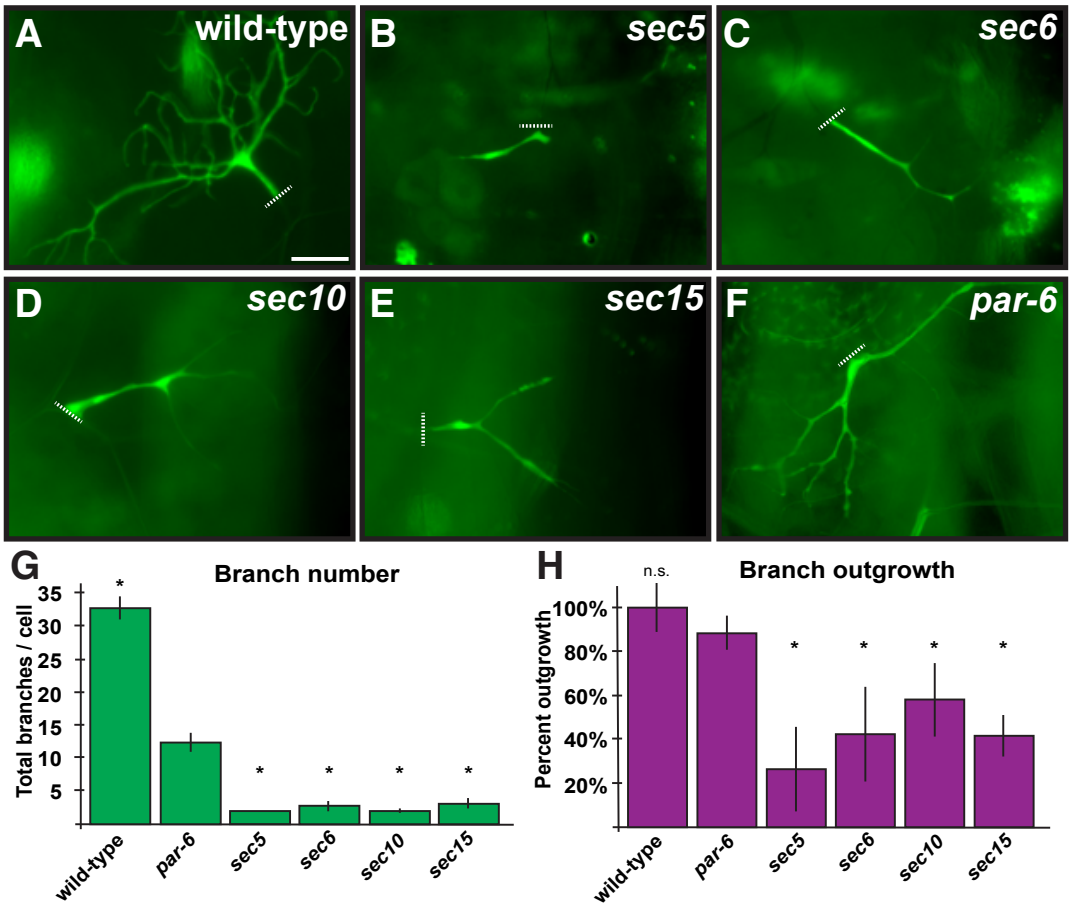
A
wild-type
B
sec5
C
sec6
D
sec10
E
sec15
F
par-6
G
Branch number
Total branches / cell
35
30
25
20
15
10
5
*
*
*
*
*
wild-type
par-6
sec5
sec6
sec10
sec15
H
Branch outgrowth
Percent outgrowth
100%
80%
60%
40%
20%
n.s.
*
*
*
*
wild-type
par-6
sec5
sec6
sec10
sec15

Figure 3.2. The exocyst is required for terminal cell branch outgrowth. (A-O) MARCM was used to generate mosaic animals with GFP-marked terminal cells expressing RNAi transgenes directed against specific exocyst genes. (A) Wild-type terminal cells have many subcellular branches and individual branches (F) have a smooth tapered appearance. (B-E) Terminal cells expressing RNAi directed against exocyst complex members have fewer branches than wild-type cells. (G-J) Individual branches of exocyst RNAi cells show numerous short extensions along their lengths. (K) Terminal cells homozygous for a null allele of *par-6,* show branching defects, but normal outgrowth. (L-O) RNAi of exocyst components in a *par-6* mutant result in defects similar to those observed with RNAi alone. (P) Quantification of terminal cell branch number measured by counting the total number of branches per cell. † ($p=0.05$); n.s., not significant ($p<0.05$). Dashed white lines indicate the proximal ends of the GFP-labeled cell. Scale bars are 75 μm within each column. Error bars represent ±2 SEM.

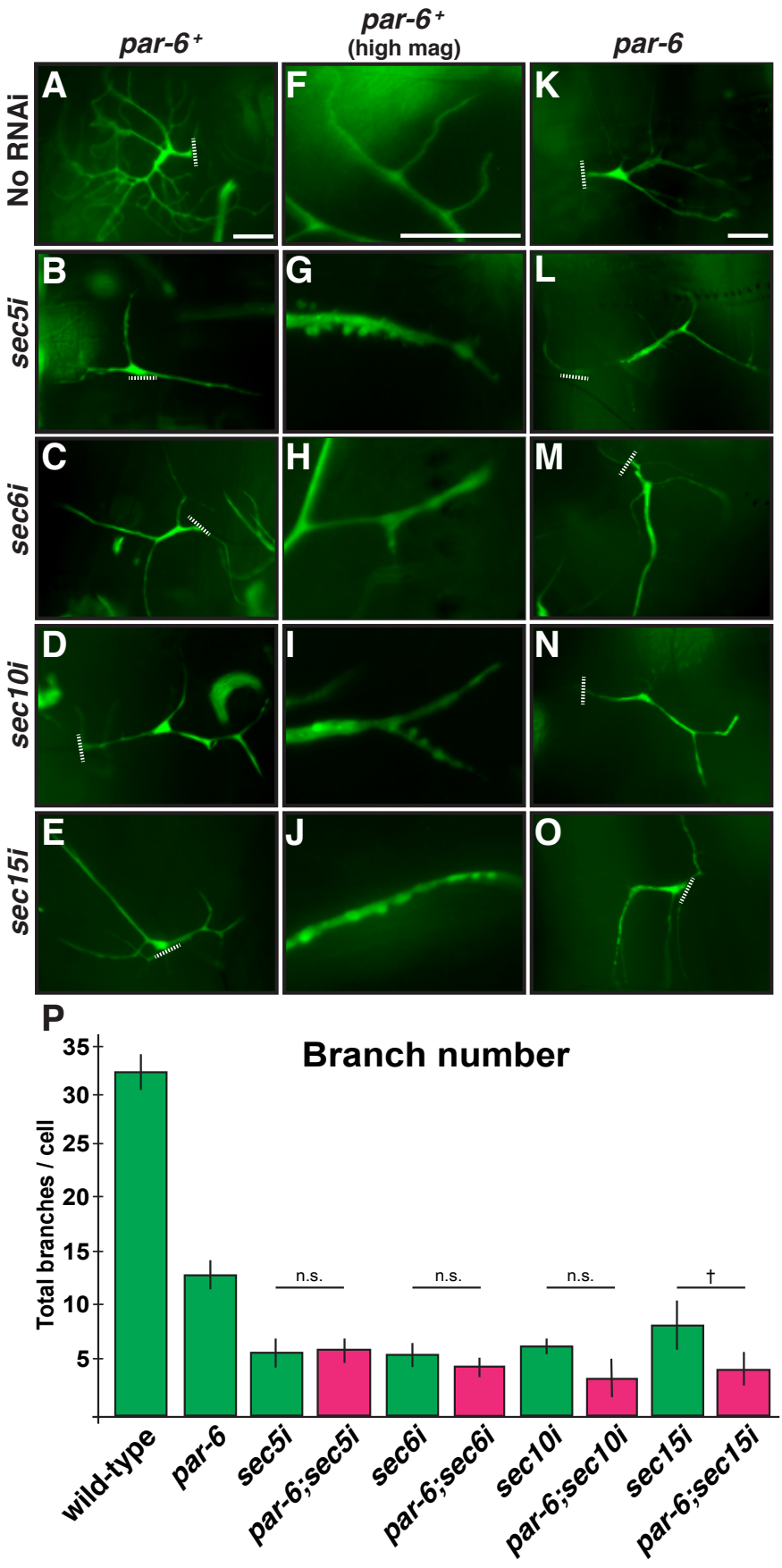
par-6+
par-6+
(high mag)
par-6
No RNAi
sec5i
sec6i
sec10i
sec15i
A
B
C
D
E
F
G
H
I
J
K
L
M
N
O
P
Branch number
Total branches / cell
35
30
25
20
15
10
5
n.s.
n.s.
n.s.
†
wild-type
par-6
sec5i
par-6;sec5i
sec6i
par-6;sec6i
sec10i
par-6;sec10i
sec15i
par-6;sec15i

Figure 3.3. The PAR complex is required for exocyst membrane concentration in terminal cells. Terminal cells in L3 mosaic larvae were identified by cytoplasmic GFP expression and then probed with anti-GFP (A, D, and G) and anti-Sec8 (B, E, and H) antisera. (C, F and I) merged channels (GFP in green, anti-Sec8 in red). (B and B') In wild-type cells, Sec8 is found diffusely throughout the membrane and in distinct puncta. Terminal cells homozygous for *Cdc42* (E and E') or *aPKC* (H and H') lose the punctate but not the diffuse membrane staining. In the image of the *aPKC* mutant cell, normal Sec8 puncta can be observed in an adjacent, non-GFP labeled wild-type cell (asterisk). B', E', and H' show magnified views of B, E, and H (boxed regions). Scale bars: A-I, 10 μm; B', E', and H', 2.5 μm.

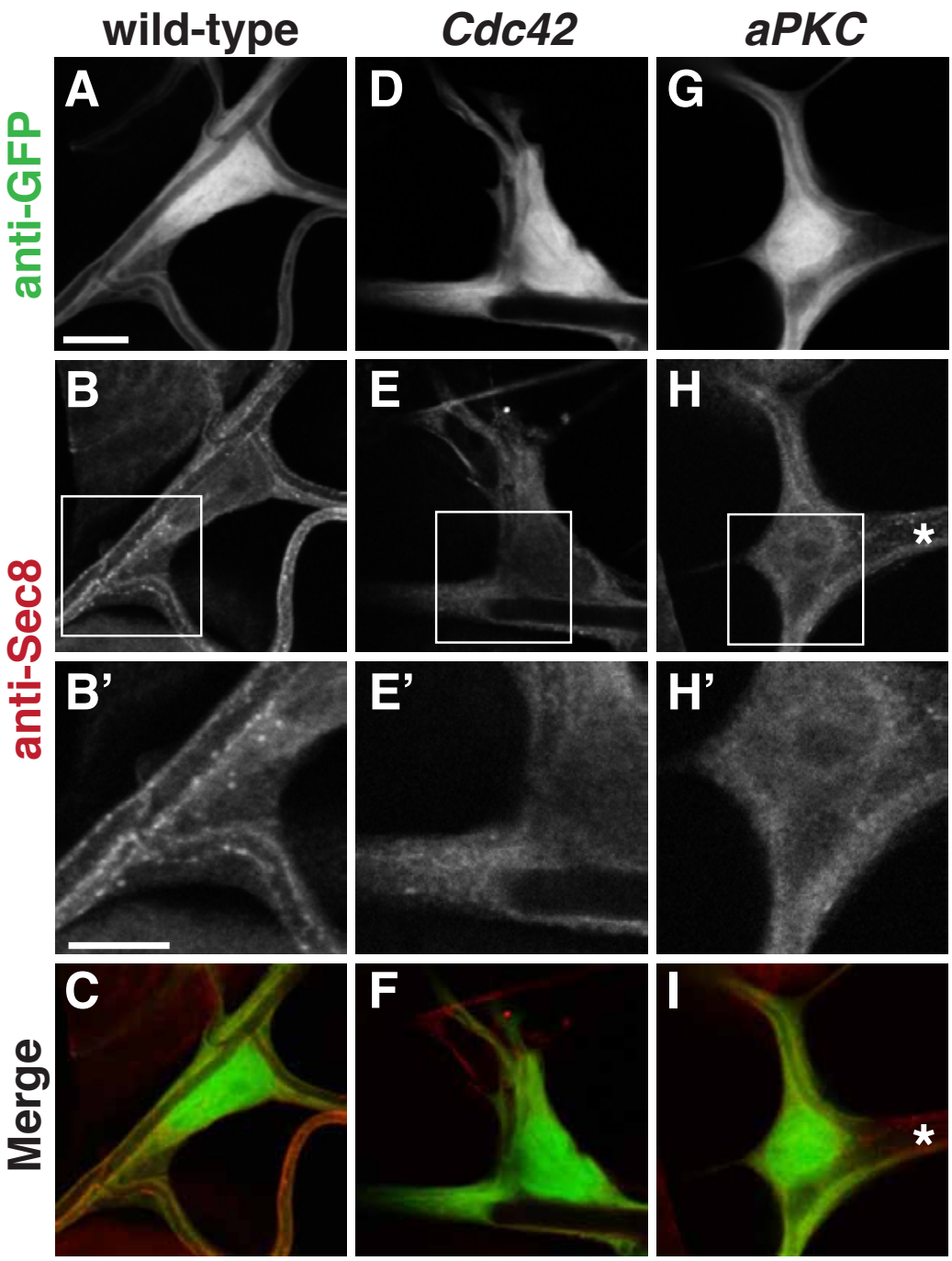
wild-type
Cdc42
aPKC
anti-GFP
anti-Sec8
Merge
A
D
G
B
E
H
B'
E'
H'
C
F
I
*
*

Figure 3.4. Terminal cells defective for the exocyst complex or Cdc42 accumulate cytoplasmic vesicles. (A-D) Terminal cell branch ultrastructure observed in thin cross-section using transmission electron microscopy (TEM). Cytoplasmic vesicles are outlined in orange and green shows an apparently swollen Golgi. (A) Wild-type terminal cell branches show circular crosssectional morphology, the lumen is expanded and clear of cytoplasmic material and the cytoplasm is devoid of large vesicles. Notes lysosomes appear as circular structures containing electron dense staining. (B and C) Terminal cells expressing RNAi for exocyst complex member *sec5* or *sec15*, show an accumulation of vesicles in their cytoplasm. (D) Terminal cells expressing a dominant-negative Cdc42 also show vesicle accumulation. Arrows in A indicate microtubules (MT), which are much smaller than cytoplasmic vesicles (close up in inset). Scale bars, 400 nm.

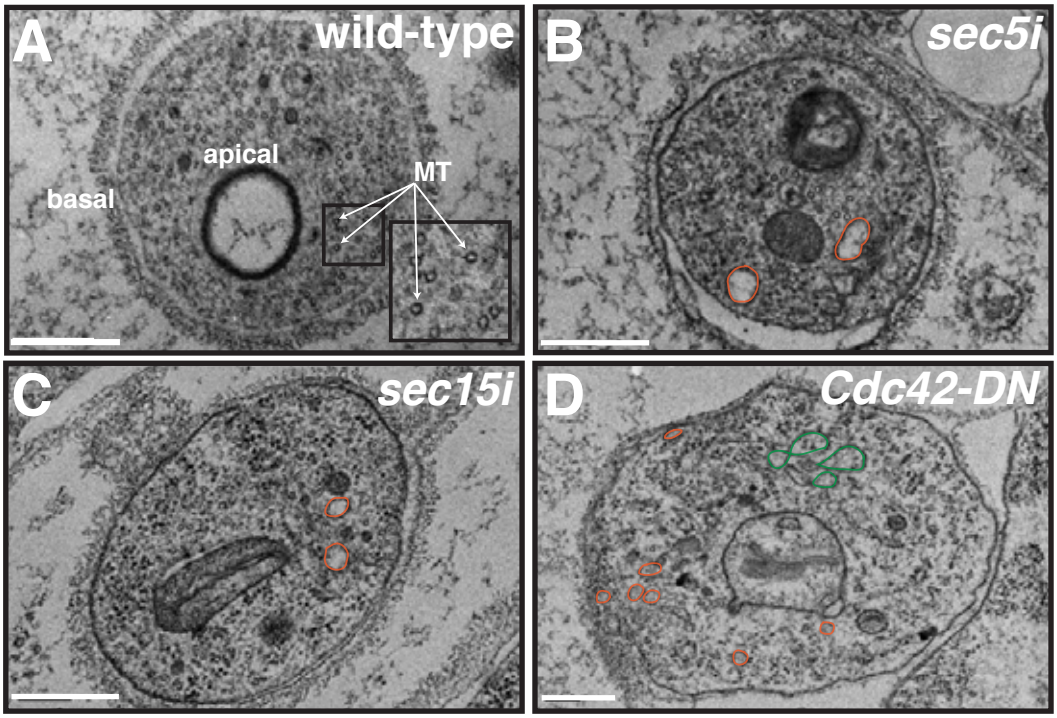
A
wild-type
apical
basal
MT
B
sec5i
C
sec15i
D
Cdc42-DN

Figure 3.5. Rab GTPases Rab10 and Rab11 are required for terminal cell branch development. (A-C) Mosaic animals were generated using MARCM and GFP co-expressed with dominant-negative transgenes for the indicated Rab. (A and B) Terminal cells expressing dominant-negative Rab10 or dominant-negative Rab11 show defects in branching, but only mild defects in outgrowth. (C) Coexpression of Rab10-DN and Rab11-DN leads to severe branching and outgrowth defects. (D and E) TEM of branch ultrastructure in terminal cells expressing dominant-negative Rab10 or RNAi directed against Rab11 show accumulation of vesicles within the cell cytoplasm. Cytoplasmic vesicles are pseudo-colored orange. (F and G) Quantification of branch number and outgrowth. * ($p<0.01$). Dashed white lines indicate the proximal end of the GFP-labeled cell (A-C). Scale bars, A-C, 75 μm; D and E, 200 nm.

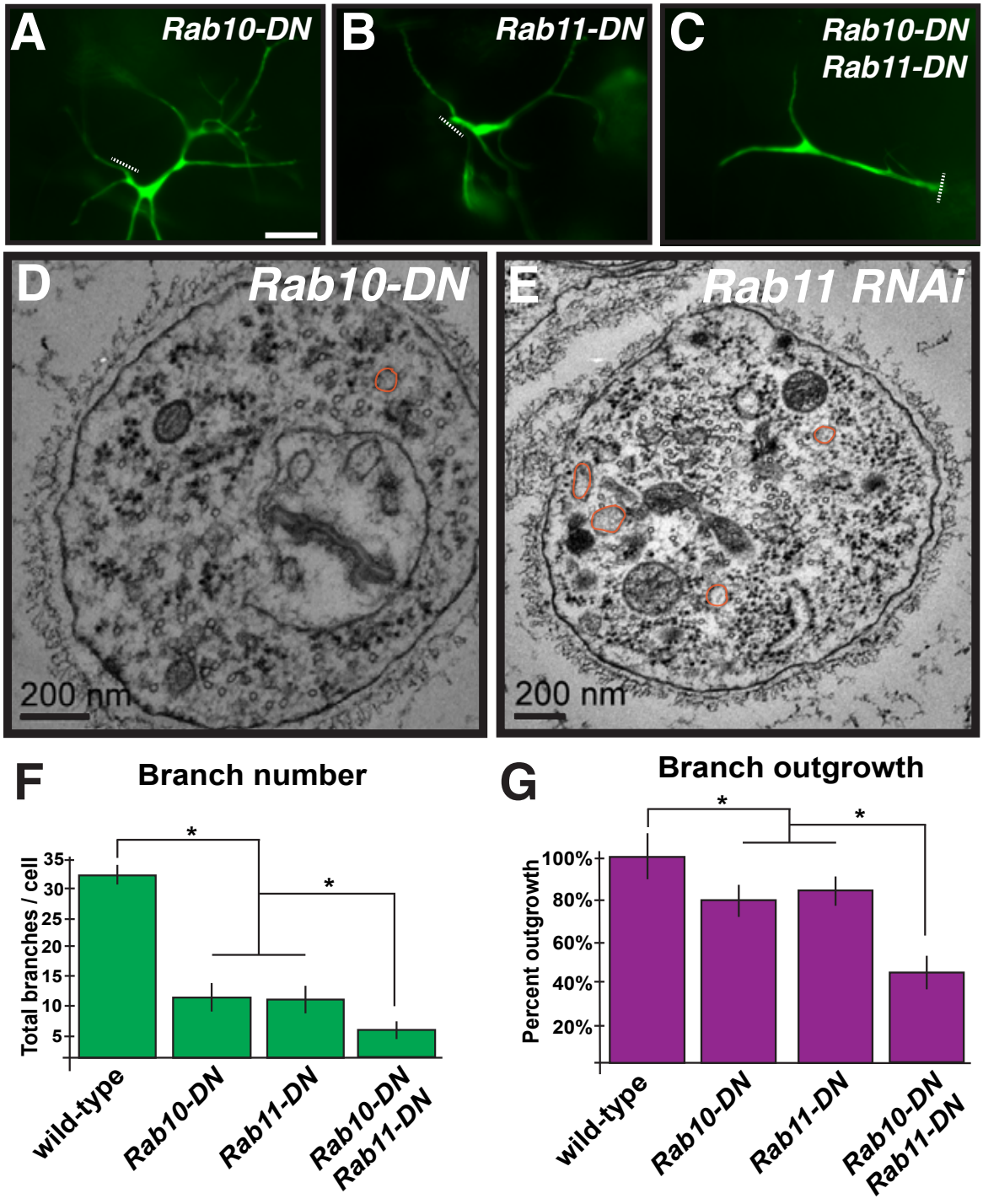
A
Rab10-DN
B
Rab11-DN
C
Rab10-DN
Rab11-DN
D
Rab10-DN
200 nm
E
Rab11 RNAi
200 nm
F
Branch number
Total branches / cell
35
30
25
20
15
10
5
*
*
wild-type
Rab10-DN
Rab11-DN
Rab10-DN
Rab11-DN
G
Branch outgrowth
Percent outgrowth
100%
80%
60%
40%
20%
*
*
wild-type
Rab10-DN
Rab11-DN
Rab10-DN
Rab11-DN

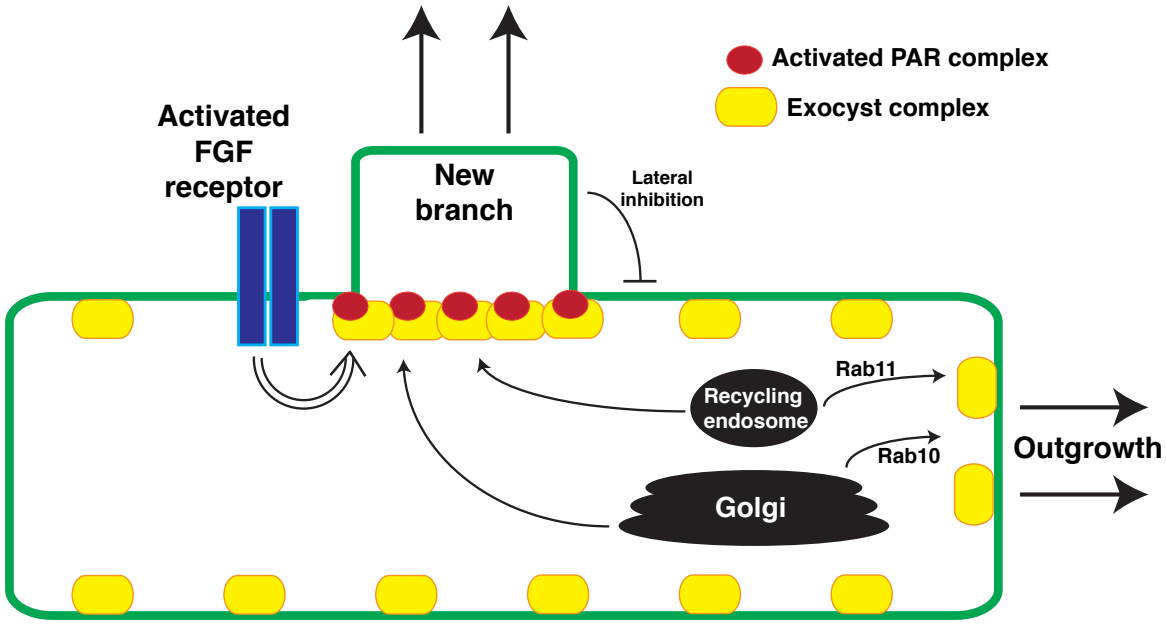

Figure 3.6. Branching morphogenesis model. Activation of the FGF receptor leads to local concentration of the exocyst complex, via activation of the PAR complex. General cell growth and branch elongation is controlled by trafficking of vesicle from the recycling endosomes or Golgi to the exocyst. Newly formed branches inhibit outgrowth of subsequent branches by a process of lateral inhibition.

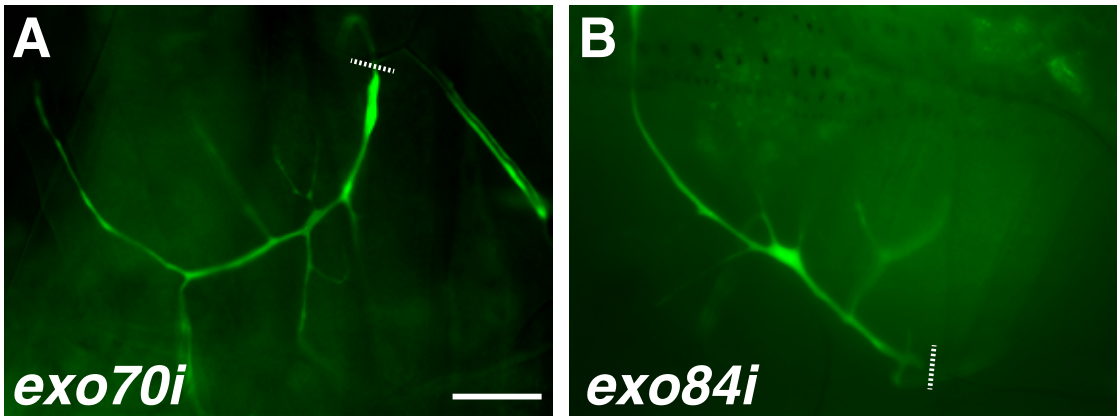

Figure S3.1. Terminal cells expressing RNAi directed against exocyst complex members show branching and outgrowth defects. (A and B) GFP labeled terminal cells in MARCM mosaic L3 larvae expressing RNAi directed against exocyst complex members exo70 and exo84 have defects in branching and branch outgrowth. Scale bar, 75 μm.

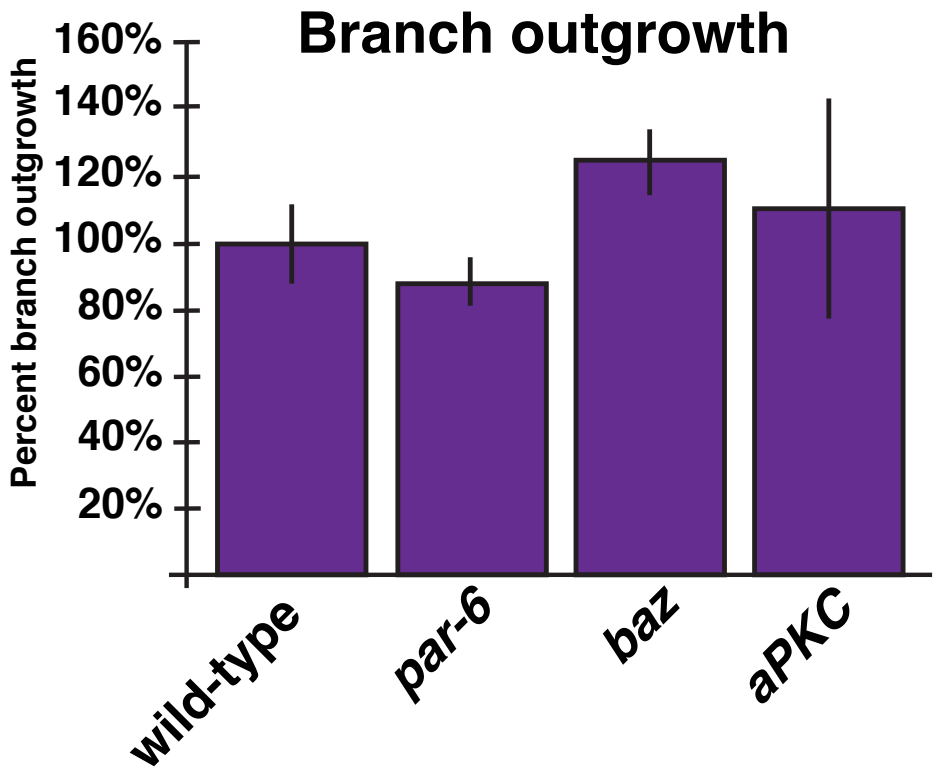

Figure S3.2. The PAR-polarity complex is not required for terminal cell branch outgrowth. Quantification of terminal cell branch outgrowth measured as the average length of class I branches (the first side branches to emerge from a terminal cell). Error bar represent ±2 SEM.

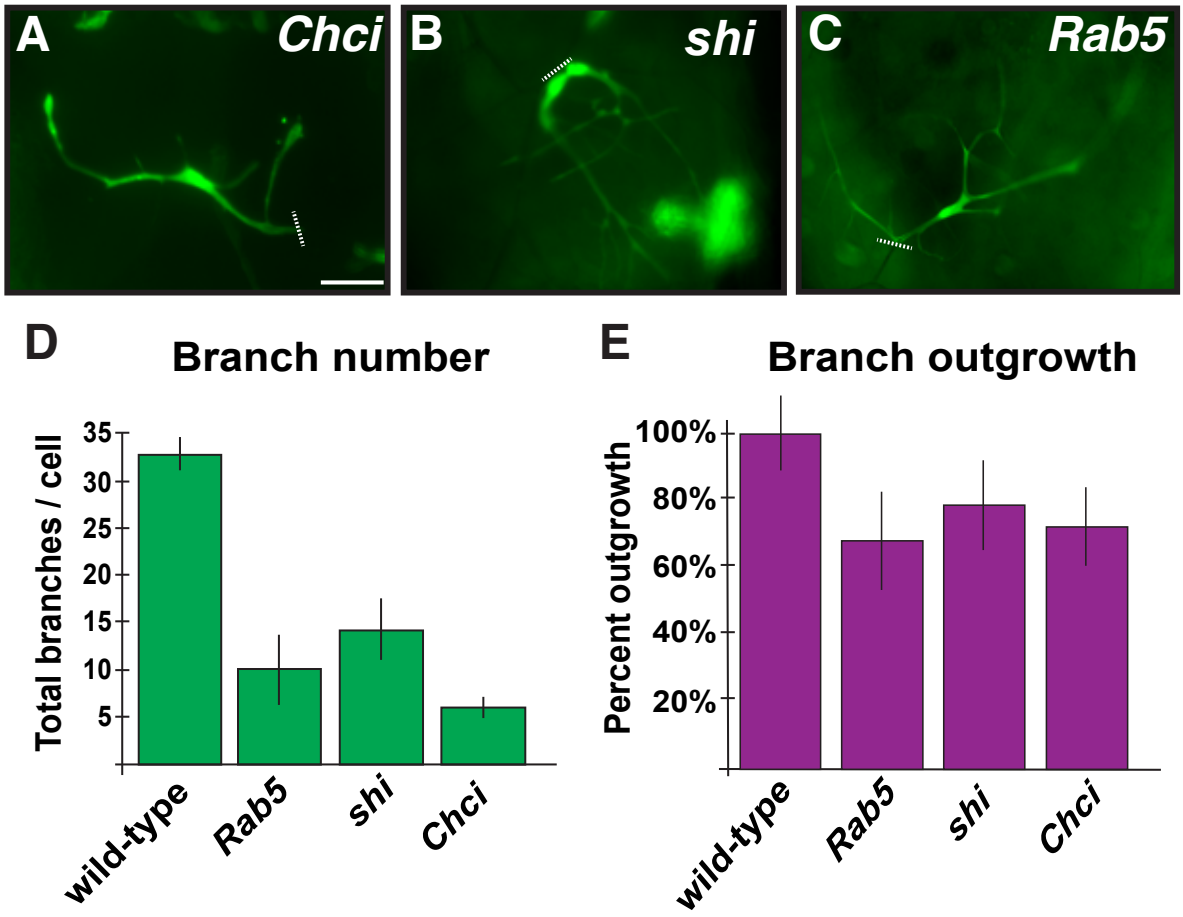

Figure S3.3. The endocytic recycling pathway is required for terminal cell branch development. Terminal cells in MARCM mosaic L3 larvae with homozygous mutant cells labeled with GFP. (A-C) Terminal cells expressing RNAi directed against Chc (clathrin heavy chain), or homozygous mutant for shi (dynamin), or Rab5 have defects in branching and mild outgrowth defects. (D and E) Quantification of branch number and outgrowth. Error bars represent ±2 SEM. Dashed white lines indicate the proximal end of the GFP-labeled cell (A-C). Scale bar, 75 µm.

References

Babbey, C.M., Bacallao, R.L., and Dunn, K.W. (2010). Rab10 associates with primary cilia and the exocyst complex in renal epithelial cells. Am. J. Physiol. Renal Physiol. *299*, F495–F506.

Baer, M.M., Bilstein, A., and Leptin, M. (2007). A clonal genetic screen for mutants causing defects in larval tracheal morphogenesis in Drosophila. Genetics *176*, 2279–2291.

Beronja, S., Laprise, P., Papoulas, O., Pellikka, M., Sisson, J., and Tepass, U. (2005). Essential function of Drosophila Sec6 in apical exocytosis of epithelial photoreceptor cells. The Journal of Cell Biology *169*, 635–646.

Bilimoria, P.M., and Bonni, A. (2013). Molecular control of axon branching. Neuroscientist *19*, 16–24.

Bryant, D.M., Datta, A., Rodríguez-Fraticelli, A.E., Peränen, J., Martín-Belmonte, F., and Mostov, K.E. (2010). A molecular network for de novo generation of the apical surface and lumen. Nat Cell Biol *12*, 1035–1045.

Carmeliet, P., and Jain, R.K. (2011). Molecular mechanisms and clinical applications of angiogenesis. Nature *473*, 298–307.

Chen, W., Feng, Y., Chen, D., and Wandinger-Ness, A. (1998). Rab11 is required for trans-golgi network-to-plasma membrane transport and a preferential target for GDP dissociation inhibitor. Mol. Biol. Cell *9*, 3241–3257.

Chou, T. (1996). The autosomal FLP-DFS technique for generating germline mosaics in Drosophila melanogaster. Genetics *144*, 1673–1679.

Cole, R.A., and Fowler, J.E. (2006). Polarized growth: maintaining focus on the tip. Curr. Opin. Plant Biol. *9*, 579–588.

Conibear, E. (2010). Converging views of endocytosis in yeast and mammals. Current Opinion in Cell Biology *22*, 513–518.

Conway, E.M., Collen, D., and Carmeliet, P. (2001). Molecular mechanisms of blood vessel growth. Cardiovasc. Res. *49*, 507–521.

Das, A., and Guo, W. (2011). Rabs and the exocyst in ciliogenesis, tubulogenesis and beyond. Trends in Cell Biology *21*, 383–386.

Englund, C., Steneberg, P., Falileeva, L., Xylourgidis, N., and Samakovlis, C. (2002). Attractive and repulsive functions of Slit are mediated by different receptors in the Drosophila trachea. Development *129*, 4941–4951.

Estravís, M., Rincón, S.A., Santos, B., and Pérez, P. (2011). Cdc42 regulates multiple membrane traffic events in fission yeast. Traffic *12*, 1744–1758.

Feng, S., Knödler, A., Ren, J., Zhang, J., Zhang, X., Hong, Y., Huang, S., Peränen, J., and Guo, W. (2012). A Rab8 guanine nucleotide exchange factor-effector interaction network regulates primary ciliogenesis. Journal of Biological Chemistry *287*, 15602–15609.

Funamoto, S., Meili, R., Lee, S., Parry, L., and Firtel, R.A. (2002). Spatial and temporal regulation of 3-phosphoinositides by PI 3-kinase and PTEN mediates chemotaxis. Cell *109*, 611–623.

Gehr, P., Mwangi, D.K., Ammann, A., Maloiy, G.M., Taylor, C.R., and Weibel, E.R. (1981). Design of the mammalian respiratory system. V. Scaling morphometric pulmonary diffusing capacity to body mass: wild and domestic mammals. Respir Physiol *44*, 61–86.

Gervais, L., and Casanova, J. (2010). In Vivo Coupling of Cell Elongation and Lumen Formation in a Single Cell. Current Biology *20*, 359–366.

Gervais, L., and Casanova, J. (2011). The Drosophila homologue of SRF acts as a boosting mechanism to sustain FGF-induced terminal branching in the tracheal system. Development *138*, 1269–1274.

Ghabrial, A.S., Levi, B.P., and Krasnow, M.A. (2011). A systematic screen for tube morphogenesis and branching genes in the Drosophila tracheal system. PLoS Genet *7*, e1002087.

Ghabrial, A.S., Luschnig, S., Metzstein, M.M., and Krasnow, M.A. (2003). Branching morphogenesis of the drosophila tracheal system. Annu. Rev. Cell Dev. Biol. *19*, 623–647.

Guillemin, K., Groppe, J., Ducker, K., Treisman, R., Hafen, E., Affolter, M., and Krasnow, M.A. (1996). The pruned gene encodes the Drosophila serum response factor and regulates cytoplasmic outgrowth during terminal branching of the tracheal system. Development *122*, 1353–1362.

Guo, W., Grant, A., and Novick, P. (1999). Exo84p is an exocyst protein essential for secretion. J. Biol. Chem. *274*, 23558–23564.

Hazuka, C.D., Foletti, D.L., Hsu, S.-C., Kee, Y., Hopf, F.W., and Scheller, R.H. (1999). The sec6/8 complex is located at neurite outgrowth and axonal synapse-assembly domains. The Journal of Neuroscience *19*, 1324–1334.

He, B., and Guo, W. (2009). The exocyst complex in polarized exocytosis. Current Opinion in Cell Biology *21*, 537–542.

Heider, M.R., and Munson, M. (2012). Exorcising the exocyst complex. Traffic *13*, 898–907.

Jarecki, J., Johnson, E., and Krasnow, M.A. (1999). Oxygen regulation of airway branching in Drosophila is mediated by branchless FGF. Cell *99*, 211–220.

Jones, T.A., and Metzstein, M.M. (2011). A novel function for the PAR complex in subcellular morphogenesis of tracheal terminal cells in Drosophila melanogaster. Genetics *189*, 153–164.

Jones, T.A., and Metzstein, M.M. (2013). Examination of Drosophila Larval Tracheal Terminal Cells by Light Microscopy. JoVE e50496.

Kanzaki, M., and Pessin, J.E. (2003). Insulin signaling: GLUT4 vesicles exit via the exocyst. Curr. Biol. *13*, R574–R576.

Kawase, K., Nakamura, T., Takaya, A., Aoki, K., Namikawa, K., Kiyama, H., Inagaki, S., Takemoto, H., Saltiel, A.R., and Matsuda, M. (2006). GTP hydrolysis by the Rho family GTPase TC10 promotes exocytic vesicle fusion. Developmental Cell *11*, 411–421.

Lee, T., and Luo, L. (1999). Mosaic analysis with a repressible cell marker for studies of gene function in neuronal morphogenesis. Neuron *22*, 451–461.

Lee, T., Hacohen, N., Krasnow, M., and Montell, D.J. (1996). Regulated Breathless receptor tyrosine kinase activity required to pattern cell migration and branching in the Drosophila tracheal system. Genes & Development *10*, 2912–2921.

Lerner, D.W., McCoy, D., Isabella, A.J., Mahowald, A.P., Gerlach, G.F., Chaudhry, T.A., and Horne-Badovinac, S. (2013). A Rab10-dependent mechanism for polarized basement membrane secretion during organ morphogenesis. Developmental Cell *24*, 159–168.

Levi, B.P., Ghabrial, A.S., and Krasnow, M.A. (2006). Drosophila talin and integrin genes are required for maintenance of tracheal terminal branches and luminal organization. Development *133*, 2383–2393.

Lipschutz, J.H., and Mostov, K.E. (2002). Exocytosis: The Many Masters of the Exocyst. Current Biology *12*, R212–R214.

Locke, M. (1957). The structure of insect tracheae. Journal of Microscopical Science *98*, 487–492.

Masur, S.K., Kim, Y.-T., and Wu, C.-F. (1990). Reversible Inhibition of Endocytosis in Cultured Neurons from the Drosophila Temperature-Sensitive Mutant Shibire. Journal of Neurogenetics *6*, 191–206.

McDonald, K., and Müller-Reichert, T. (2002). Cryomethods for thin section electron microscopy. Meth. Enzymol. *351*, 96–123.

Mehta, S.Q., Hiesinger, P.R., Beronja, S., Zhai, R.G., Schulze, K.L., Verstreken, P., Cao, Y., Zhou, Y., Tepass, U., Crair, M.C., et al. (2005). Mutations in Drosophila sec15 reveal a function in neuronal targeting for a subset of exocyst components. Neuron *46*, 219–232.

Murthy, M., Garza, D., Scheller, R.H., and Schwarz, T.L. (2003). Mutations in the Exocyst Component Sec5 Disrupt Neuronal Membrane Traffic, but Neurotransmitter

Release Persists. Neuron *37*, 433–447.

Novick, P., Medkova, M., Dong, G., Hutagalung, A., Reinisch, K., and Grosshans, B. (2006). Interactions between Rabs, tethers, SNAREs and their regulators in exocytosis. Biochem. Soc. Trans. *34*, 683–686.

Ory, S., and Gasman, S. (2011). Rho GTPases and exocytosis: what are the molecular links? Semin. Cell Dev. Biol. *22*, 27–32.

Pfeffer, S.R. (2001). Rab GTPases: specifying and deciphering organelle identity and function. Trends in Cell Biology *11*, 487–491.

Pfeffer, S.R. (2012). Rab GTPase localization and Rab cascades in Golgi transport. Biochem. Soc. Trans. *40*, 1373–1377.

Ponnambalam, S., and Baldwin, S.A. (2003). Constitutive protein secretion from the trans-Golgi network to the plasma membrane. Mol. Membr. Biol. *20*, 129–139.

Prigent, M., Dubois, T., Raposo, G., Derrien, V., Tenza, D., Rosse, C., Camonis, J., and Chavrier, P. (2003). ARF6 controls post-endocytic recycling through its downstream exocyst complex effector. The Journal of Cell Biology *163*, 1111–1121.

Ramachandran, R. (2011). Vesicle scission: dynamin. Semin. Cell Dev. Biol. *22*, 10–17.

Rivera-Molina, F., and Toomre, D. (2013). Live-cell imaging of exocyst links its spatiotemporal dynamics to various stages of vesicle fusion. The Journal of Cell Biology *201*, 673–680.

Rogers, K.K., Wilson, P.D., Snyder, R.W., Zhang, X., Guo, W., Burrow, C.R., and Lipschutz, J.H. (2004). The exocyst localizes to the primary cilium in MDCK cells. Biochem. Biophys. Res. Commun. *319*, 138–143.

Ruiz, O.E., Nikolova, L.S., and Metzstein, M.M. (2012). Drosophila Zpr1 (Zinc Finger Protein 1) Is Required Downstream of Both EGFR And FGFR Signaling in Tracheal Subcellular Lumen Formation. PLoS ONE *7*, e45649.

Samakovlis, C., Hacohen, N., and Manning, G. (1996). Development of the Drosophila tracheal system occurs by a series of morphologically distinct but genetically coupled branching events. Development *122*, 1395–1407.

Sann, S., Wang, Z., Brown, H., and Jin, Y. (2009). Roles of endosomal trafficking in neurite outgrowth and guidance. Trends in Cell Biology *19*, 317–324.

Sano, H., Eguez, L., Teruel, M.N., Fukuda, M., Chuang, T.D., Chavez, J.A., Lienhard, G.E., and McGraw, T.E. (2007). Rab10, a target of the AS160 Rab GAP, is required for insulin-stimulated translocation of GLUT4 to the adipocyte plasma membrane. Cell Metab. *5*, 293–303.

Satoh, A.K., O'Tousa, J.E., Ozaki, K., and Ready, D.F. (2005). Rab11 mediates post-Golgi trafficking of rhodopsin to the photosensitive apical membrane of Drosophila photoreceptors. Development *132*, 1487–1497.

Schottenfeld-Roames, J., and Ghabrial, A.S. (2012). Whacked and Rab35 polarize dynein-motor-complex-dependent seamless tube growth. Nature *14*, 386–393.

Steneberg, P., and Samakovlis, C. (2001). A novel stop codon readthrough mechanism produces functional Headcase protein in Drosophila trachea. EMBO Rep. *2*, 593–597.

Sutherland, D., Samakovlis, C., and Krasnow, M.A. (1996). branchless encodes a Drosophila FGF homolog that controls tracheal cell migration and the pattern of branching. Cell *87*, 1091–1101.

Swan, L.E. (2013). Initiation of clathrin-mediated endocytosis: all you need is two? Bioessays *35*, 425–429.

Takahashi, S., Kubo, K., Waguri, S., Yabashi, A., Shin, H.-W., Katoh, Y., and Nakayama, K. (2012). Rab11 regulates exocytosis of recycling vesicles at the plasma membrane. Journal of Cell Science *125*, 4049–4057.

Tekirian, T.L. (2002). The central role of the trans-Golgi network as a gateway of the early secretory pathway: physiologic vs nonphysiologic protein transit. Exp. Cell Res. *281*, 9–18.

TerBush, D.R., Maurice, T., Roth, D., and Novick, P. (1996). The Exocyst is a multiprotein complex required for exocytosis in Saccharomyces cerevisiae. Embo J. *15*, 6483–6494.

Vega, I.E., and Hsu, S.C. (2001). The exocyst complex associates with microtubules to mediate vesicle targeting and neurite outgrowth. J. Neurosci. *21*, 3839–3848.

Vetter, P., Roth, A., and Häusser, M. (2001). Propagation of action potentials in dendrites depends on dendritic morphology. J. Neurophysiol. *85*, 926–937.

Walther, P., and Ziegler, A. (2002). Freeze substitution of high-pressure frozen samples: the visibility of biological membranes is improved when the substitution medium contains water. J Microsc *208*, 3–10.

Wang, T., Liu, Y., Xu, X.-H., Deng, C.-Y., Wu, K.-Y., Zhu, J., Fu, X.-Q., He, M., and Luo, Z.-G. (2011). Lgl1 Activation of Rab10 Promotes Axonal Membrane Trafficking Underlying Neuronal Polarization. Developmental Cell 1–14.

Warburton, D., Bellusci, S., De Langhe, S., Del Moral, P.-M., Fleury, V., Mailleux, A., Tefft, D., Unbekandt, M., Wang, K., and Shi, W. (2005). Molecular mechanisms of early lung specification and branching morphogenesis. Pediatr. Res. *57*, 26R–37R.

Warburton, D., El-Hashash, A., Carraro, G., Tiozzo, C., Sala, F., Rogers, O., De Langhe,

S., Kemp, P.J., Riccardi, D., Torday, J., et al. (2010). Lung organogenesis. Curr. Top. Dev. Biol. *90*, 73–158.

Warburton, D., Schwarz, M., Tefft, D., Flores-Delgado, G., Anderson, K.D., and Cardoso, W.V. (2000). The molecular basis of lung morphogenesis. Mech. Dev. *92*, 55–81.

Whyte, J.R.C., and Munro, S. (2002). Vesicle tethering complexes in membrane traffic. Journal of Cell Science *115*, 2627–2637.

Wodarz, A., Ramrath, A., Grimm, A., and Knust, E. (2000). Drosophila atypical protein kinase C associates with Bazooka and controls polarity of epithelia and neuroblasts. The Journal of Cell Biology *150*, 1361–1374.

Wu, H., Turner, C., Gardner, J., Temple, B., and Brennwald, P. (2010). The Exo70 subunit of the exocyst is an effector for both Cdc42 and Rho3 function in polarized exocytosis. Mol. Biol. Cell *21*, 430–442.

Wu, S., Mehta, S.Q., Pichaud, F., Bellen, H.J., and Quiocho, F.A. (2005). Sec15 interacts with Rab11 via a novel domain and affects Rab11 localization in vivo. Nat. Struct. Mol. Biol. *12*, 879–885.

Wucherpfennig, T., Wilsch-Bräuninger, M., and González-Gaitán, M. (2003). Role of Drosophila Rab5 during endosomal trafficking at the synapse and evoked neurotransmitter release. The Journal of Cell Biology *161*, 609–624.

Xu, T., and Rubin, G.M. (1993). Analysis of genetic mosaics in developing and adult Drosophila tissues. Development *117*, 1223–1237.

Yang, H.W., Shin, M.-G., Lee, S., Kim, J.-R., Park, W.S., Cho, K.-H., Meyer, T., and Do Heo, W. (2012). Cooperative activation of PI3K by Ras and Rho family small GTPases. Mol. Cell *47*, 281–290.

Zhang, J., Schulze, K.L., Hiesinger, P.R., Suyama, K., Wang, S., Fish, M., Acar, M., Hoskins, R.A., Bellen, H.J., and Scott, M.P. (2007). Thirty-one flavors of Drosophila rab proteins. Genetics *176*, 1307–1322.

Zhang, X. (2001). Cdc42 Interacts with the Exocyst and Regulates Polarized Secretion. Journal of Biological Chemistry *276*, 46745–46750.

Zhang, X.-M., Ellis, S., Sriratana, A., Mitchell, C.A., and Rowe, T. (2004). Sec15 is an effector for the Rab11 GTPase in mammalian cells. J. Biol. Chem. *279*, 43027–43034.

Zhou, D., Xue, J., Chen, J., Morcillo, P., Lambert, J.D., White, K.P., and Haddad, G.G. (2007). Experimental selection for Drosophila survival in extremely low O(2) environment. PLoS ONE *2*, e490.

Zuo, X., Guo, W., and Lipschutz, J.H. (2009). The exocyst protein Sec10 is necessary for primary ciliogenesis and cystogenesis in vitro. Mol. Biol. Cell *20*, 2522–2529.

CHAPTER 4

MOLECULAR INTERACTIONS OF THE PAR COMPLEX AND THE ROLE OF THE PAR- AND EXOCYST COMPLEX IN SUBCELLULAR TUBE FORMATION

Introduction

We have shown previously that the conserved PAR-polarity complex is required for branching in terminal cells (Jones and Metzstein, 2011). However, the molecular interactions that occur between PAR proteins during terminal cell branching are unknown. In addition, the upstream processes that function to initiate localization or local activation of the PAR complex, which are presumably required for terminal cell branching, remain unclear. Previous work in epithelial cells showed that the PAR complex member Par-6 acts as a scaffold protein and interacts with the Rho GTP binding protein Cdc42 (Hutterer et al., 2004; Joberty et al., 2000), another scaffold protein, Baz, and a protein kinase, aPKC (Figure 4.1A). aPKC is negatively regulated by Baz, a process facilitated by the PDZ domain of Par-6 (Hung and Kemphues, 1999; Nance and Zallen, 2011). Once activated, aPKC phosphorylates Baz at a conserved serine residue, and the inhibitory effect of Baz on aPKC is suppressed (Horikoshi et al., 2009; Morais-de-Sá et al., 2010; Nance and Zallen, 2011). The aPKC kinase can be transformed by proteolytic cleavage of the regulatory domain to a constitutively active kinase, called PKM, which is sufficient to

rescue some of the defects associated with loss of aPKC in *Drosophila* (Drier et al., 2002; Ruiz-Canada et al., 2004).

The *15N* allele of *par-6* contains a 592-bp deletion in the *par-6* gene. This mutation is predicted to truncate the PDZ domain, which is located in the C-terminal region of the Par-6 protein (Jones and Metzstein, 2011; Mehta et al., 2005). Since the PDZ domain of Par-6 is required for Baz binding, this mutation presumably abrogates the interaction between Par-6 and Baz. However, we expect the Par-6^{15N} truncated protein to still efficiently bind aPKC and Cdc42. In addition, the Par-6^{15N} transcript is expected to be stable as there is no premature termination codon and the 3' UTR is mostly intact. We previously showed that terminal cells homozygous for the *par-6^{15N}* allele have branching defects, lack a visible air-filled lumen, and also display an abnormal tip morphology (Bloomington Drosophila Stock Center,, 2004; Jones and Metzstein, 2011) . These defects are quantitatively more severe than defects observed in *par-6* null mutants with *15N* mutant terminal cells having approximately 2-fold fewer branches than either *par-6* or *baz* null terminal cells. This suggests that the PDZ domain of *par-6* is important for regulating aspects of terminal cell development. Since the PDZ domain of Par-6 is required to bind Baz, and Baz acts to inhibit aPKC, we propose that in the absence of the Par-6 PDZ domain, as in *15N,* there is no inhibition of aPKC by Baz, resulting in mis-regulation of aPKC. Unregulated kinase activity could be the cause of the severe branching defects observed in *15N* mutant terminal cells. Alternatively, the *15N* defects could be caused by mislocalization or misregulation of Baz itself. In this model, loss of the Par-6 PDZ domain prevents interaction with Baz, resulting in a Baz gain-of-function phenotype. Here, we use double mutant analysis and expression of a constitutively active

version of aPKC, called PKM, to differentiate between these models. We find the defects observed in *15N* mutant terminal cells are not ameliorated by loss of Baz, suggesting the defects are not a result of unregulated Baz. In addition, we find that constitutive kinase activity of aPKC is sufficient to induce severe branching defects, both in wild-type and *aPKC* mutant cells. This suggests that both the positive and negative modulation of aPKC kinase is required for terminal cell branching morphogenesis.

In epithelial cells, apical and basolateral plasma membrane domains can be distinguished by their different lipid and protein compositions (Drubin and Nelson, 1996; Hung and Kemphues, 1999; Hutterer et al., 2004; Joberty et al., 2000; Jones and Metzstein, 2011; Nance and Zallen, 2011; Rodriguez-Boulan and Nelson, 1989; Zhu and Nelson, 2012). Similarly, in neurons, the polarized axonal and dendritic membrane domains also display differences in lipid composition (Drier et al., 2002; Horikoshi et al., 2009; Hsu et al., 1999; Jones and Metzstein, 2011; Morais-de-Sá et al., 2010; Nance and Zallen, 2011). The activity and localization of polarity complexes, including the PAR complex, is regulated by spatially restricted molecular signals. Phosphoinositides are membrane-tethered lipid molecules derived from phosphatidylinositol (PI), or phosphoinositides, synthesized from PI by the sequential action of lipid kinases. Localization of particular phosphoinositides is controlled by local concentrations of lipid kinases and lipid phosphatases at the membrane (Gassama-Diagne et al., 2006; Mehta et al., 2005). For example, localization of PI 3-kinase to the plasma membrane is triggered by growth factors that activate receptor tyrosine kinases (RTKs) (Funamoto et al., 2002). This localization causes a local accumulation of PI(3,4,5)P3 (PIP_3), which in turn is required for axon formation (Jones and Metzstein, 2011; Shi et al., 2003). Individual

phosphoinositides are known to control a variety of cellular processes. PIP_2, has diverse targets and functions in the context of sperm polarization by regulating trafficking of actin and membrane proteins and has been associated with localization of the exocyst complex (Fabian et al., 2010; Simões et al., 2010). Additionally, PIP_3 can participate in local activation of Cdc42 and localization of Par-3, which is required for axon outgrowth in neurons (Keely et al., 1997; Nguyen et al., 2002; Tolias et al., 1995; Wodarz et al., 2000). Additionally, PI 3-kinase and PIP_3 have been shown to play an instructive role in cell polarization and migration by controlling localization of Par-3 (Baz) (Funamoto et al., 2002; Iijima and Devreotes, 2002; Ruiz-Canada et al., 2004; Sciorra et al., 2002; Weiner et al., 2002). Based on their role in localization of PAR proteins in other cell types, we investigated a role for specific kinases of the PI pathway in terminal cell branch development. We found PI 3-kinase is required for terminal cell branching, but that no other component of the pathway appears necessary for terminal cell development.

The exocyst, a conserved protein complex composed of proteins Sec3, Sec5, Sec6, Sec8, Sec10, Sec15, Exo70 and Exo84, is required for docking and fusion of vesicles at target membranes, where it facilitates cell outgrowth. Chapter 3 of this dissertation shows that exocyst mutants fail to form fully-grown branches, demonstrating that the exocyst is required for branch outgrowth in terminal cells. Interestingly, members of the exocyst have recently been shown to participate in early regulatory steps and assembly of autophagy machinery (Bodemann et al., 2011; Farré and Subramani, 2011; Shiga et al., 1996), thus implicating the exocyst in a process that requires intracellular membrane assembly. Such assembly is reminiscent of the membrane accumulation that is thought to occur in the cell-hollowing process necessary for subcellular lumen formation in terminal

cells. Here, we show members of the exocyst complex are required for a step in terminal cell lumen maturation.

Materials and methods

Fly stocks and genetics

Flies were reared on standard cornmeal/dextrose media and larvae were raised at 25°C. The control chromosomes for these experiments were *y w FRT*^{19A} and *FRT*^{82B} (Jones and Metzstein, 2011; Xu and Rubin, 1993) and *FRT*^{G13} (Chou, 1996). Alleles analyzed were *sec5*^{E10} (Murthy et al., 2003), *sec6*^{KG08199} (Mehta et al., 2005), *sec10*^{f03085}(Bloomington Drosophila Stock Center,, 2004), *sec15*^{1} (Mehta et al., 2005), *par-6*^{15N} (Jones and Metzstein, 2011), *baz*^{FA50} (Simões et al., 2010) [*a gift from T.Schüpbach (Princeton University, Princeton, New Jersey) via J. Zallen (Sloan-Kettering Institute, New York, New York)*], *aPKC*^{k06403} (Wodarz et al., 2000) and *UAS-PKM* (Ruiz-Canada et al., 2004) a gift from V. Budnik. For mosaic analysis we used the tracheal specific *breathless* (*btl*) promoter (Shiga et al., 1996) in the stocks *y w P{w+,btl-Gal80} FRT19A, hsFLP122 ; btl-Gal4 UAS-GFP* (Jones and Metzstein, 2011). *UAS-Sec5* RNAi (27526), *UAS-Sec15* RNAi (27499), *UAS-fwd* (29396*, 31187, 35257) RNAi, *UAS-sktl* (35198*, 27715) RNAi, *UAS-PLC* (31269, 31270*, 32438) RNAi, *UAS-PI3K* (35265, 35798, 31252, 27690*) RNAi were obtained from the Bloomington *Drosophila* Stock Center (stock numbers shown in parentheses, * indicates the lines imaged). Homozygous mutant cells were generated using the mosaic analysis with a repressible cell marker (MARCM) technique (Lee and Luo, 1999). To generate the mosaics, 0-6 hr

embryos were collected in fly food vials at 25° C and treated to a 45 minute heat shock at 38° C in a circulating water bath before being returned to 25° C for development.

Construction of *baz par-6^{15N}* double mutant

Because *baz* and *par-6* are located close to each other on the *Drosophila* X chromosome (*baz* is ~1.3 m.u. to the left of *par-6*), we used a two-step recombination process to construct the *baz par-6^{15N}* double mutant. First, we recombined the viable visible marker, *scalloped* (*sd^{1}*), located about 7 m.u. to the left of *par-6* (thus ~5.7 m.u. from *baz*) onto *par-6^{15N}*. *par-6^{15N} FRT^{19A}/FM7c* females were crossed to *sd^{1}/Y* males, nonbalancer female progeny (sd^{1}/par-6^{15N} FRT^{19A}) were collected and crossed to *Dp(1;Y)W73, y B f^{+}* bearing males. *Dp(1;Y)W73* is a Y-linked duplication that covers *par-6* and *baz*, but not *sd*. Individual *sd* males were used to establish lines balanced with *FM7c*. Lethal lines, were chosen and complementation tests, using a null allele of *par-6*, were performed to confirm the presence of *par-6^{15N}*. In addition, terminal cell defects in these presumptive *15N* mutants were also evaluated in mosaic animals and found to be identical to those observed in *par-6^{15N}*, confirming the presence of *15N* as well as *FRT^{19A}*. Next, *sd^{1} par-6^{15N} FRT^{19A}/FM7c* females were crossed to *baz^{FA50} FRT^{19A}/Dp(1;Y)W73, y B f^{+}* males, nonbalancer female offspring were collected and crossed to *Dp(1;Y)W73, y B f^{+}* bearing males. Single *sd^{+}* males were selected, and crossed to *baz* and to *par-6* carrying females. Animals that failed to complement both *par-6* and *baz* were used to establish lines.

Light microscopy of terminal cells

Wandering third instar larvae were collected and heat-fixed according to a standard protocol developed in our lab (Jones and Metzstein, 2013). Images were obtained using a Zeiss AxioImager M1 equipped with an AxioCam MRm.

Quantification of terminal cell branch number

Terminal cell branch number was determined using methods described previously (Jones and Metzstein, 2011).

Immunocytochemistry

Wandering third instar larvae were dissected in 1X PBS to make fillets exposing the tracheal system. Fillets were fixed for 30 minutes in 4% PFA in 1X PBS, rinsed 3 times for 15 minutes in 1X PBST (1X PBS + 0.1% TX100), blocked 30 minutes at room temperature in PBSTB (1X PBST + 0.02% BSA), then incubated with primary antibody overnight at 4°C. Fillets were then rinsed 3 times for 15 minutes in 1X PBSTB and incubated with secondary antibody for 2 hr at room temperature. Fillets were then rinsed and mounted on glass slides in ProLong® Gold antifade reagent (Invitrogen). Antibodies were used in the following concentrations: rabbit anti-pio, 1:100 (Jaźwińska et al., 2003) and mouse anti-GFP, 1:1000 (Clontech, #632375). Secondary antibodies, conjugated to Alexa-488 or Alexa-568 (Molecular Probes), were used at 1:1000. Imaging was performed using a Leica TCS SP2 confocal microscope. A Z-stack of 10-25 slices was imaged for each setting sequentially. An average intensity projection was generated in Image-J.

Transmission electron microscopy

High pressure freezing, resin infiltration and embedding, sectioning and imaging were performed using methods described in Chapter 3.

Results

The PDZ domain of Par-6 is required for regulation of aPKC

The *par-6* allele *15N* shows more severe branching defects than a null mutant allele (Jones and Metzstein, 2011), suggesting that the Par-6 15N protein has neomorphic or gain-of function activity. The 15N allele truncates the PDZ domain, which has been shown to bind Baz in canonical PAR complex formation. We therefore predict that, in a 15N mutant, Baz cannot interact with Par-6, and this loss of binding causes a gain-of-function phenotype. The resulting branching defects could be due to the loss of Baz interacting with the rest of the PAR complex and failure to negatively regulate aPKC, causing constitutive kinase activity in aPKC. Alternatively, unbound Baz may negatively affect the overall polarity of the cell, if it has intrinsic gain-of-function activity.

To distinguish between these models, we aimed to generate a *15N baz* double mutant. This would allow us to determine if the defects observed in the *15N* mutant were due to Baz gain-of-function activity. To do this we used MARCM to generate homozygous *baz par-6*^{15N} double mutant terminal cells. Wild-type terminal cells show many subcellular branches (Figure 4.1B) and a gas-filled lumen (Figure 4.1B'), and each branch tip has a smooth, tapered appearance (Figure 4.1B''). Terminal cells homozygous for *15N* show defects in branching (Figure 4.1C), almost no gas-filled lumen (Figure 4.1C'), and tip morphology defects (Figure 4.1C''). In contrast, while *baz* homozygous

terminal cells show similar branching defects (Figure 4.1D), they have a complete gas-filled lumen (Figure 4.1D') and smooth, tapered tip morphology (Figure 4.1D''). We found double mutant *baz par-6*^{15N} terminal cells had branching defects (Figure 4.1E), lumen defects (Figure 4.1E') and tip morphology defects (Figure 4.1E''). These defects were both qualitatively and quantitatively (Figure 4.1F) similar to those observed for *15N*. These data indicate the severe defects seen in *15N* are not caused by a Baz gain of function, but instead suggest that unregulated aPKC is responsible for the defects observed in Par-6^{15N}.

To test this hypothesis, we expressed a truncated version of the mouse homolog of aPKC, PKM, which functions as a constitutively active kinase (Drier et al., 2002; Ruiz-Canada et al., 2004). We found that wild-type mosaic terminal cells that expressed *PKM* had severe branching defects (Figure 4.2A). Similarly, expressing PKM in *aPKC* homozygous terminal cells also resulted in branching defects (Figure 4.2B), suggesting regulation of the kinase activity of aPKC is critical for terminal cell branch development.

The phosphoinositide PI(3,4,5)P_3 is required for terminal cell branching morphogenesis

To examine mechanisms of PAR protein localization, we tested whether specific phosphoinositides are required for terminal cell branching. When we generated mosaic animals with terminal cells expressing RNAi for kinases required for phosphoinoside production, we found the PI4K *fwd* (Figure 4.3B), PI5K *sktl* Figure 4.3B), or *PLC* (Figure 4.3D) had normal branching and gas-filled lumens (Figured 4.3B'- 4.3D'). However, terminal cells expressing RNAi for *PI3K* showed mild branching defects

(Figure 4.3E) but no lumen defects (Figure 4.3E'). These data suggest PI3K is important in terminal cell branch development and suggests the phosphoinositide $PI(3,4,5)P_3$, the product of PI3K and PIP_2, is required for branching.

Par-6 and aPKC organize apical membranes required for lumen formation

Previously, we showed PAR-polarity proteins Par-6 and aPKC, but not Baz, are required for terminal cell lumen morphogenesis (Jones and Metzstein, 2011). However, the methods used in this study could only detect fully mature, gas-filled lumens. Therefore, we could not distinguish lumens that never form from lumens that are defective at an intermediate stage of development, such as air filling. To distinguish between these possibilities, we used immunofluorescence to visualize localization of Pio, an apically secreted luminal protein (Jaźwińska et al., 2003), in mutant and wild-type terminal cells. Pio is required in the embryonic tracheal system as a vital component of the extracellular matrix to facilitate cell elongation and intercalation in multicellular and unicellular tubes (Jaźwińska et al., 2003). However, it is not required for terminal cell development and simply acts as a marker to visualize the apical membrane (Jaźwińska et al., 2003). We used GFP expression to identify homozygous terminal cells in MARCM mosaics (Figure 4.4A-E) and found that in wild-type cells, Pio is localized to distinct puncta lining the entire lumen (Figure 4.4F and F'). Terminal cells homozygous null for *baz*, which have an air-filled lumen, also show punctate luminal localization of Pio (Figure 4.4G and G'). Conversely, *aPKC* (Figure 4.4H and H'), or *par-6* (Figure 4.4I and I') null mutant terminal cells show diffuse, sporadic localization of Pio protein in

regions devoid of GFP. This segregation suggests some sort of compartmentalization of Pio, possibly within membrane bound vesicles. In terminal cells homozygous for *15N* (Figure 4.4J and J'), Pio protein is mostly diffuse throughout the cytoplasm, but it accumulates in the cytoplasmic blobs found at terminal cell branch tips (as seen in Figure 4.1B''). Since Pio is only secreted onto apical domains, these data suggest *aPKC, par-6,* and *15N* mutant terminal cells contain regions or compartments with apical identity, suggestive of partial lumens. In addition, TEM of *15N* mutant terminal cells shows the apical membrane takes up a much larger portion of the cell and contains large vesicle like structures in place of the lumen, something never observed in wild-type (Figure 4.5A and B).

Exocyst complex components are required for lumen maturation in terminal cells

In Chapter 3 of this thesis, we showed the exocyst complex is required for vesicle tethering events that facilitate branch outgrowth in terminal cells. To test the role of the exocyst in lumen formation we used MARCM to generate homozygous mutant terminal cells for exocyst complex members *sec5, sec6, sec10,* and *sec15*. We used GFP to identify homozygous cells and brightfield microscopy to visualize the air-filled lumen (Figure 4.6A-E and A'-E'). We found terminal cells homozygous for any of these exocyst components had no air-filled lumens (Figure 4.6B'-E'), indicating members of the exocyst complex are required for lumen development. However, using brightfield microscopy only shows portions of the lumen that are gas-filled and does not differentiate between defects that may occur in earlier steps of lumen formation.

The process of lumen formation likely requires multiple steps including cell regionalization, membrane accumulation, domain identification, and lumen maturation and clearing. The exocyst could participate in any one of these steps. To further investigate the role of the exocyst in lumen formation we used transmission electron microscopy (TEM) to visualize the lumen ultrastructure in wild type and exocyst defective terminal cells (Figure 4.7A-C). We found that in wild-type cells, the lumen is generally found near the center of the cell, and the envelope and thin, waxy water-resistant outer layer, called the epicuticle are electron dense, and are closely associated with the less electron dense chitinous underlayer, called the procuticle (Figure 4.7A). In contrast, when we express RNAi directed against exocyst components *sec5* (Figure 4.7B) or *sec15* (Figure 4.7C) lumen ultrastructure appears defective. In *sec5* terminal cells the epicuticle, is irregularly shaped and the procuticle, is often not easily identified, and the luminal space appears filled with membrane bound structures (Figure 4.7B). In *sec15* deficient terminal cells the epicuticle has a more regular shape, but the procuticle is misshapen and the space between these two membranes is much larger than is ever observed in wild-type cells (Figure 4.7C). These data demonstrate that exocyst complex members are not required for trafficking membrane for lumen assembly or initial organization, but instead suggest the exocyst is required for a lumen maturation step, possibly through maturation of the cuticle.

One important aspect of terminal cell development is the regionalization and specification of apical and basal domains. In terminal cells, the apical domain is tightly associated with the cuticle that lines the lumen and is critical for lumen formation. One prediction for the role of the exocyst in lumen formation is that it would be required for

delivering components to the membrane that are necessary for apical identity. To test this possibility we used immunohistochemistry to visualize localization of the apical membrane marker Pio in wild-type and exocyst-deficient terminal cells. Here, GFP identifies homozygous terminal cells (Figure 4.7D-F). In the wild-type cells Pio protein was localized to distinct puncta lining the lumen (Figure 4.7D'). Conversely, when we used RNAi to inhibit expression of *sec5* (Figure 4.7E-E'') or *sec15* (Figure 4.7F-F''), this punctate localization is lost and Pio protein appears diffuse or nearly absent (Figure 4.7E' and F'). Taken together these data suggest members of the exocyst are required for a lumen maturation step.

Discussion

We have shown previously that the PAR-polarity complex, composed of the proteins, Par-6, Baz, aPKC, and Cdc42, is required for terminal cell branching. In addition, we have also shown that physical interactions known to occur between aPKC and Par-6, and Par-6 and Baz, are also required for terminal cell branching. Finally, we also found that terminal cells homozygous for the neomorphic allele of *par-6, 15N* have more severe branching defects than a null allele. Here, we investigate the potential cause of the additional defects observed in *15N* mutants in more detail. One possibility is that this is due to loss of Par-6 mediated Baz regulation. We found that the strong defects observed in *15N* mutants are not ameliorated by the loss of Baz, showing that they are not due to a Baz gain of function defect, which suggests the PDZ domain of Par-6 is important for regulation of aPKC, likely through its ability to bind Baz, which negatively regulates aPKC. Furthermore, evidence to support the idea that *15N* could have aPKC

gain of function activity comes from expression of PKM. Here, we show expression of PKM in tracheal terminal cells is sufficient to cause severe branching defects in both wild-type and *aPKC* mutant terminal cells, suggesting a gain of function effect, although we did not test this directly. We propose that the interaction between the PDZ domains of Par-6 and Baz is required to govern the activation and kinase activity of aPKC. In the absence of a functional PDZ domain, as in *15N,* Par-6 can still bind and activate aPKC*,* however, Baz is unable to bind and negatively regulate this process. We propose that the excess branching defects seen in *15N,* are a result of the unregulated kinase activity of aPKC, which might result in unregulated phosphorylation of downstream targets that could disrupt the polarization of potential branch sites. This type of regulation is reminiscent of the regulation that occurs in epithelial cells, where Baz is required to negatively regulate aPKC in the context of establishing apical and basolateral domains. *15N* is the first gain-of-function allele of *par-6* described in *Drosophila* and would therefore be an interesting allele to test in other cellular contexts where the PAR complex is required, such as in axon outgrowth.

PAR proteins participate in terminal cell branching morphogenesis downstream of the FGF signaling pathway. However, the molecular cues that are required for PAR protein positioning remain unknown. In neurons, regional activation of phosphatidylinositol 3-kinase (PI3K), an enzyme that converts PIP_2 to PI 3,4,5-trisphosphate (PIP_3), is required for localization of Baz, and this is necessary for axon specification. We predict loss of PI3K would inhibit localized PIP_3 production and subsequent PAR protein localization. If this were the case, we would expect inhibition of PI3K to lead to phenotypes similar to PAR complex loss of function alleles. However,

we found inhibiting expression of PI3K in terminal cells resulted in only mild branching defects, suggesting PI3K, PIP_3, have no major role in terminal cell branching. We also predicted other PI kinases would be important for lumen formation, based on predictions that the apical or luminal membrane of a terminal cell would have a different lipid composition than the basal or branching membrane of the cell. Surprisingly, no other PI kinase we tested showed any terminal cell defects in branching or lumen formation. It is possible that using RNAi, which results in an incomplete knockdown, could confound these results and PI3K and other PI kinases and phosphatases may indeed play major roles in terminal cell development. The minor defects in branching were unexpected and we propose examination of null alleles would better decipher the role of various phosphatidylinositides in terminal cell branching and lumen formation.

Lumen formation is thought to occur by a process of cell hollowing, and this process likely includes numerous steps including, polarization, scaffold assembly, vesicle trafficking, and vesicle fusion. Additionally, proper secretion and assembly of the luminal cuticle is also required to generate a function lumen. Previously, we found PAR-polarity proteins aPKC and Par-6, but not Baz, are required for terminal cell lumen development. However, the methods used previously could only detect mature gas-filled lumens thus did not provide information about the specific step at which defects occurred. Par-6 and aPKC are required for apical membrane identity in epithelial cells (Bryant et al., 2010). We predicted these polarity proteins could participate in either organization membrane bound vesicle (polarization) at a presumptive lumen site or provide apical identity for vesicles that make up the luminal membrane. Using localization of an apically secreted protein, Pio as a marker, we found aPKC and Par-6 mutant terminal

cells have unorganized and discontinuous regions of apical membrane throughout the cells. Additionally, we found the Par-6 allele *15N* has a massively expanded apical membrane. Despite this, as we showed previously, *15N* shows no lumen by brightfield microscopy (Jones and Metzstein, 2011). These data suggest a model in which the PAR-polarity proteins Par-6 and aPKC are required for apical membrane organization, which is necessary for terminal cell lumen development.

The exocyst complex is required for trafficking, docking and tethering of vesicles at the plasma membrane. We showed in Chapter 3, that the exocyst complex facilitates fusion of vesicles required for terminal cell branch outgrowth. We expected the exocyst would also play a role in lumen formation. We found loss of the exocyst complex showed defects in the formation of terminal cell lumen gas-filling as assayed by brightfield microscopy. We further predicted the exocyst would participate in the trafficking of vesicles necessary for luminal membrane formation. However, we instead found the exocyst complex is not required for lumen initiation, as we can observe an immature luminal structure by TEM in exocyst defective cells. The lumen in these cells does show a defective cuticular lining in which the envelope and epicuticle are disorganized and the procuticle domain is expanded. Additionally, we found the normally apically secreted Pio protein, is not found in the presumptive lumens. Therefore, we propose the exocyst complex is not required for initial membrane assembly steps in terminal cell lumen formation, but instead is required for secretion and maturation of the cuticle. The cuticle is in turn necessary for terminal cell air filling and for maturation of the lumen.

Figure 4.1 *baz 15N* double mutants show severe terminal cell defects. (A) PAR complex protein-protein interaction model. Dashed lines indicate interaction domains. Abbreviations: **P**ost synaptic density protein (PSD95), **D**rosophila disc large tumor suppressor (Dlg1), and **Z**onula occludens-1 protein (zo-1) (**PDZ** domain), **P**hox and **B**em**1** (**PB1** domain), **C**dc42/**R**ac **I**nteractive **B**inding (**CRIB**). (B-E) Mosaic larvae were generated using MARCM, with homozygous mutant cells labeled with GFP to visualize cytoplasmic branching (B-E) and brightfield microscopy to visualize the darkly contrasting air-filled lumen (B'-E'). Wild-type terminal cells show extensive outgrowth and subcellular branching (B) a complete air-filled lumen (B') and smooth tapered tip morphology (B''). Terminal cells homozygous for *par-6*^{15N} show defects in branching (C), no visible air-fill lumen (C') and abnormal tip blobs (C''). *baz* mutant cells show branching defects (D), but an air-filled lumen (D') and normal tip morphology (D''). Terminal cells homozygous for *baz par-6*^{15N} show branching defects (E), no visible air-filled lumen (E') and abnormal tip blobs (E''). (F) Quantification of total terminal cell branch number per cell. (G) Gene interaction model. Dashed white lines indicate the proximal end of the cell. White arrows highlight the air-filled lumen. Scale bar, B-E, B'-E' 75 μm and B''-E'', 25 μm.

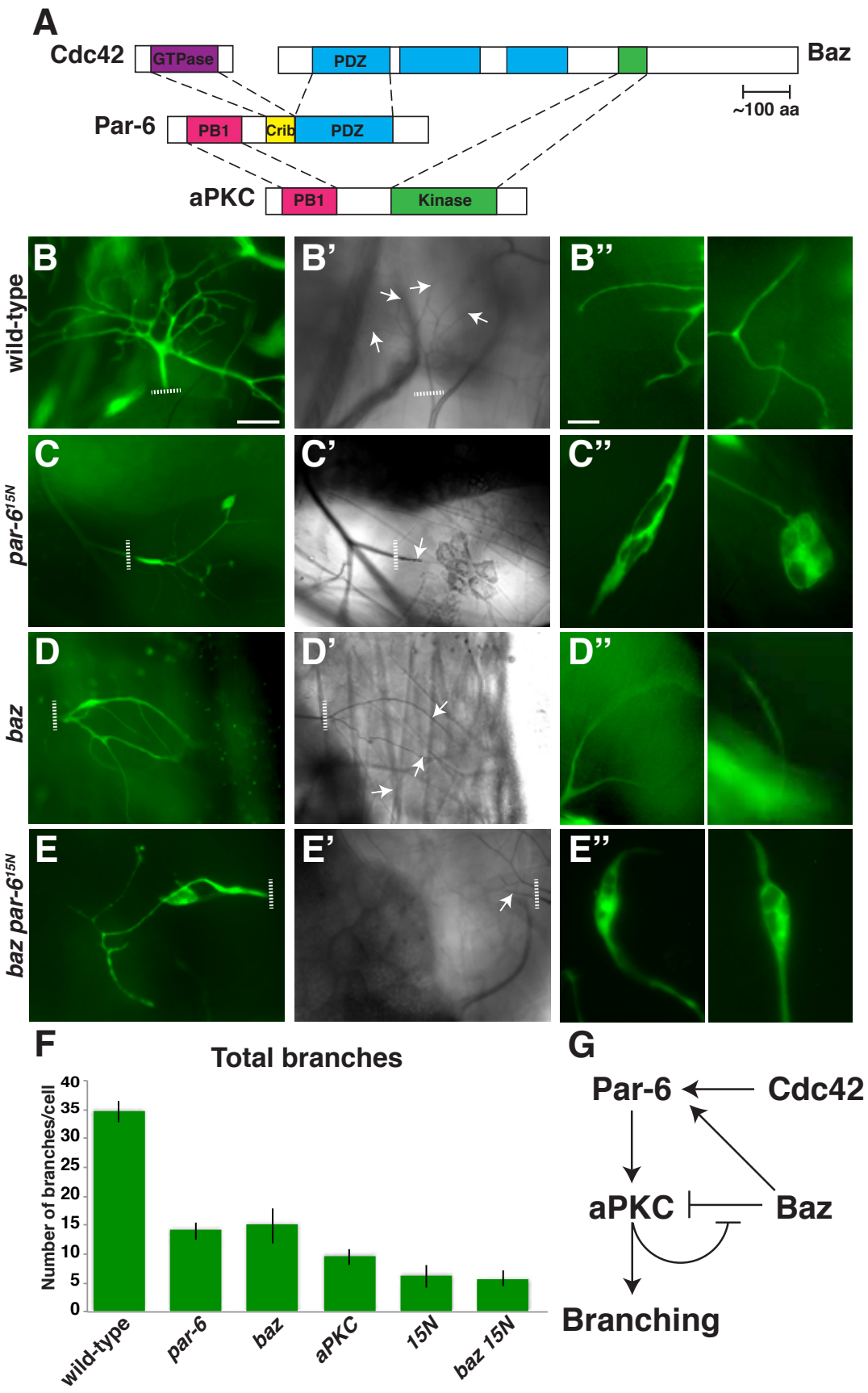
A
Cdc42
GTPase
PDZ
Baz
~100 aa
Par-6
PB1
Crib
PDZ
aPKC
PB1
Kinase
wild-type
par-6^15N
baz
baz par-6^15N
B
B'
B''
C
C'
C''
D
D'
D''
E
E'
E''
F
Total branches
Number of branches/cell
40
35
30
25
20
15
10
5
0
wild-type
par-6
baz
aPKC
15N
baz 15N
G
Par-6
Cdc42
aPKC
Baz
Branching

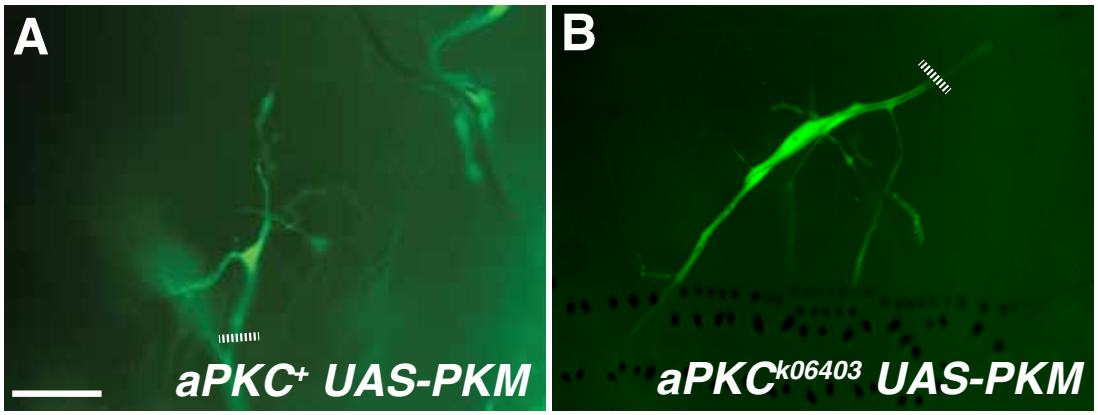

Figure 4.2 Activated aPKC causes branching defects in terminal cells. As in Figure 4.1, homozygous terminal cell branches are visualized and identified by expression of GFP in L3 mosaic animals. (A) Expression of PKM in wild-type terminal cells shows defects in terminal cell branch number and morphology. (B) Terminal cells homozygous for aPKC and expressing PKM also show branch number and morphology defects. Dashed white lines indicate the proximal end of the cell. Scale bar, 75 μm.

Figure 4.3 PI3K is required for branching in tracheal terminal cells. (A) Phosphatidylinositol (PI) pathway. PI 4-kinase (*fwd)* phosphorylates PI to yield PI4P. PIP 5-kinase (*sktl)* phosphorylates PI4P to produces PI (4,5)P also called PIP_2, can then be phosphorylated by PI 3-kinase to produce PIP_3. PIP_2 can also be hydrolyzed by PLC to produce inositol triphosphate (IP3) and diacylglycerol (DAG) second messenger molecules. As in Figure 4.1, homozygous terminal cell branches are visualized and identified by expression of GFP in L3 mosaic animals (B-E) and brightfield microscopy shows the air-filled lumen (B'-E'). Terminal cells homozygous for *fwd*, *sktl*, or *PLC*, show no defects in branching (B-D) and complete air-filled lumens (B'-D'). In contrast, *PI3K* homozygous terminal cells show mild branching defects (E) but have a complete air-filled lumen (E'). Dashed white lines indicate the proximal end of the GFP-labeled cell. Scale bar, 75 μm.

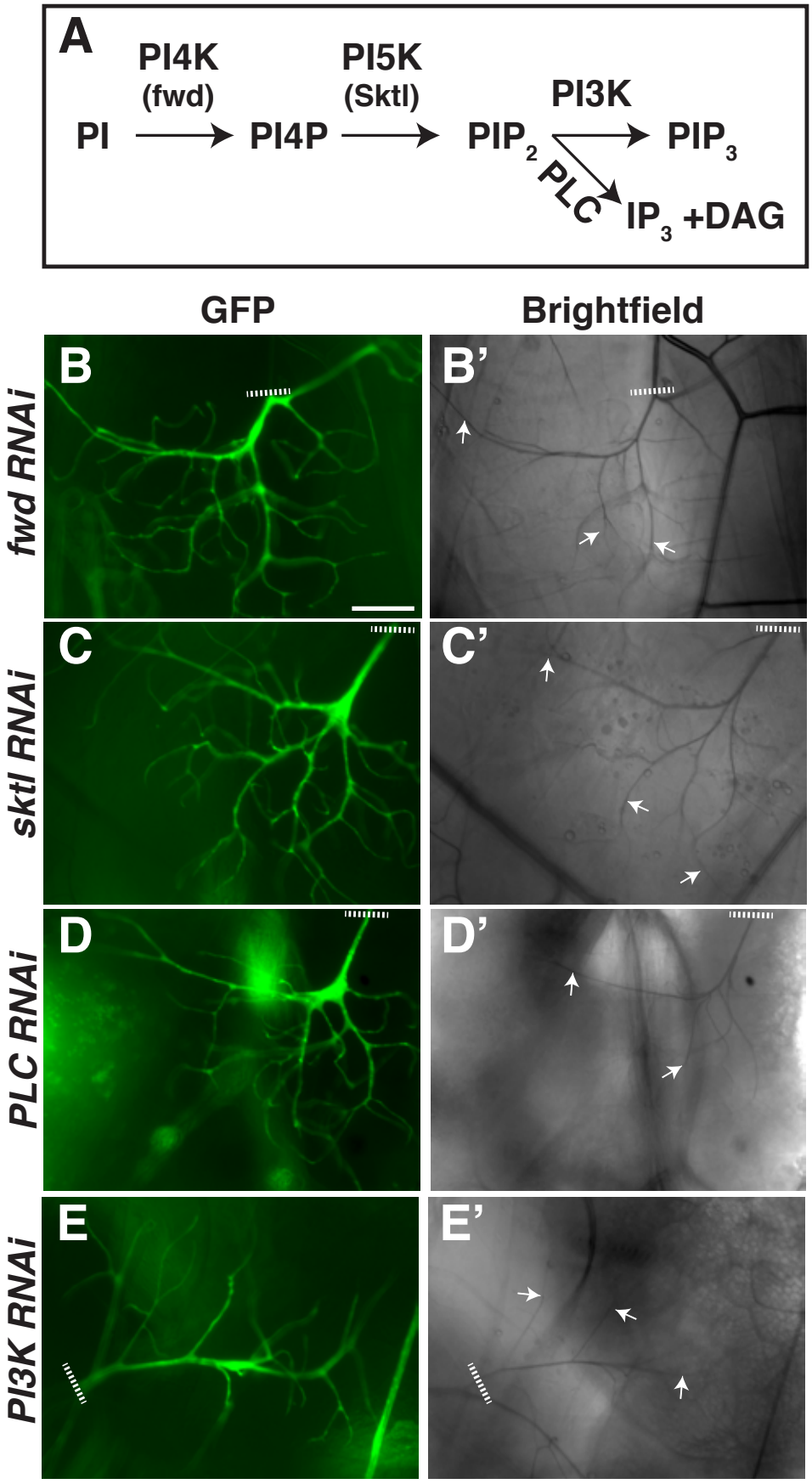
A
PI4K
(fwd)
PI5K
(Sktl)
PI3K
PI
PI4P
PIP2
PIP3
PLC
IP3 +DAG
GFP
Brightfield
fwd RNAi
sktl RNAi
PLC RNAi
PI3K RNAi
B
B'
C
C'
D
D'
E
E'

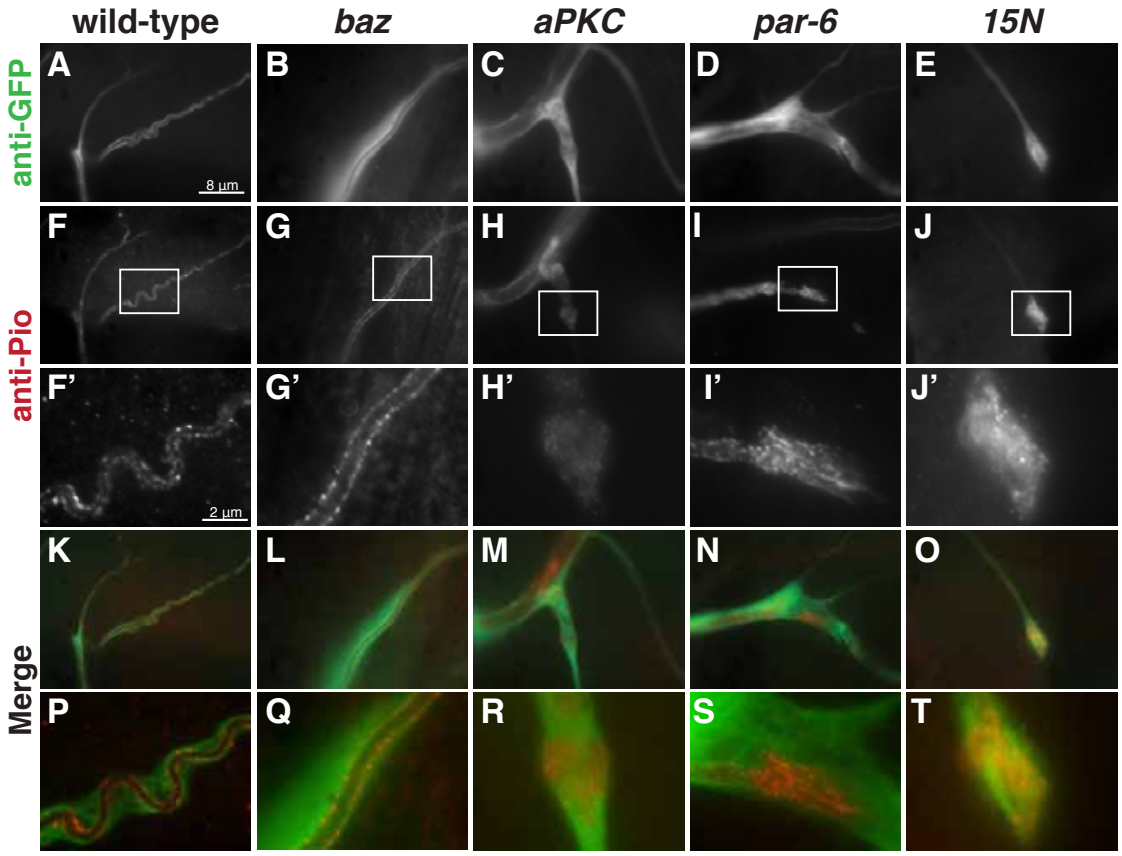

Figure 4.4 PAR-polarity mutant terminal cells show accumulation of the apical membrane marker, Pio. Terminal cells in L3 mosaic larvae were identified by cytoplasmic GFP expression and then probed with anti-GFP (A - E) and anti-Pio (F-J & F'-J') antisera. Panels K-O show merged channels, P-T show merged channels of F'-J' (GFP in green, anti-Pio in red). In wild type (F & F') and baz (G & G') cells, Pio is found in distinct puncta lining the luminal membrane. In terminal cells homozygous for aPKC (H & H') or par-6 (I & I') Pio appears in distinct, but random regions, which are usually devoid of GFP. Terminal cell homozygous for par-615N (J & J') show accumulation of Pio only in cytoplasmic tip blobs (Highlighted in J').

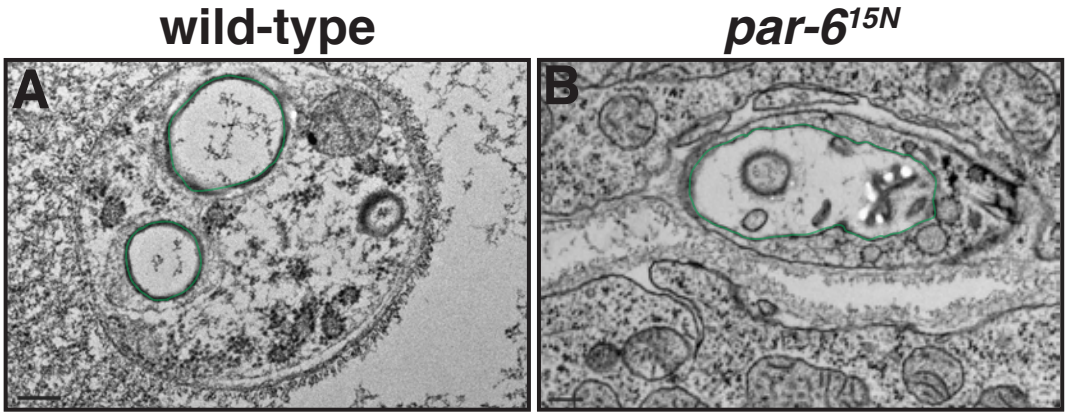

Figure 4.5 Ultrastructure of 15N mutant terminal cells. Terminal cell branch ultrastructure observed in thin cross-section using transmission electron microscopy (TEM). The luminal membrane (apical) is pseudo-colored green. Wild-type terminal cell branches show a circular cross-sectional morphology, the lumen is expanded and clear of cytoplasmic material (A). Terminal cells homozygous for 15N (B) show an abnormal extensive apical domain and an accumulation of membranous structures in the luminal space. Scale bar, 200 nm.

Figure 4.6 Exocyst complex members are required for lumen formation in terminal cells. As in Figure 4.1, homozygous terminal cell branches are identified by expression of GFP. (A-E) Shows the GFP image merged with the brightfield image that shows the air-filled lumen (A'-E'). Wild-type terminal cells show a complete air-filled lumen running through each branch (A & A'). Terminal cells homozygous for *sec5, sec6, sec10,* or *sec15* show branching defects (B-E) and no air-filled lumen appears in any of the branches (B'-E'). Dashed line indicates the region that contains the GFP-labeled cell. Scale bar, 75 μm.

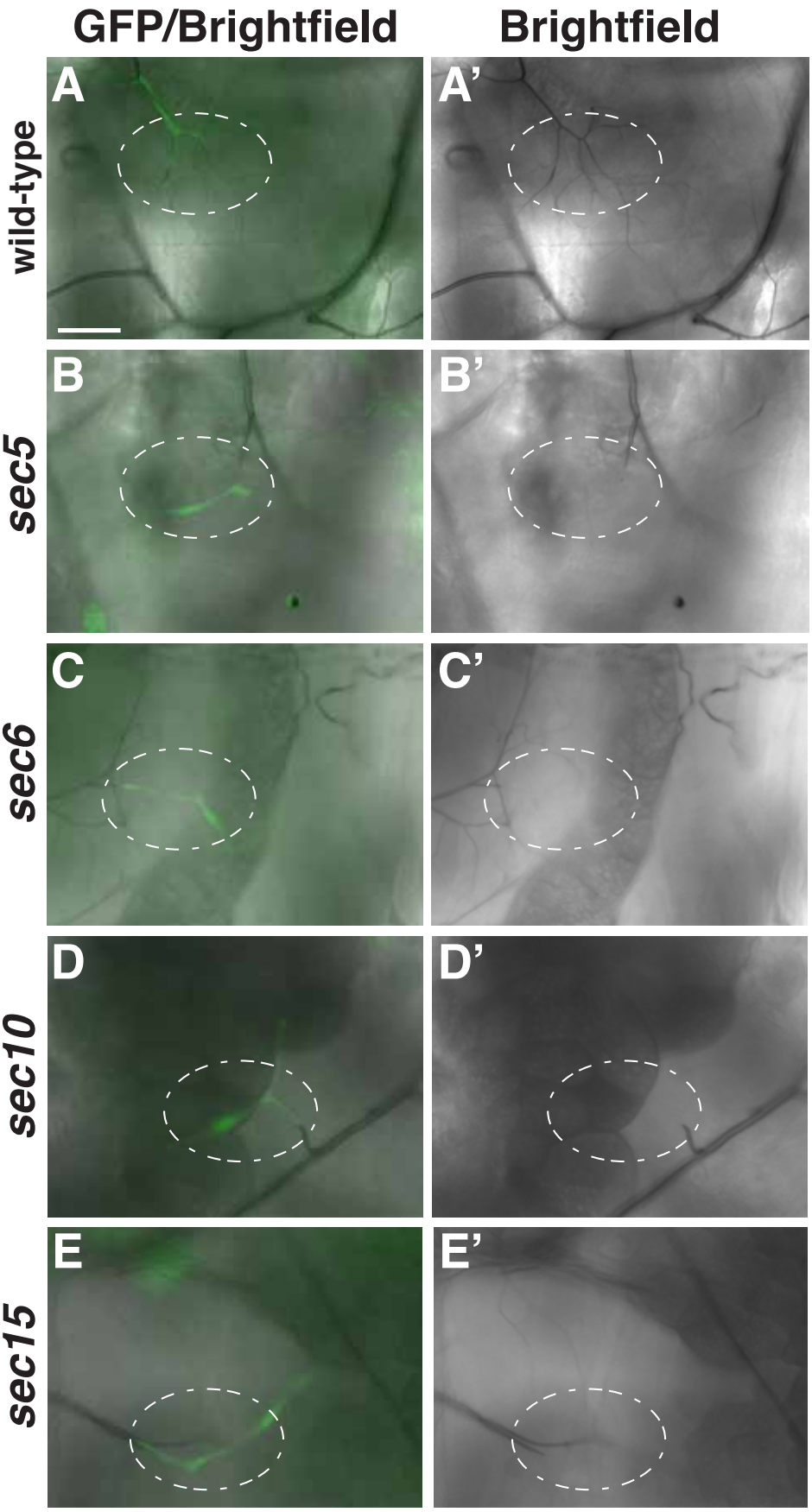
GFP/Brightfield
Brightfield
wild-type
sec5
sec6
sec10
sec15
A
A'
B
B'
C
C'
D
D'
E
E'

Figure 4.7 Exocyst complex members are required for lumen maturation in terminal cells. (A-C) Transmission electron microscopy (TEM) of terminal cell branch ultrastructure. The procuticle (white double-headed arrows) fills the space between the apical membrane (red arrows) and the epicuticle (red arrowheads). Wild-type terminal cell branches show a normal circular cross-sectional morphology with little space between the epi- and procuticle (A). Expression of RNAi for *sec5* (B) or *sec15* (C) shows severe defects in lumen ultrastructure and the distance between the epicuticle and the procuticle is much larger and is filled with membrane bound structures. (D-F) Terminal cells in L3 mosaic larvae were identified by cytoplasmic GFP expression and then probed with anti-GFP (D-F) and anti-Pio (D'-F') antisera. Panels D''-F'' show merged channels (GFP in red, anti-Pio in green). Wild-type terminal cells show punctate localization of Pio at the luminal membrane. Expression of RNAi for *sec5* (E-E'') or *sec15* (F-F'') show very diffuse cytoplasmic staining with Pio (E' & F') but Pio protein can be seen lining the lumen of the adjacent unicellular tube. Scale bar, A-C, 50 nm.

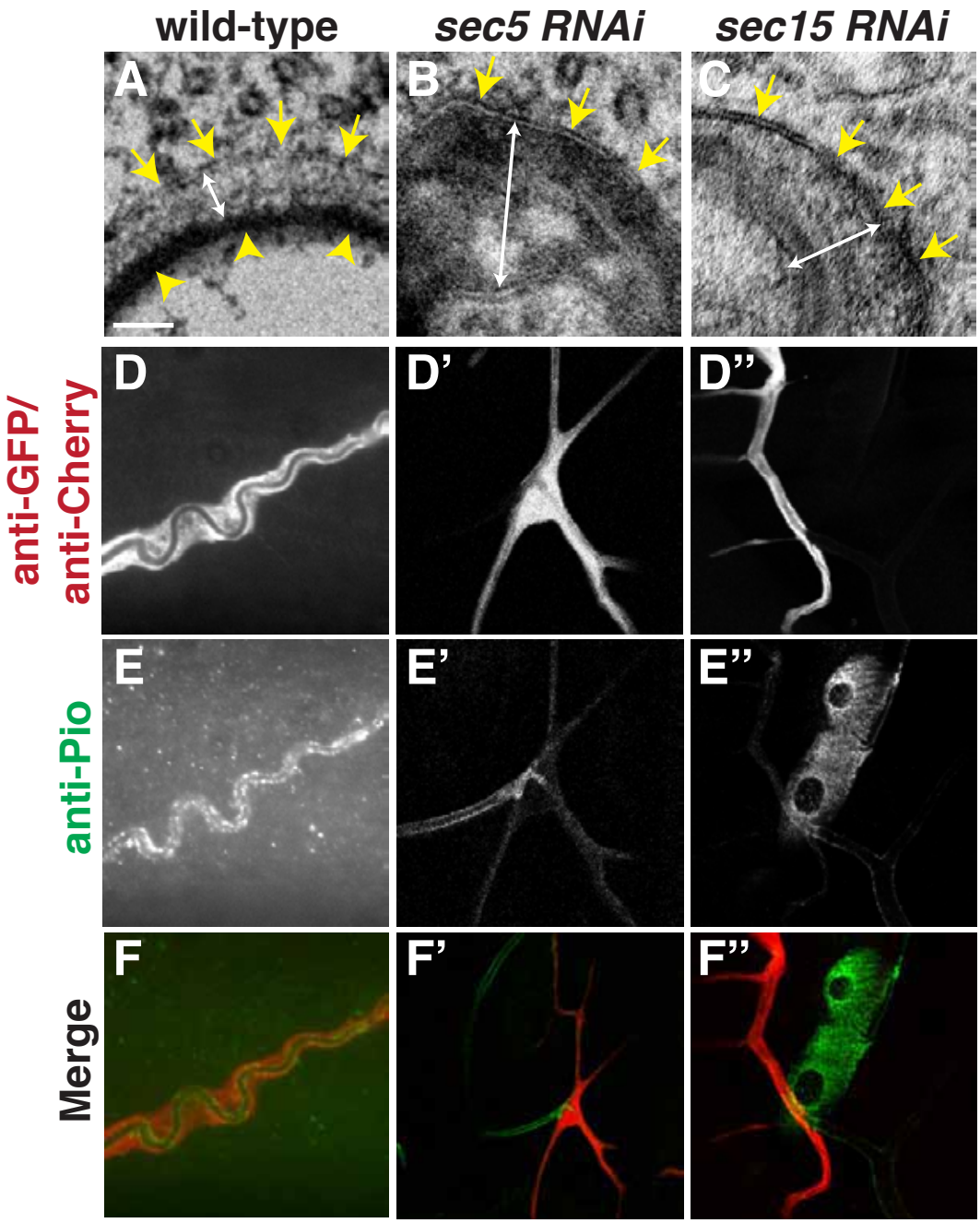
wild-type
sec5 RNAi
sec15 RNAi
A
B
C
D
D'
D''
anti-GFP/
anti-Cherry
E
E'
E''
anti-Pio
F
F'
F''
Merge

References

Bloomington *Drosophila* Stock Center, (2004). Exelixis insertion alleles that are not in FlyBase.

Bodemann, B.O., Orvedahl, A., Cheng, T., Ram, R.R., Ou, Y.-H., Formstecher, E., Maiti, M., Hazelett, C.C., Wauson, E.M., Balakireva, M., et al. (2011). RalB and the exocyst mediate the cellular starvation response by direct activation of autophagosome assembly. Cell *144*, 253–267.

Bryant, D.M., Datta, A., Rodríguez-Fraticelli, A.E., Peränen, J., Martín-Belmonte, F., and Mostov, K.E. (2010). A molecular network for de novo generation of the apical surface and lumen. Nat Cell Biol *12*, 1035–1045.

Chou, T. (1996). The autosomal FLP-DFS technique for generating germline mosaics in *Drosophila* melanogaster. Genetics *144*, 1673–1679.

Drier, E.A., Tello, M.K., Cowan, M., Wu, P., Blace, N., Sacktor, T.C., and Yin, J.C.P. (2002). Memory enhancement and formation by atypical PKM activity in *Drosophila* melanogaster. Nat Neurosci *5*, 316–324.

Drubin, D.G., and Nelson, W.J. (1996). Origins of cell polarity. Cell *84*, 335–344.

Fabian, L., Wei, H.-C., Rollins, J., Noguchi, T., Blankenship, J.T., Bellamkonda, K., Polevoy, G., Gervais, L., Guichet, A., Fuller, M.T., et al. (2010). Phosphatidylinositol 4,5-bisphosphate directs spermatid cell polarity and exocyst localization in *Drosophila*. Mol. Biol. Cell *21*, 1546–1555.

Farré, J.-C., and Subramani, S. (2011). Rallying the exocyst as an autophagy scaffold. Cell *144*, 172–174.

Funamoto, S., Meili, R., Lee, S., Parry, L., and Firtel, R.A. (2002). Spatial and temporal regulation of 3-phosphoinositides by PI 3-kinase and PTEN mediates chemotaxis. Cell *109*, 611–623.

Gassama-Diagne, A., Yu, W., Beest, ter, M., Martín-Belmonte, F., Kierbel, A., Engel, J., and Mostov, K. (2006). Phosphatidylinositol-3,4,5-trisphosphate regulates the formation of the basolateral plasma membrane in epithelial cells. Nature *8*, 963–970.

Horikoshi, Y., Suzuki, A., Yamanaka, T., Sasaki, K., Mizuno, K., Sawada, H., Yonemura, S., and Ohno, S. (2009). Interaction between PAR-3 and the aPKC-PAR-6 complex is indispensable for apical domain development of epithelial cells. Journal of Cell Science *122*, 1595–1606.

Hsu, S.-C., Hazuka, C.D., Foletti, D.L., and Scheller, R.H. (1999). Targeting vesicles to specific sites on the plasma membrane: the role of the sec6/8 complex. Trends in Cell Biology *9*, 150–153.

Hung, T.J., and Kemphues, K.J. (1999). PAR-6 is a conserved PDZ domain-containing protein that colocalizes with PAR-3 in Caenorhabditis elegans embryos. Development *126*, 127–135.

Hutterer, A., Betschinger, J., Petronczki, M., and Knoblich, J.A. (2004). Sequential Roles of Cdc42, Par-6, aPKC, and Lgl in the Establishment of Epithelial Polarity during *Drosophila* Embryogenesis. Developmental Cell *6*, 845–854.

Iijima, M., and Devreotes, P. (2002). Tumor suppressor PTEN mediates sensing of chemoattractant gradients. Cell *109*, 599–610.

Jaźwińska, A., Ribeiro, C., and Affolter, M. (2003). Epithelial tube morphogenesis during *Drosophila* tracheal development requires Piopio, a luminal ZP protein. Nat Cell Biol *5*, 895–901.

Joberty, G., Petersen, C., Gao, L., and Macara, I.G. (2000). The cell-polarity protein Par6 links Par3 and atypical protein kinase C to Cdc42. Nat Cell Biol *2*, 531–539.

Jones, T.A., and Metzstein, M.M. (2011). A novel function for the PAR complex in subcellular morphogenesis of tracheal terminal cells in *Drosophila* melanogaster. Genetics *189*, 153–164.

Jones, T.A., and Metzstein, M.M. (2013). Examination of *Drosophila* Larval Tracheal Terminal Cells by Light Microscopy. JoVE.

Keely, P.J., Westwick, J.K., Whitehead, I.P., Der, C.J., and Parise, L.V. (1997). Cdc42 and Rac1 induce integrin-mediated cell motility and invasiveness through PI(3)K. Nature *390*, 632–636.

Lee, T., and Luo, L. (1999). Mosaic analysis with a repressible cell marker for studies of gene function in neuronal morphogenesis. Neuron *22*, 451–461.

Mehta, S.Q., Hiesinger, P.R., Beronja, S., Zhai, R.G., Schulze, K.L., Verstreken, P., Cao, Y., Zhou, Y., Tepass, U., Crair, M.C., et al. (2005). Mutations in *Drosophila* sec15 reveal a function in neuronal targeting for a subset of exocyst components. Neuron *46*, 219–232.

Morais-de-Sá, E., Mirouse, V., and St Johnston, D. (2010). aPKC phosphorylation of Bazooka defines the apical/lateral border in *Drosophila* epithelial cells. Cell *141*, 509–523.

Murthy, M., Garza, D., Scheller, R.H., and Schwarz, T.L. (2003). Mutations in the exocyst component Sec5 disrupt neuronal membrane traffic, but neurotransmitter release persists. Neuron *37*, 433–447.

Nance, J., and Zallen, J.A. (2011). Elaborating polarity: PAR proteins and the cytoskeleton. Development *138*, 799–809.

Nguyen, K.T., Zong, C.S., Uttamsingh, S., Sachdev, P., Bhanot, M., Le, M.-T., Chan,

J.L.-K., and Wang, L.-H. (2002). The role of phosphatidylinositol 3-kinase, rho family GTPases, and STAT3 in Ros-induced cell transformation. J. Biol. Chem. *277*, 11107–11115.

Rodriguez-Boulan, E., and Nelson, W. (1989). Morphogenesis of the polarized epithelial cell phenotype. Science *245*, 718–725.

Ruiz-Canada, C., Ashley, J., Moeckel-Cole, S., Drier, E., Yin, J., and Budnik, V. (2004). New synaptic bouton formation is disrupted by misregulation of microtubule stability in aPKC mutants. Neuron *42*, 567–580.

Sciorra, V.A., Rudge, S.A., Wang, J., McLaughlin, S., Engebrecht, J., and Morris, A.J. (2002). Dual role for phosphoinositides in regulation of yeast and mammalian phospholipase D enzymes. The Journal of Cell Biology *159*, 1039–1049.

Shi, S.-H., Jan, L.Y., and Jan, Y.-N. (2003). Hippocampal neuronal polarity specified by spatially localized mPar3/mPar6 and PI 3-kinase activity. Cell *112*, 63–75.

Shiga, Y., Tanaka-Matakatsu, M., and Hayashi, S. (1996). A nuclear GFP/beta-galactosidase fusion protein as a marker for morphogenesis in living *Drosophila*. Dev Growth Differ *38*, 99–106.

Simões, S. de M., Blankenship, J.T., Weitz, O., Farrell, D.L., Tamada, M., Fernandez-Gonzalez, R., and Zallen, J.A. (2010). Rho-kinase directs bazooka/Par-3 planar polarity during *Drosophila* axis elongation. Developmental Cell *19*, 377–388.

Tolias, K.F., Cantley, L.C., and Carpenter, C.L. (1995). Rho family GTPases bind to phosphoinositide kinases. J. Biol. Chem. *270*, 17656–17659.

Weiner, O.D., Neilsen, P.O., Prestwich, G.D., Kirschner, M.W., Cantley, L.C., and Bourne, H.R. (2002). A PtdInsP3- and Rho GTPase-mediated positive feedback loop regulates neutrophil polarity. Nat Cell Biol *4*, 509–513.

Wodarz, A., Ramrath, A., Grimm, A., and Knust, E. (2000). *Drosophila* atypical protein kinase C associates with Bazooka and controls polarity of epithelia and neuroblasts. The Journal of Cell Biology *150*, 1361–1374.

Xu, T., and Rubin, G.M. (1993). Analysis of genetic mosaics in developing and adult *Drosophila* tissues. Development *117*, 1223–1237.

Zhu, W., and Nelson, C.M. (2012). PI3K signaling in the regulation of branching morphogenesis. BioSystems *109*, 403–411.

CHAPTER 5

EXAMINATION OF *DROSOPHILA* LARVAL TRACHEAL TERMINAL CELLS BY LIGHT MICROSCOPY

Reprint of: Jones and Metzstein (2013) Examination of *Drosophila* Larval Tracheal Terminal Cells by Light Microscopy. *JoVE,* 77,e50496.

Reprinted with permission from The Journal of Visualized Experiments.

jove Journal of Visualized Experiments www.jove.com

Video Article

Examination of *Drosophila* Larval Tracheal Terminal Cells by Light Microscopy

Tiffani A Jones, Mark M. Metzstein
Department of Human Genetics, University of Utah

Correspondence to: Mark M. Metzstein at markm@genetics.utah.edu

URL: http://www.jove.com/video/50496
DOI: doi:10.3791/50496

Keywords: Developmental Biology, Issue 77, Genetics, Molecular Biology, Cellular Biology, Biochemistry, Biophysics, Bioengineering, Cellular Structures, Epithelial Cells, Drosophila melanogaster, Microscopy, Phase-Contrast Microscopy, Fluorescence Microscopy, genetics (animal and plant), animal biology, animal models, Respiratory System, trachea, terminal cell, intact animal, larvae, cell morphology, Drosophila, fluorescence, branching, lumen, fruit fly, animal model

Date Published: 7/9/2013

Citation: Jones, T.A., Metzstein, M.M. Examination of *Drosophila* Larval Tracheal Terminal Cells by Light Microscopy. *J. Vis. Exp.* (77), e50496, doi:10.3791/50496 (2013).

Abstract

Cell shape is critical for cell function. However, despite the importance of cell morphology, little is known about how individual cells generate specific shapes. *Drosophila* tracheal terminal cells have become a powerful genetic model to identify and elucidate the roles of genes required for generating cellular morphologies. Terminal cells are a component of a branched tubular network, the tracheal system that functions to supply oxygen to internal tissues. Terminal cells are an excellent model for investigating questions of cell shape as they possess two distinct cellular architectures. First, terminal cells have an elaborate branched morphology, similar to complex neurons; second, terminal cell branches are formed as thin tubes and contain a membrane-bound intracellular lumen. Quantitative analysis of terminal cell branch number, branch organization and individual branch shape, can be used to provide information about the role of specific genetic mechanisms in the making of a branched cell. Analysis of tube formation in these cells can reveal conserved mechanisms of tubulogenesis common to other tubular networks, such as the vertebrate vasculature. Here we describe techniques that can be used to rapidly fix, image, and analyze both branching patterns and tube formation in terminal cells within *Drosophila* larvae. These techniques can be used to analyze terminal cells in wild-type and mutant animals, or genetic mosaics. Because of the high efficiency of this protocol, it is also well suited for genetic, RNAi-based, or drug screens in the *Drosophila* tracheal system.

Video Link

The video component of this article can be found at http://www.jove.com/video/50496/

Introduction

Cell shape is critical for function of individual cells within an organism, as well as cells that function as part of a tissue or organ. We use *Drosophila* tracheal terminal cells, a component of the insect respiratory system, to investigate the molecular mechanisms that participate in controlling two conserved types of cellular morphology: branching and tube formation (lumenogenesis). Terminal cells are located at the tips of a network of branched tubes that functions to deliver oxygen to internal tissues[1] and have an elaborate branched morphology which depends on an FGF signaling pathway that is controlled by local oxygen levels within target tissues[2]. Terminal cell branches are thin tubes, with a gas-filled subcellular lumen running through each branch. The distinct cellular architectures of terminal cells, along with the ease by which genetic analysis can be performed in *Drosophila,* make these cells an excellent model for investigating mechanisms of cellular outgrowth, branching, and intracellular tube formation. Terminal cells have proved a useful model for understanding some of the signaling pathways leading to branched cell differentiation, outgrowth, and maturation[2-4]. Using this system unbiased, forward genetic screens for cell morphogenesis mutants have been performed, yielding insights into mechanisms controlling cell shape[5,6]. For instance, these screens have revealed that a specific RabGAP is required for cytoskeletal polarity and vesicle trafficking in lumen formation and positioning[7]; that integrin-mediated adhesion is required for branch stability[8]; and that epithelial PAR-polarity proteins regulate polarized membrane trafficking required for both branching and lumen formation[9]. Other studies in terminal cells have shown that asymmetric actin accumulation and microtubule organization is required for cell elongation and lumenogenesis[10]. Thus, diverse, conserved cell biological mechanisms contribute to terminal cell morphogenesis.

Here, we describe a method to rapidly fix intact third-instar *Drosophila* larvae for analysis of terminal cell branching and lumen formation. This protocol can also be carried out on both first and second instar animals. Key to this technique is the ability to visualize terminal cells that are genetically labeled by fluorescent protein expression directly through the larval cuticle of intact animals. Since this procedure does not require any post-fixation manipulations, such as antibody staining, to observe the cells, it is well suited to high throughput analysis, including genetic or drug screening. Fluorescent protein expression reveals the structure of the cytoplasmically-filled branches. Tube formation can be monitored in parallel using brightfield microscopy to identify the gas-filled lumen, which contrasts with the surrounding fluid-filled tissues.

Included in this protocol is the method for generating genetic mosaics based on the MARCM system[11], to produce homozygous mutant terminal cells labeled with fluorescent proteins in otherwise unlabeled animals. This is necessary, since terminal cells only elaborate their complex

structures relatively late in development; genetic mosaics allow for bypass of gene requirements in other tissues earlier in development.
To generate MARCM clones, trachea are labeled using the tracheal-specific driver *breathless (btl)*[12]. Described here is the protocol for the *Drosophila* X chromosome; for other chromosomes, a similar procedure can be used, with genetic reagents appropriate to the chromosome being examined. Here, trachea are labeled by expression of a cytoplasmically localized GFP, but the procedure works equally well with expression of other fluorescent proteins, such as DsRed.

Additionally, we have included a method to quantify branching patterns and lumen formation in terminal cells, based on methods developed for characterizing neuronal branch patterns[13]. This kind of quantitative data can be critical in discerning the precise role of genes in the branching or lumenogenesis process, as well as allowing for direct comparisons between different mutants[9].

Protocol

1. Mosaic Generation

1. **Genetic Cross**

   w FRT^{19A} *tub:GAL80* FLP^{122}*/Y; Btl-GAL4, UAS-GFP* (males) X * FRT^{19A}*/Bal* (females), where * represents the mutant to be examined. Note: Set up cross at least one day prior to experiment, as this allows animals to mate appropriately.
2. **Pre-lay:** Transfer cross to fly-food vials with a small smear of fresh yeast paste placed on the media. Allow to lay for 1 hr at 25 °C.
3. **Lay:** Transfer animals from pre-lay vial to a fresh vial with a small smear of fresh yeast paste. Allow to lay for 6 hr at 25 °C.
4. Transfer adults back to pre-lay vial for storage and use in subsequent experiments. Immediately heat shock the lay vial containing 0-6 hr old embryos for 45 min at 38 °C, in a circulating water bath. Note: The surface of the food should be below the water level to verify all embryos are appropriately heat shocked.
5. Incubate heat shocked vials at 25 °C for 4-5 days until third instar larvae start to wander.

2. Screen for Mosaic Animals

1. Using fine forceps gently pick wandering third-instar larvae from the sides of the vial and place them into chilled 100% glycerol in a small plastic plate.
2. Examine larvae using a high magnification-dissecting microscope equipped with fluorescent optics. Identify larvae with mosaic expression of fluorescently labeled tracheal cells. Typically, this can be done at 10-20X magnification.

3. Heat Fixation

1. Using fine forceps carefully pick mosaic animals out of the dish and place in a drop of fresh 100% glycerol on a 75x25x1 mm white glass microscope slide. Note: multiple animals can be placed in the drop (**Figure 1A**).

   Animals can also be placed in a drop of glycerol directly onto a coverslip, but care must be taken during fixation (step 3.2), as the animals will heat very quickly and can become over-fixed.
2. Place glass slide onto 70 °C heat block until the animals just stop moving, no more than 20 sec for a slide, and 10 sec for a cover slip (**Figure 1B**). Animals will wriggle initially but stop and become rigid and elongated once dead. Note: overlong exposure to heat will damage terminal branches and lumens as well as make the GFP signal dim and diffuse. For optimal efficiency it is recommended to have the heat block in the same room as the microscopes.
3. Using fine forceps carefully orient all larvae in the drop in a single direction, such that all larvae on the slide are oriented parallel to one another (**Figure 1C**).
4. Gently place an 18x18mm micro cover glass on top of larvae (or invert the coverslip onto a glass slide) and avoid forming bubbles (**Figure 1D**). Note: coverslip may not lie exactly flat over larvae, this is not a problem.
5. Image larvae within 30 min. Heat fixed terminal cells will degrade and GFP signal will become very diffuse.

4. *In vivo* Imaging of Tracheal Terminal Cells

1. Place slide on the stage of a compound stereomicroscope. Using a 5X objective locate the two parallel dorsal trunks running from anterior to posterior on the dorsal surface of the animal (**Figure 1F**). Locate the two dorsal terminal cells, directly between the two dorsal trunks. This helps identify the appropriate segment for analysis.
2. Once oriented, rotate the animals to image desired terminal cells. To do this, carefully push the coverslip on the edge with the forceps perpendicular to the long axis of the larvae, slowly rolling the larvae underneath the coverslip (**Figures 1E** and **1G**).
3. Selecting the appropriate terminal cells is critical for consistent results and comparisons between mutants. The fat body branch (FB) terminal cells are easily found adjacent to the dorsal trunk, lateral to the midline. The lateral group G terminal cells (LG) are easily found and are located just lateral of the ventral midline (**Figure 1H**). Note: in the most anterior (Tr1) and posterior (Tr10) segments the arrangement of terminal cell is divergent from other segments. We only analyze terminal cells in segments Tr2-Tr9. Dorsal terminal cells have a more stereotyped branching pattern than other tracheal terminal cells. This may depend on additional, non-cell autonomous signals, and this should be considered when deciding whether to include them in analysis.
4. Once a terminal cell of interest has been identified, capture an image using the desired magnification; typically 10X or 20X is best (**Figure 2A**). Note: due to variable branching patterns, try to capture images that include as many branches and branch tips as possible.

5. Without moving the stage, switch off the fluorescence and turn on the transmitted light to capture a brightfield image of the same cell and focal plane (**Figure 2B**). The lumen will be visualized as darkly contrasting within the terminal cell space. If planning on quantify terminal cell branches and lumens, collect multiple images in multiple focal planes of each terminal cell.

5. Analysis and Quantification of Terminal Cell Morphology Using ImageJ

1. Open the fluorescent and brightfield images using the ImageJ (http://rsb.info.nih.gov/ij/) plug-in NeuronJ (http://www.imagescience.org/meijering/software/neuronj/).
2. Using the "Add tracings" tool, manually trace the branches and lumen of the entire terminal cell.
3. Using the "Label tracings" tool, rename and recolor to assign each line within the trace a specific designation.
4. Using the "Set parameters" tool, adjust the line width from 6-10 pixels (for 512x512 images obtained from the digital camera connected to the compound microscope. For higher or lower resolution cameras, the pixel width should be scaled appropriately), using all other default settings, and choose "OK". Then use the "Make snapshot" tool to take an image. Choose "Draw trace" to get a snapshot of the trace that can be shown side-by-side with the original.
5. Select the "Measure tracings" tool and select the tracing type (*i.e.* which branches to measure based on the specific designations assigned in step 5.3). Next, select "Display tracing measurements" and "Clear previous measurements" then click "RUN". This will produce a spreadsheet that contains the name, label, length (in pixels), and other data for the image. This data can then be saved as a Microsoft Excel spreadsheet for further statistical analysis.

Representative Results

Results are shown in **Figure 2**. A single lateral group (LG) terminal cell shows extensive subcellular branching (visualized by GFP; A) and a gas-filled subcellular lumen running through each of the branches (visualized by brightfield microscopy; B). These images were collected from a mosaic L3 larva, generated using the MARCM system described in sections 1 & 2, and heat fixed and imaged, as described in sections 3 & 4. Panels C & D show a NeuronJ generated trace, as described in section 5, of the branches and the lumen respectively of the images shown in A & B. Panels E & F show the location of the fat body (FB) branch in a larva prepared for imaging as described in sections 3 & 4. Note that in this example, the animal is not a mosaic, and GFP is expressed throughout the entire tracheal system. Panels G and H show an example of a GFP-labeled terminal cell that was heat fixed for too long a time. GFP is diffuse (G), branches have broken down and portions of lumens are no longer gas filled, thus appearing as breaks in the brightfield image.

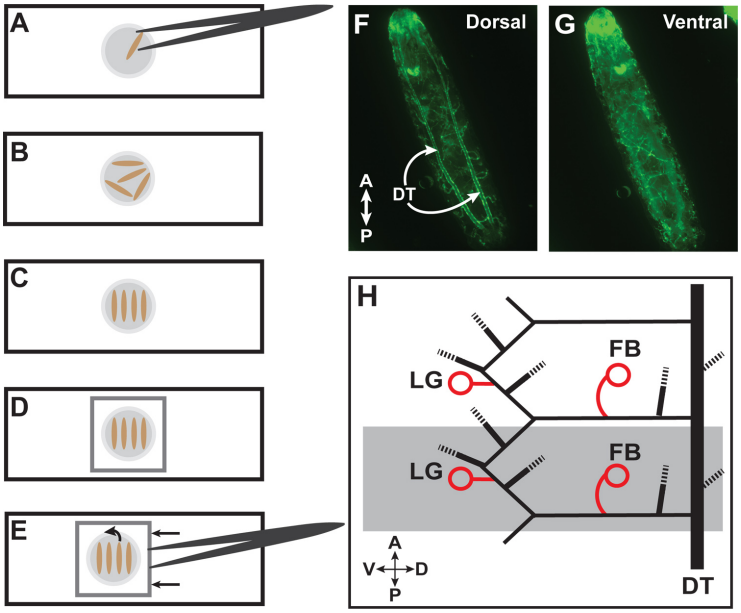

Figure 1. Larvae preparation and identification of terminal cells. (A) Place larva in a drop of 100% glycerol on a glass slide. **(B)** Multiple larvae can be placed for heat fixation. **(C)** After heat fixation, organize larvae parallel to each other and perpendicular to the long axis of the slide. **(D)** Place cover glass over larvae. **(E)** To reorient larvae, carefully push cover glass with forceps to roll the animals. **(F)** Wild-type third instar larva with GFP expressed throughout the tracheal system. The paired dorsal trunks (DT) are visible on the dorsal side. **(G)** The same larva after the rolling technique with the ventral side now facing upwards. **(H)** Diagram of lateral view of two third-instar tracheal hemisegments (one hemisegment is highlighted in grey). Circles indicate lateral group (LG) and fat body (FB) terminal cells which we use for quantitation. Dashed lines represent other branches of the tracheal system which we do not routinely quantitate. For a full description of the tracheal branches in a larval segment, refer to Ref [1].

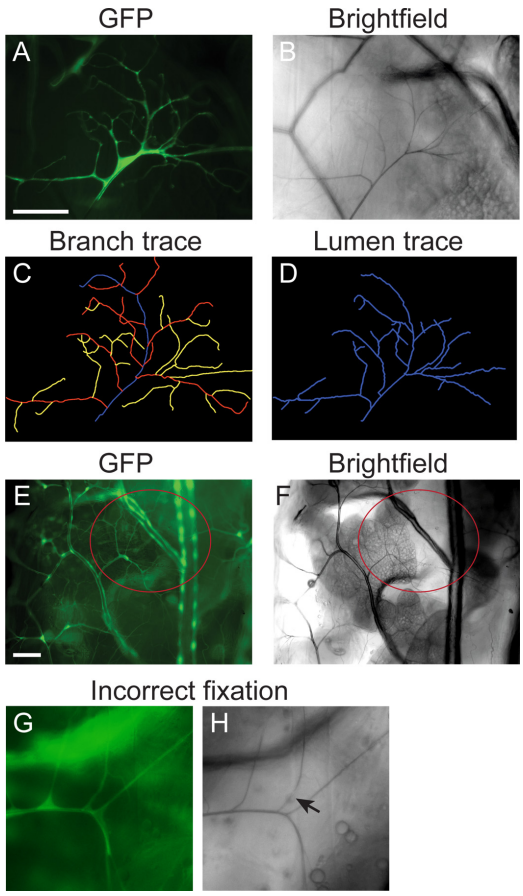

Figure 2. Representative images. (A-D) Mosaic L3 larvae were generated using the MARCM technique (section 1) and fixed and imaged using the protocol in sections 2-4. The branching pattern of a single LG terminal cell was visualized by mosaic expression of GFP **(A)**; the gas-filled lumen visualized with brightfield microscopy **(B)**. **(C)** Tracing of the branching pattern of the cell in **A**, generated using NeuronJ (section 5). **(D)** Tracing of the gas-filled lumen of the cell in **B**, generated using NeuronJ (protocol section 5). **(E, F)** A fat body (FB) terminal cell (highlighted by the red circle) visualized by GFP expression throughout the tracheal system **(E)** and brightfield microscopy **(F)** in a larva prepared by the protocol in sections 2-4. **(G, H)** Example of fixation artifacts obtained when the sample is heated for too long a period. GFP is diffuse and small branches have degraded **(G)**. Areas of lumen also no longer appear air-filled (arrow in **H**). Scale bar: 100 µm.

Discussion

The heat fixation technique described here is a rapid and convenient tool for imaging *Drosophila* larval tracheal terminal cells. Here, we use this technique to examine the branching and lumen pattern of wild-type cells. Tracheal cells expressing GFP, driven by the tracheal specific promoter *breathless*, can be easily visualized through the larval cuticle after heat fixation. The specific branching patterns of individual terminal cells, as well as those of the air-filled lumen, can be quickly visualized and measured using this method. This technique can also be performed on both first and second instar larvae. However, care must be taken in fixing smaller animals, as fluorescent protein expression can easily be disrupted.

In the method shown here, we describe an analysis of mosaic animals with GFP expressed in single tracheal cells. However, the same techniques are applicable to analysis of tracheal cells under a number of experimental manipulations. For instance, animals in which gene expression has been altered by molecular approaches, throughout the tracheal system or in individual cells by expression of RNAi transgenes or modified proteins, can also be examined with this approach. Non-genetic treatments which affect terminal cell development, such as drugs or hypoxia[2,14], can also be characterized using these methods. In these latter cases, it is necessary to start with a *Drosophila* stock constitutively

expressing GFP or another fluorescent protein throughout its tracheal system in order to visualize branching patterns. Gas-filling can be examined regardless of fluorescent protein expression.

Here, we only show examples of untagged (cytoplasmically localized) GFP being used to label the tracheal system. However, the methods described here are also suitable for detection of other native fluorescent proteins, such as DsRed, as well as fluorescent proteins which have been modified to be localized to specific subcellular structures. For instance, actin:GFP or tubulin:GFP fusions can be used to visualize the tracheal cytoskeleton[10].

Disclosures

The authors declare that they have no competing financial interest.

Acknowledgements

We thank Gillian Stanfield for comments on the manuscript. T.A.J. is supported by the University of Utah Genetics Training Grant T32-GM007464 from NIH NIGMS.

References

1. Manning, G. & Krasnow, M.A. Development of the *Drosophila* Tracheal System. *The Development of Drosophila melanogaster.*, 609-685 (1993).
2. Jarecki, J., Johnson, E., & Krasnow, M.A. Oxygen regulation of airway branching in Drosophila is mediated by branchless FGF. *Cell.* **99** (2), 211-20 (1999).
3. Ghabrial, A.S. & Krasnow, M.A. Social interactions among epithelial cells during tracheal branching morphogenesis. *Nature.* **441** (7094), 746-749 (2006).
4. Ruiz, O.E., Nikolova, L.S., & Metzstein, M.M. *Drosophila* Zpr1 (Zinc Finger Protein 1) Is Required Downstream of Both EGFR And FGFR Signaling in Tracheal Subcellular Lumen Formation. *PLoS ONE.* **7** (9), e45649 (2012).
5. Ghabrial, A.S., Levi, B.P., & Krasnow, M.A. A systematic screen for tube morphogenesis and branching genes in the Drosophila tracheal system. *PLoS Genetics.* **7** (7), e1002087 (2011).
6. Baer, M.M., Bilstein, A., & Leptin, M. A clonal genetic screen for mutants causing defects in larval tracheal morphogenesis in Drosophila. *Genetics.* **176** (4), 2279-2291 (2007).
7. Schottenfeld-Roames, J. & Ghabrial, A.S. Whacked and Rab35 polarize dynein-motor-complex-dependent seamless tube growth. *Nat. Cell Biol.* **14** (4), 386-393 (2012).
8. Levi, B.P., Ghabrial, A.S., & Krasnow, M.A. Drosophila talin and integrin genes are required for maintenance of tracheal terminal branches and luminal organization. *Development.* **133** (12), 2383-2393 (2006).
9. Jones, T.A. & Metzstein, M.M. A novel function for the PAR complex in subcellular morphogenesis of tracheal terminal cells in Drosophila melanogaster. *Genetics.* **189** (1), 153-164 (2011).
10. Gervais, L. & Casanova, J. *In vivo* coupling of cell elongation and lumen formation in a single cell. *Curr. Biol.* **20** (4), 359-366 (2010).
11. Lee, T. & Luo, L. Mosaic analysis with a repressible cell marker for studies of gene function in neuronal morphogenesis. *Neuron.* **22** (3), 451-461 (1999).
12. Shiga, Y., Tanaka-Matakatsu, M., & Hayashi, S. A nuclear GFP/ß-galactosidase fusion protein as a marker for morphogenesis in living *Drosophila. Dev. Growth Differ.* **38**, 99-106 (1996).
13. Meijering, E., Jacob, M., Sarria, J.-C.F., Steiner, P., Hirling, H., & Unser, M. Design and validation of a tool for neurite tracing and analysis in fluorescence microscopy images. *Cytometry. Part A: The Journal of the International Society for Analytical Cytology.* **58** (2), 167-176 (2004).
14. Centanin, L., Dekanty, A., Romero, N., Irisarri, M., Gorr, T.A., & Wappner, P. Cell autonomy of HIF effects in Drosophila: tracheal cells sense hypoxia and induce terminal branch sprouting. *Dev. Cell.* **14** (4), 547-558 (2008).

CHAPTER 6

SUMMARY

Cellular branching is a unique and highly specialized type of morphology that facilitates many interactions between a single cell and its surrounding environment. This interconnectivity is often observed in systems that require a cell to propagate or affect cellular processes with many neighboring cells. The best-known and well-studied type of branched cells are mammalian neurons, which are often characterized solely by their distinct branching patterns. In the case of neurons, the highly branched dendritic and axonal projections allow a single cell to make many individual contacts that facilitate rapid, multiplicative signal propagation. However, branching morphology is also specialized to facilitate delivery of fluids or gases to broad areas of tissue, where the branches contact many cells at once. In this case, the branched cell also requires a cellular tube through which gases or fluids can flow. Tubular cells that display a branched morphology transport material from a single cell to many target cells, which allows the system to satisfy the nutrient requirements of a target tissue quickly and efficiently. An example of this can be seen in the human vasculature, in capillaries or in the alveolar sacs of the human lung. In both cases, these branched tubular cells lie at the end of a network of interconnected tubes that facilitate diffusion of liquid or gases. The development of a branched cell is a dynamic and highly regulated process that involves a

number of organization steps to regionalize domains within the cell. Domain organization is coupled with membrane trafficking events necessary for growing a cellular branch. Additionally, a branched tubular cell has the complexity of having to organize a cellular tube. Similar to branching, tube formation requires the regionalization of domains that will support a cellular tube, as well as delivery and organization of membrane required for the tube structure. In addition, tube formation requires a process of clearing the space within the tube to create the lumen, which also requires the generation of structures that provide mechanical support to keep the lumen open. Both branching morphogenesis and tube formation likely require much of the same molecular machinery, however, surprisingly little is known about the genes and molecular mechanisms that govern their development. Using a component of the *Drosophila* larval tracheal system (respiratory system) called terminal cells we have begun to elucidate some of the cellular machinery required for elaborating a branched tubular cell.

Terminal cells are single cells located at the ends of a network of cellular tubes that provide oxygen and other gases to tissues in *Drosophila*. These cells have an elaborately branched cytoplasm that is dynamic and highly variable as its development is controlled by the oxygen requirement of target tissues. Located within each cellular branch is a subcellular tube that is connected at its base to the rest of the tracheal system. This tube contains no cell-cell junctions and is generated *de novo* within the terminal cells during development.

To investigate the genes that are required for terminal cell branch and tube formation, a forward genetic screen of the X chromosome was performed (Jones and Metzstein, 2011). This screen yielded thirty-two lethal lines that had defects in various

aspects of terminal cell development, including branch morphogenesis, cell outgrowth, and lumen formation. Mapping and sequencing of two mutant lines, designated *29VV* and *15N,* which showed defects in branching and lumen formation, revealed the causative mutation was in the same gene, *par-6.* Our analysis showed *29VV* is a null allele, and *15N* is a neomorphic allele. Both of these mutants showed defects in branch number and lumen development, and also showed abnormal tip morphologies; however, these defects were much more severe in *15N.*

Par-6 is a member of the conserved PAR-polarity complex best known for its role is establishing apical/basal polarity in epithelial cells. We found that other members of the complex, Bazooka (Par-3), aPKC, and Cdc42, are also required for terminal cell branching. We also found that the direct physical interaction known to occur between complex members aPKC and Par-6 is required for terminal cell branching. Furthermore, the Par-6^{15N} allele indicates that the interaction with Baz is also necessary for this process. Additionally, we found the PAR complex functions downstream of the FGF receptor to facilitate branching but does not participate in the branch outgrowth process, thus genetically separating these two previously coupled processes. The identification of PAR proteins as potential regulators of branching was a novel discovery and, based on their roles in other cell types, suggested these proteins could act to specify branch sites. However, our localization studies were not able to confirm this hypothesis. Additionally, terminal cells mutant for *par-6, baz,* or *aPKC* show defects in the number of class II and class III branches, but the number of class I branches as well as the positioning of those branches, is comparable to wild-type, but differ only by a thin and spindly appearance. This result suggests that PAR proteins do not act to specify branch points for at least class

I branches, and instead suggest that this complex could be required for localization of other factors that act in a branch specification process.

Interestingly, the par-6 mutant *15N,* showed branching and tip morphology defects that were more severe than those seen in the null allele. This allele truncates the PDZ domain of the protein, which is required for its interaction with Baz. I found that these additional defects were likely due to the misregulation of aPKC. As these defects are not ameliorated in the absence of Baz. Additionally, expression of PKM, which has constitutive aPKC kinase activity, also results in severe branching defects. Together these data indicate that regulation of aPKC, both positively and negatively, is necessary for terminal cell branching morphogenesis. However, the exact phosphorylation targets and how this process affects terminal cell branching remains unclear.

In addition to branch specification, terminal cell branches must also undergo polarized membrane addition for outgrowth of a branch. Using a reverse genetic approach, we determined that a conserved protein complex called the exocyst is required for terminal cell branch outgrowth. The exocyst, composed of, Sec3, Sec5, Sec6, Sec8, Sec10, Sec15, Exo70 and Exo84, is known for its role in docking and tethering of vesicles at the plasma membrane. We showed that exocyst deficient terminal cells accumulate cytoplasmic vesicles and have fewer branches that do not extend as far as wild-type branches. We also showed the exocyst is localized to both the basal (branching) membrane and the apical (luminal) membrane and that this localization is dependent upon PAR proteins. Taken together, we propose that the exocyst is localized to the membrane by the PAR complex where it functions to facilitate the docking and fusion of vesicles required for terminal cell branch outgrowth. Additionally, we found this process

required the Rab GTP binding proteins, Rab10 and Rab11 and that these proteins function in redundant pathways to facilitate this process. One of these pathways may be the endocytic recycling pathway, which requires proteins such as dynamin, Clathrin and Rab5. We showed that these factors are required for terminal cell branching, thus suggesting this pathway is a source of at least some of the membrane necessary to outgrow a terminal cell branch.

In addition to branching and outgrowth, many of these same proteins are required for subcellular lumen formation in terminal cells. We found PAR-polarity proteins Par-6 and aPKC, but not Baz, are required for terminal cell lumen development. Interestingly, the physical interaction known to occur between complex members is not required for this process, indicating Par-6 and aPKC participate in lumen formation in a novel way, independent of their role in the canonical PAR complex. Terminal cells mutant for *aPKC* or *par-6* do not exhibit air-filled lumens but instead contain local accumulations, in what may be large vesicles, of apical membrane. This indicates that these proteins could act to organize vesicles at the center of the cell or possibly define the membrane as apical and in the absence of aPKC or Par-6 only a portion of the lumen is properly organized. Ultrastructural analysis of *aPKC* and *par-6* mutant terminal cells would help differentiate these models.

We also found that, in addition to its role in branch outgrowth, the exocyst is required for terminal cell lumen formation. We found exocyst mutants do not show an air-filled lumen by brightfield microscopy. Ultrastructural analysis showed the presumptive lumen of exocyst deficient cells are defective in the development of the cuticle that lies adjacent to the apical membrane and is therefore required for maturation

of the lumen. Additionally, these same mutants failed to properly position the apical membrane marker Pio. Both cuticle formation and positioning of Pio on the apical domain require secretion from the apical membrane; therefore it is likely that the exocyst is required for a secretory step necessary for lumen maturation.

The work presented in this thesis contributes to a growing literature on terminal cell branch and lumen development, but also gives the field of cell biology a better understanding of the cellular processes that govern the generation of a branched cell and cellular tubes. Despite our contribution to the understanding of terminal cell development, many questions still remain. Some of these questions include: How does FGF signaling position the molecular machinery required for branching? How is the PAR-polarity complex positioned within the terminal cell, and is this important for branch site specification? What cytoskeletal rearrangements are necessary for branching and lumen formation? Analysis and characterization of the remaining mutants from the X chromosome screen will begin to elucidate many of these questions. We identified a noncanonical role for polarity proteins, aPKC and Par-6, which provides a new understanding of previously well-studied developmental pathways. Lastly, the allele of *par-6, 15N,* will be a useful tool for dissecting the cellular interactions and regulatory mechanism required for the PAR complex in many contexts.

Using *Drosophila* terminal cells to model cellular branching and subcellular tube formation has proven fruitful and we have identified multiple molecular complexes required for their development. However, future investigation using this model system would benefit greatly from the development of additional tools and metrics for evaluating terminal cell morphologies. For example, little is known about the temporal nature of

terminal cell branching and how this process correlates with lumen formation. Developing live imaging techniques will be critical for answering these questions. Live imaging would also be useful for detecting transient localization events that are likely required for branch specification. Additionally, throughout the course of this graduate dissertation work our methods of detecting branch abnormalities such as measuring absolute number of branches and quantifying branch outgrowth ratios, have evolved drastically. However, many of the finer branch defects, such as wispy branches, branches with uneven diameter and a misplaced cell body, have largely been ignored. Future projects would benefit greatly from the development of more stringent methods for measuring these small morphological abnormalities.

References

Jones, T.A., and Metzstein, M.M. (2011). A novel function for the PAR complex in subcellular morphogenesis of tracheal terminal cells in Drosophila melanogaster. Genetics *189*, 153–164.